

# Linear Robust Model Predictive Control for Urban Traffic Networks

Dik Jansen

Master of Science Thesis



# Linear Robust Model Predictive Control for Urban Traffic Networks

MASTER OF SCIENCE THESIS

For the degree of Master of Science in Systems and Control at Delft  
University of Technology

Dik Jansen

December 14, 2016

Faculty of Mechanical, Maritime and Materials Engineering (3mE) · Delft University of  
Technology



The work in this survey is the result of a collaboration with Swinburne University of Technology



Copyright © Delft Center for Systems and Control (DCSC)  
All rights reserved.



---

# Abstract

In the last decades there has been a significant increase of traffic demand in urban areas due to the development of the economy and the increase of population. The increase in traffic demand leads to a more congested road network. Congestion causes unwanted delays, resulting in higher travel costs, noise, and pollution. Popular methods to resolve the problem of congestion are, for instance, to improve the use of the existing infrastructure or to extend the current infrastructure. Most of the time the latter is not possible, because there is no space for extension of road network.

To improve the use of the existing infrastructure, the available capacity should be utilized as efficiently as possible. In an urban road network traffic travels from intersection to intersection. Hence, the intersections are influenced by each other with some time delay, and therefore it would be useful to predict the evolution of the traffic demands. For this reason an Model Predictive Control (MPC) strategy will be suitable for controlling traffic. However, this is to realize in practice due to the long computation time and the presence of uncertainty in traffic.

The goal of this thesis is to develop a predictive model-based urban traffic controller that accounts for uncertainty while not losing performance in every traffic regime and while remaining real-time feasible. The aim of the controller is to improve the throughput of an urban traffic network by aggregating the traffic dynamics to (several) tens of seconds, and this is evaluated by means of simulation.

In order to reach this goal, a literature survey is conducted to identify the possibilities in urban traffic control in combination with robust control. In this literature survey it is shown that there are different types and sources of uncertainty in urban traffic control. There are various control approaches that can handle uncertainties, while robust MPC is an approach that can also take into account predicted future traffic dynamics. Robust MPC shows promising results in terms of performance when uncertainty is present. However, the main disadvantage of robust MPC is the computation time.

The control strategy that is developed will be based on the linear MPC controller proposed by Van de Weg et al. (2016a). The reason for this is that the controller of Van de Weg et al. (2016a) is real-time feasible and has promising performance in each traffic regime. There are

two ways to extend the controller of Van de Weg et al. (2016a) to account for uncertainty: (1) by using existing robust MPC strategies, or (2) by redefining the control strategy so that it avoids traffic situations that are sensitive to uncertainty. It is expected that the first option may yield a real-time infeasible controller. Therefore, in this thesis the second option is explored to develop a robust urban traffic controller.

The MPC controller of Van de Weg et al. (2016a) consists of three main components: the prediction model, the objective function, and the optimization algorithm. To account for uncertainty the proposed extension adjusts the objective function by introducing an extra variable. It is expected that uncertainty has a greater impact in the saturated and over-saturated traffic regime, because spill-back is more likely to occur then. The extra variable is used as a penalty that describes the number of vehicles that exceeds a given threshold for each link at each time step. The value of the penalty increases with an increasing number of vehicles when the threshold is exceeded. By minimizing the penalty the controller tries to avoid that the number of vehicles exceeds this threshold, and therefore the controller incorporates a safety margin in every link.

The proposed extension does not require any additional measurements compared to the controller of Van de Weg et al. (2016a). However, the implementation of the penalty does require an extra state variable and two extra constraints per link. Thus, the optimization problem will become larger than the optimization problem of Van de Weg et al. (2016a). Nevertheless, the optimization problem is kept linear. Hence, it is expected that the proposed extension is real-time feasible.

The control strategy is evaluated by means of simulation. Four different case studies have been conducted on a network consisting of two intersections. The four case studies evaluate the performance of the controller when there is uncertainty in the demand, turn fractions, bottleneck capacity, or in the model. These evaluations show that the controller does not increase the performance for uncertainty in the demand. In contrast, the controller can increase the performance for uncertainty in the turn fractions, bottleneck capacity, or in the model. However, the performance increase is not due to the avoidance of spill-back, but due to the placement of more vehicles at the exits of the network. This causes the outflow of the network to be less affected by the uncertainty. During the first three cases the computation time of the optimization problem is tracked, which shows that the controller needs up to 18% more computation time.

Concluding, a control strategy has been developed that can improve the throughput of an urban traffic network when uncertainty is present. However, the performance improvement is due to a non-foreseen reason. Further research has to be conducted with more suitable case studies to verify the concept. It is expected that the performance of the controller can be further improved by tailoring the control parameters for individual links. It would be interesting for future research to evaluate the controller for more realistic uncertainties and for more complex and larger traffic networks.

---

# Table of Contents

<b>Preface</b>	<b>vii</b>
<b>1 Introduction</b>	<b>1</b>
1-1 Challenges in urban traffic control . . . . .	2
1-2 Research objective . . . . .	3
1-3 Research scope . . . . .	4
1-4 Relevance . . . . .	5
1-5 Outline . . . . .	5
<b>2 Literature survey on robust urban traffic control</b>	<b>7</b>
2-1 Introduction . . . . .	7
2-2 Traffic controllers . . . . .	8
2-2-1 Fixed-time control . . . . .	8
2-2-2 Traffic-responsive control . . . . .	9
2-2-3 Traffic-responsive control: Model-based strategies . . . . .	11
2-3 Robust traffic control . . . . .	14
2-3-1 Uncertainties in traffic control . . . . .	14
2-3-2 Robust control theory . . . . .	15
2-3-3 Robust urban traffic control . . . . .	17
2-4 Discussions and Conclusions . . . . .	18
<b>3 The design of the robust urban traffic controller</b>	<b>21</b>
3-1 Introduction . . . . .	21
3-1-1 MPC . . . . .	22
3-1-2 Assumptions . . . . .	22
3-2 Current control framework . . . . .	23
3-2-1 Prediction model: the Link Transmission Model (LTM) . . . . .	24
3-2-2 Linear optimization problem formulation . . . . .	28

3-3	Analysis of uncertainty in the current control framework . . . . .	31
3-3-1	Uncertainty in the measurement of the state . . . . .	32
3-3-2	Uncertainty in the measurement of the disturbances . . . . .	32
3-3-3	Uncertainty in the prediction model . . . . .	33
3-4	Extension of the control framework . . . . .	34
3-4-1	General idea . . . . .	34
3-4-2	Mathematical formulation . . . . .	36
3-4-3	Additional Assumptions . . . . .	37
3-4-4	Linear optimization formulation . . . . .	37
3-5	Conclusions and discussions . . . . .	41
<b>4</b>	<b>Evaluation of the robust urban traffic controller</b>	<b>43</b>
4-1	Introduction . . . . .	43
4-2	Simulation set-up . . . . .	44
4-2-1	Timing parameters . . . . .	45
4-2-2	Network . . . . .	45
4-3	Case Study 1: Uncertainty in the demand . . . . .	47
4-3-1	Case study 1 - evaluation set-up . . . . .	47
4-3-2	Case study 1 - quantitative results . . . . .	48
4-3-3	Case study 1 - qualitative results . . . . .	50
4-4	Case Study 2: Uncertainty in the turn fractions . . . . .	52
4-4-1	Case study 2 - Evaluation set-up . . . . .	52
4-4-2	Case study 2 - quantitative results . . . . .	53
4-4-3	Case study 2 - qualitative results . . . . .	56
4-5	Case Study 3: Uncertainty in the outflow constraint . . . . .	58
4-5-1	Case study 3 - Evaluation set-up . . . . .	58
4-5-2	Case study 3 - quantitative results . . . . .	59
4-5-3	Case study 3 - qualitative results . . . . .	62
4-6	Case Study 4: Model uncertainty . . . . .	64
4-6-1	Case study 4 - Evaluation set-up . . . . .	64
4-6-2	Case study 4 - quantitative results . . . . .	66
4-6-3	Case study 4 - qualitative results . . . . .	67
4-7	Computation time . . . . .	67
4-8	Conclusions and recommendations . . . . .	68
<b>5</b>	<b>Conclusions and recommendations</b>	<b>71</b>
5-1	Conclusions . . . . .	71
5-1-1	Conclusions on the literature survey . . . . .	71
5-1-2	Conclusions on the development of the control strategy . . . . .	72
5-1-3	Conclusions on the evaluation of the control strategy . . . . .	73
5-2	Recommendations . . . . .	74
5-2-1	Further research - extension of the case study . . . . .	74
5-2-2	Further research - improvements and extensions on the control strategy . . . . .	75
5-2-3	Further research - regarding robust urban traffic control . . . . .	75
5-2-4	Further research - regarding urban traffic control . . . . .	76

---

<b>A</b>	<b>Specification of control matrices</b>	<b>79</b>
A-1	Matrices of current control method . . . . .	79
A-1-1	Specification of the objective function matrices . . . . .	79
A-1-2	Specification of the inequality constraints . . . . .	82
A-2	Matrices of extended control method . . . . .	85
A-2-1	Specification of the objective function matrices . . . . .	85
<b>B</b>	<b>Local control strategy</b>	<b>87</b>
B-1	Control framework . . . . .	87
B-2	Assumptions . . . . .	88
B-3	Network control . . . . .	89
B-4	Local control . . . . .	90
	<b>Bibliography</b>	<b>93</b>
	<b>Glossary</b>	<b>97</b>
	List of Acronyms . . . . .	97
	List of Symbols . . . . .	97



---

# Preface

During the past thirteen months I had the opportunity to work on a project that allowed me to have an amazing four months in Melbourne and a very instructive year in Delft. I am very grateful towards the people that made this possible.

First of all, I would like to thank Bart de Schutter for his support, feedback and patience throughout this thesis. Bart was always very positive in the monthly meetings and he was always spot-on with his guidance.

I want to thank Goof van de Weg for all his effort. Goof was very supportive, and was always willing to make time for me. Without the confidence Goof gave me I would not made it this far by now. He introduced me to most of his research, which made me far more enthusiastic about traffic control.

Furthermore, I would like to thank Hai le Vu for making it possible for me to come to the Swinburne University of Technology in Melbourne. Hai looked from a totally different and refreshing perspective at the conducted research.

Last but not least, I would like to thank many of my fellow students in Delft for the fruitful discussions and chats on how to deal with the process of graduation. Finally, I want to express my gratitude towards my girlfriend and family whom have granted me the opportunity and encouraged me to perform to the best of my ability.



---

# Chapter 1

---

## Introduction

In the last decades there has been a significant increase of traffic demand in urban areas, due to the development of the economy and the increase of population. The increase in traffic demand leads to a more congested road network. Congestion causes unwanted delays, resulting in higher travel cost, noise, and pollution. A growing queue can even become so large that it reaches a neighboring intersection, the so-called spill-back of a queue. Spill-back will lead to a waste of green time at the intersection itself and at neighboring intersections, because vehicles cannot enter the street with the spilled back queue.

Another drawback of congestion is the clockwise hysteresis loop as shown by Gayah and Daganzo (2011) and the clockwise hysteresis loop can be seen in Figure 1-1. Gayah and Daganzo (2011) show that traffic networks tend to recover more slowly from very congested areas, compared to from less congested areas. Especially when drivers do not act adaptively to disturbances in traffic, traffic networks are more unstable as they recover from congestion than when they are loaded. This instability causes clockwise hysteresis loops to appear in the macroscopic fundamental diagram. The clockwise hysteresis is better known for freeway traffic and causes the so-called capacity drop.

Methods to resolve the problem of congestion are, for instance, to improve the control of the existing infrastructure or to extend the current infrastructure. Most of the time, the latter is not possible because there is no space for extension of the road network. Therefore, the most convenient way to resolve the problem is to make the use of intersections as efficient as possible.

The efficiency of traffic control is not only of great importance for congested traffic, because unwanted delays can also occur when there is no congestion at the intersection in case of the lack of efficient control. Consider, for example a situation in which there are two incoming roads at a single intersection, one with a queue and the other without a queue. It would be very inefficient if the road without the queue gets green. Hence, for both congested and free-flow traffic situations traffic use should be efficient and should not lead to unwanted delays.

To improve the use of the existing infrastructure, the available road capacity should be utilized

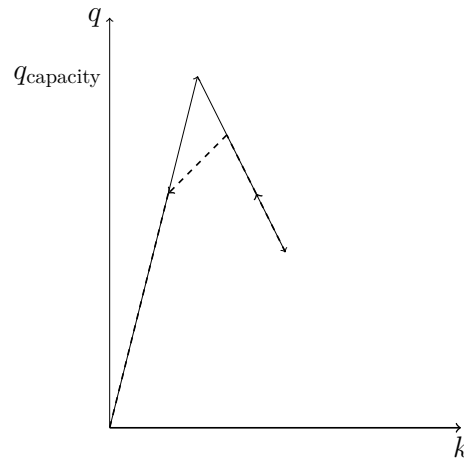


**Figure 1-1:** Fundamental diagram where  $q$  [veh/h] is the flow and  $k$  [veh/m] the density. The solid line represents the loading of the traffic network and the dashed line represents the recovery from congestion of the traffic network.

as efficient as possible. In an urban road network traffic travels from one intersection to another. Hence, the intersections are influenced by each other with some time delay. Therefore, it would be useful to predict the traffic to utilize the road capacity as efficiently as possible.

## 1-1 Challenges in urban traffic control

Already a lot of research has been done in the field of urban traffic control. However, there are still a lot of opportunities for improvement, because the urban traffic control problem is a very complex problem. This complexity is due to the several requirements a traffic controller has to satisfy when implemented in practice. The most important requirements are:

1. The ability to improve the network throughput in the different traffic regimes (e.g. in the under-saturated, saturated, and over-saturated regime);
2. The computation time required by the controller should be less than the real-time sampling time (so the controller should be real-time feasible);
3. The ability to control signal timings and signal plans (e.g. green times, offsets, cycle times, etc.);
4. The ability to control an intersection, while subjected to heterogeneous traffic, such as vehicles, cyclists, pedestrians, public transport, and emergency vehicles;
5. The ability to improve the network throughput when noise, disturbance, and uncertainty are influencing the dynamics of traffic.

It can be a very challenging task to design an urban traffic controller that satisfies all the above mentioned requirements. Hence, this research is only focused on improving throughput

in the different traffic regimes while subjected to uncertainty and while remaining real-time feasible.

Why should we account for uncertainty in urban traffic controller design? Traffic is by its nature influenced by uncertainty. In modern-day traffic vehicles are still controlled by humans. Humans can make their own decisions, and therefore they can act unpredictable. Note that not only humans can be unpredictably but unexpected events can happen as well, such as a change of weather, accidents, or unexpected road works. Furthermore, some traffic controllers use sensors to measure queue lengths. These sensors (e.g. induction loops) are not very reliable, because they are easily broken and they are not always very accurate. Thus, it can be very difficult to determine the exact queue length with the use of induction loops. As the previous examples show, there can be various uncertainties in traffic. However, the question remains whether we should account for uncertainty in urban traffic control.

## 1-2 Research objective

The main objective of this thesis is the development of an urban traffic controller that improves the traffic network throughput while subjected to uncertainty and remaining real-time feasible. In order to reach such a design, five design requirements are specified:

1. The ability to improve the network throughput when noise, disturbance, and uncertainty are influencing the dynamics of traffic;
2. The ability to improve the network throughput in the various traffic regimes;
3. The computation time required by the controller should be less than the real-time sampling time;
4. The ability to control signal timings by controlling green times;
5. The ability to control an intersection with only vehicular traffic.

In order to reach this objective, the design process is subdivided in the following steps: analysis, development, and evaluation. First, the literature is studied to analyze where the major opportunities lie in the field of robust urban traffic control. More specifically, the following objectives are stated for the literature survey:

- create an overview of relevant existing urban traffic controllers;
- identify the different causes of uncertainty in urban traffic control;
- create an overview of existing urban traffic controllers that explicitly account for uncertainty.

The identified opportunities will form the basis for the development of the controller. During the evaluation, the impact of the different uncertainties on the performance for not accounting for uncertainty is assessed first. Subsequently, the proposed controller will be assessed on its ability to improve the throughput.

## 1-3 Research scope

The focus in this thesis lies on developing a controller that satisfies the five design requirements that are mentioned in the previous section. This section tries to make the requirements more concrete and discuss their limitations.

### **Focus on various sources of uncertainty**

Section 1-1 lists some of the reasons why there is uncertainty in urban traffic control. There are many ways to mathematically describe these uncertainties such that they can be used for controller design. The focus in this thesis lies on uncertainties that fluctuate around a known and given mean. However, this mathematical description of uncertainty may not be the most realistic representation of uncertainty.

### **Focus on the characteristics of urban traffic**

When designing an urban traffic controller it is important to realize what the characteristics of urban traffic are and what the challenges are when controlling urban traffic. In this thesis a potential undesired effect in particular, spill-back of a queue is identified that causes additional delays. The phenomenon of spill-back may be prevented for one arterial by distributing the traffic more evenly or by introducing a safety margin in every link.

### **Focus on a model-based predictive control approach**

This thesis focuses on improving the network throughput by means of Model Predictive Control (MPC), the reason being that in a road network traffic travels from intersection to intersection. Hence, the intersections are influenced by each other with some delay, and therefore it would be useful to predict the traffic. Model-based approaches, such as MPC, are able to predict the future traffic dynamics, and therefore are able to improve network throughput in all three traffic regimes. However, one of the challenges of an MPC strategy is its long computation time. Another challenge of MPC strategies is that to accurately predict the future traffic dynamics there is the need for a suitable model and suitable measurements, which are not always available in practice.

### **Focus on a small network and vehicular traffic**

This thesis evaluates the proposed control framework on a network with only two intersections, while in reality a traffic network may consist of hundreds of intersections. Furthermore, the network is only considered for one type of traffic: vehicles, whereas in reality traffic consists of multiple participants (e.g. cyclists, public transport, lorries). The reason for this is that it is more important to demonstrate that the concept of the newly developed control framework works as expected than assessing the performance on a very realistic traffic situation. Considering a more realistic traffic situation is more relevant when the concept has proven itself to avoid the phenomena of spill-back, and therefore account for uncertainty.

## Evaluation criteria

For the evaluation of the proposed control strategy multiple case studies should be conducted, where a different uncertainty source is applied to each case study. Every case study should provide insights into the impact of every uncertainty, the quantitative behavior, qualitative behavior of the control strategy. In this thesis, the following indicators will be evaluated:

- The impact of different uncertainties is evaluated for various demands. The demands with the most significant impact can then be used to assess the proposed control strategy specifically for those regions;
- This impact consist of the throughput decrease or increase obtained by the controller of Van de Weg et al. (2016a) compared to the situation without uncertainty;
- The Total Time Spent (TTS) and the computation time of the optimization algorithm are used as performance indicators. The TTS is commonly used to evaluate the performance of traffic control strategies that aim at improving traffic throughput. The TTS is the sum of the time spent by all vehicles in the network (including the origin queues) during a certain time interval. The computation time is used to evaluate whether the control strategy will be real-time feasible;
- The qualitative behavior can provide insights into the behavior of the control strategy. This behavior should be in accordance with the expectations that are presented during the development of the control strategy.

## 1-4 Relevance

The main contributions of the research presented in this thesis are

- the impact analysis of the different sources of uncertainty on the controller of Van de Weg et al. (2016a). This provides insight in how the performance of the controller of Van de Weg et al. (2016a) is affected due to uncertainty;
- a robust urban traffic control approach with an efficient formulation that tries to avoid spill-back ;
- the proposed controller is able to increase performance when uncertainty in the turn fractions, uncertainty in the outflow constraint or model uncertainty is present.
- this work is extension of the work of Van de Weg et al. (2016a), and therefore this extension makes the control strategy of Van de Weg et al. (2016a) a step closer to future implementation.

## 1-5 Outline

This report consists of five chapters. The structure of this report and relations between the chapters are illustrated in Figure 1-2. Chapter 2 introduces the challenges in robust urban

traffic control that are identified by means of a literature survey. Chapter 3 describes the control framework that is proposed in thesis. This includes details on the control strategy of Van de Weg et al. (2016a), its potential sources of uncertainty, and the proposed extension. Chapter 4 presents the simulations that have been conducted to evaluate the proposed framework and the framework of Van de Weg et al. (2016a) for different sources of uncertainty. Chapter 5 presents the conclusions and recommendations for future research.

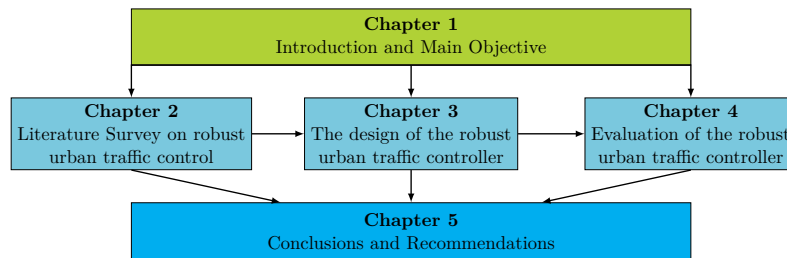


**Figure 1-2:** Overview of this thesis

# Literature survey on robust urban traffic control

This chapter provides an overview of the research related to robust urban traffic control. It does so by discussing relevant nominal traffic controllers in Section 2-2. After that, different sources of uncertainty in urban traffic control are discussed in Section 2-3-1. In Section 2-3-2 conventional methods to explicitly account for uncertainty (e.g. robust control theory) are presented. Finally, in Section 2-3-3 provides an overview of existing urban traffic controllers that explicitly account for uncertainty. The literature survey is concluded in Section 2-4.

## 2-1 Introduction

In recent years the development of model-based control strategies (e.g. Model Predictive Control (MPC)) for urban traffic has greatly increased; mainly due to their ability to predict the impact of input settings in the future. The ability to predict in urban traffic is useful, because the outflow of one intersection can affect the outflow of neighboring intersections in the future. Hence, model-based control strategies can be very suitable for urban traffic control.

However, as pointed out in the introduction in Section 1-1 the urban traffic control problem is a very complex problem, due to the several requirements an urban traffic controller has to satisfy. Therefore, it is expected that in literature no model-based approaches yet exists that satisfies all requirements of an urban traffic controller. This literature survey focuses on providing insights in (robust) urban traffic control for the development of an urban traffic controller. To find the necessary insights, this literature survey is divided into four parts.

First, in Section 2-2 an overview is created of relevant existing urban traffic controllers. This overview shows a wide variety of different solutions to the traffic control problem. The controllers are divided into: fixed-time control, traffic-responsive control, and model-based traffic-responsive control. Fixed-time controllers are discussed because robust fixed-time controllers will be discussed in Section 2-3-3. The division between traffic-responsive control with

and without prediction may show the potential benefits of using model-based approaches. The controllers are assessed and compared on the following characteristics: the computation time, performance in every traffic regime, and the ability to handle uncertainty.

Thereafter, the different causes of uncertainty in urban traffic control are identified in Section 2-3-1. In order to account for uncertainty, it has to be clear with what kind of uncertainty the controller should not lose too much performance. Subsequently, an overview of different robust controllers that can explicitly handle uncertainty is given in Section 2-3-2.

Section 2-3-3 provides an overview of existing urban traffic controllers that explicitly account for uncertainty. The controllers are further distinguished into: robust fixed-time control, stochastic traffic-responsive control, and robust traffic-responsive control. Each of these categories has its own benefits.

## 2-2 Traffic controllers

Traffic controllers can be used to improve the performance of an urban traffic network. Already a lot of research has been done in the field of urban traffic control, which resulted in a wide variety of different traffic controllers. Inspired by Papageorgiou et al. (2003), the discussed control strategies are categorized into two categories, namely, fixed-time and traffic-responsive control. In this literature survey the controllers are assessed on the performance in each traffic regime, the computation time, and on deterioration of performance when subjected to uncertainty or noise.

Fixed-time control involves offline optimization of cycle time, splits, and off-sets between nearby intersections. Contrary to fixed-time control, traffic-responsive control uses online measurements from road detectors (e.g. induction loops, cameras) to optimize the signal timings. Four traffic-responsive control strategies (SCOOT, SCATS, TUC, and Back-Pressure) will be discussed in Section 2-2-2. These strategies are discussed to show potential advantages and drawbacks of not using a model-based strategy.

According to Van de Weg et al. (2016a) there are three types of traffic regimes: under-saturated, saturated, and over-saturated in urban traffic control. In the under-saturated regime queues will dissolve totally during their green phase. There is no queue left when the traffic light turns to red. Secondly, in the (over-)saturated regime queues will not dissolve completely during their green phase. There is still a queue left when the traffic light turns to red. However, in the over-saturated regime the queues will spill-back to upstream intersections.

### 2-2-1 Fixed-time control

Fixed-time control can be divided into isolated methods and coordinated methods. According to Osorio and Bierlaire (2008), there exists a trade-off between isolated and coordinated strategies. The isolated strategies consider in detail the traffic dynamics at an intersection, but this is at the expense of not fully capturing the dynamics between intersections.

The isolated methods can be further distinguished into stage-based and phase-based control strategies. Stage-based strategies determine the optimal splits and cycle time, whereas phase-based strategies also optimize the stage sequence. According to Papageorgiou et al. (2003)

this may be important for more complex situations. The computation time of fixed-time controllers will not be a problem, because calculations are performed off-line.

Coordinated fixed-time control strategies were introduced to capture traffic dynamics between intersections. Two well known examples of coordinated control strategies are: MAXBAND and TRANSYT.

## **MAXBAND**

Little et al. (1981) proposed the traffic control strategy MAXBAND, which can create green waves in the under-saturated traffic regime. It does so by optimizing the bandwidth. The bandwidth is the proportion of the cycle time for which it is possible for a vehicle to travel from one end of a arterial to the other end without stopping. Several variations of the MAXBAND control strategy have been proposed, such as Gartner et al. (1991) proposed MULTIBAND, which is a more tailored approach for an arterial with segments with different capacities.

There will be a strong interaction between queues, if traffic becomes congested. The bandwidth strategies MAXBAND and MULTIBAND fail to describe this phenomena. Another drawback of this technology is that it is not based on actual traffic flows, and therefore it is insensitive for variations in flow. Furthermore, both strategies are based on the idea that platoons of vehicles do not fall apart while they travel along a link. This is in contrast to the reality, where platoon dispersion does take place.

## **TRANSYT**

TRANSYT is proposed by Robertson (1969). According to Robertson and Bretherton (1991); Papageorgiou et al. (2003) the traffic network study tool (TRANSYT), is well known and is frequently applied in practice, and is often used as an unofficial standard. TRANSYT calculates the optimal signal settings for different demands. The demand is assumed to be constant for specific parts of the day, and is based on historical data. TRANSYT is divided into two main parts: the traffic model and the optimization procedure. These two parts are then used in a iterative way. For given decision variables (e.g. signal settings) the model calculates the corresponding performance index, which is then fed back into the optimization procedure. The optimization procedure uses a heuristic hill climbing optimization algorithm that introduces small changes to the decision variables. After that, the decisions variables are then fed back into to the model, and so forth, until the procedure finds a (local) minimum. Unlike MAXBAND, TRANSYT uses a platoon dispersion model to describe the evolution of traffic platoons traveling on links at known speed with some dispersion. Therefore, TRANSYT describes the dynamics between intersections more accurately than MAXBAND. TRANSYT uses a vertical queuing model to describe the dynamics of the queue. Therefore, TRANSYT cannot determine the queue length appropriately in congested traffic conditions.

### **2-2-2 Traffic-responsive control**

The main drawback of fixed-time control strategies, is that they are based on historical data rather than on real-time data. Signals timings can become outdated, because demands can vary over of a day, a week, etc. Contrary to fixed-time control, the decisions of traffic-responsive control strategies are based on real-time data. The traffic-responsive control

strategies use on-line measurements from road detectors (e.g. induction loops, cameras) to determine the signal timings.

### **SCOOT and SCATS**

The Split Cycle Offset Optimization Technique (SCOOT) is proposed by Robertson and Bretherton (1991) and shares some of its basic concepts with TRANSYT. The main objectives of SCOOT are minimizing the sum of average queues and minimizing the number of stops. It does so by controlling the splits, offsets, and cycle time. Every 4 seconds SCOOT measures the flow, which is used to estimate the queue length and clearance time. Furthermore, SCOOT uses the same platoon dispersion model as TRANSYT. Hence, SCOOT is able to describe the dynamics between intersections as accurate as TRANSYT. It is assumed that the cruising speed of these platoons is known with some dispersion. This cruising speed is still to be determined by the use of historical traffic data. Every cycle the algorithm assesses whether or not the cycle time, splits, and offsets should be altered by 4 seconds to further decrease the objective function. Thus, SCOOT can only change its control input incrementally.

The Sydney Coordinated Adaptive Traffic System (SCATS) is proposed by Lowrie (1982) and works on a combination of traffic-responsive control and fixed time plans. The ratio of demand to saturation flow is used to assess the congestion level. The congestion level is then used to choose a fixed-time plan from a library of plans. SCATS divides the network of intersections into sub-networks. Therefore, the control is divided into a top layer and a lower layer. The upper level generates offset plans between the sub-networks by time of day with the use of historic data. The lower level optimizes splits, cycle times, and offsets between signalized intersections of the individual sub-networks. The optimization is based on the flows of the previous cycle, which are measured using detectors at the stop lines. Therefore, SCATS is not fully responsive to unpredictable arrival of flows.

Both SCOOT and SCATS can respond to both short-term local peaks in traffic demand, as well as following trends over time. However, the optimization procedure only allows a small change in control input. Then SCOOT and SCATS could be constraint by this during a sudden change in flow. However, Quan et al. (1993) show a case study where SCOOT is still able to increase performance during rapidly traffic conditions compared to a fixed-time controller. For this reason, SCOOT and SCATS lack a traffic-responsive behavior during rapidly changing traffic conditions according to Dion and Yagar (1996).

### **TUC**

The traffic-responsive urban control (TUC) strategy is proposed by Diakaki et al. (2002), and is based on feedback control theory. TUC tries to minimize the relative occupancy in the links and optimizes the control input by controlling the green times. The green times are adjusted every cycle, based on the queue lengths in the traffic network. The use of feedback control theory is made possible by the use of the store-and-forward modeling of the traffic network. The store-and-forward model introduces a model simplification that enables the description of the traffic flow process without the use of binary variables. This simplification causes the traffic flow to be continuous when the demand is assumed to be sufficient; the demand is sufficient when the traffic network is in the (over-)saturated traffic regime. The consequences of using the store-and-forward model is that the sampling time cannot be shorter than the

cycle time. Thus, decisions cannot be taken more frequently than every cycle. Furthermore, the oscillations of vehicles queues in the links due to green and red switching of traffic light is not captured by the model.

In order to operate in real time, TUC has to measure the occupancy of links. TUC is implemented in practice (e.g. UK, Greece, and Brazil). TUC shows high efficiency and performs especially well in the saturated traffic regime. However, TUC does not account for the capacity (number of vehicles) of downstream roads and spill-back dynamics. Although TUC tries to avoid the over-saturated traffic regime by minimizing the relative occupancy, it still may lose performance in the over-saturated traffic regime.

Avoid, but if there is going to spill-back, if its inevitable. TUC does not capture the spill-back dynamics during the over-saturated traffic regime.

### **Back-Pressure**

The TUC strategy is a form of centralized traffic control, whereas Back-Pressure is a form of decentralized, local traffic control. Decentralized control has the advantage of not having the cost of a communication infrastructure. The control decisions of Back-Pressure are based on the difference in traffic load: the difference in queue length upstream and downstream of the intersection. In contrast, most other control strategies only base their decisions on the (expected) number of vehicles upstream of the intersection during the next cycle. Furthermore, Back-Pressure does not require any a priori knowledge of the demand as stated by Le et al. (2015). However, the turn ratios are assumed to be known, which is not always the case in reality.

The Back-Pressure algorithm does not account for spill-back effects and free-flow dynamics. In other words, it is only applicable to the saturated traffic regime. Gregoire et al. (2015) proposed a capacity-aware Back-Pressure algorithm that accounts for the capacity of a link; instead of the pressure they use a normalized pressure. The capacity-aware Back-Pressure algorithm outperforms the original Back-Pressure algorithm in the over-saturated traffic regime and performs equally well in the under-saturated and saturated regime. Both Back-Pressure algorithms do not explicitly consider delays of waiting vehicles and are fully queue-length based. Hence, vehicles can be waiting for a very long time. Furthermore, no research has yet been performed on potential uncertainties in the measurement of queue lengths or uncertain parameters used by the algorithms.

### **2-2-3 Traffic-responsive control: Model-based strategies**

The previously discussed control strategies are not capable of accounting for future traffic dynamics. Not accounting for traffic flow dynamics in the future can lead to myopic control decisions of the traffic controller. A way to improve this, is the use of model-based strategies. Model-based strategies make use of a traffic model to find the optimal signal settings over a given time horizon. The main drawback of these strategies is that they have no real-time feasibility when implemented in an urban traffic network, due to their computational burden. However, by omitting some detail of the traffic model, model-based approaches can become real-time feasible. From Section 2-2-3 until Section 2-2-3 various types of model-based approaches are discussed, which show a wide variety of different solutions to the urban traffic control problem. The discussed model-based approaches are referred to as MPC strategies.

**Lo (1999)**

Lo (1999) introduces an MPC controller that minimizes the total network delay by controlling the green times and the initial offset of the major approaches. The prediction model is the Cell Transmission Model (CTM) of Daganzo (1995), which can capture every traffic regime. However, the CTM used here does not capture the dynamics of turning movements. Therefore, the controller only produces a signal plan for through-going traffic. To capture the effect of traffic light switching and thereby the fluctuating flows on an intersection a mixed-integer programming technique is used. In the under-saturated regime the controller is consistent with a controller like MAXBAND, as it creates green waves for the arterials of the traffic network. However, there is no further comparison with other urban traffic controllers and the results are based on limited computational experiences. Furthermore, the controller was only tested on a network of two intersections, and even then the computation time of 50 seconds is significant. Hence, the computational complexity remains a major problem for the controller proposed by Lo (1999).

**Lin et al. (2011, 2012)**

Lin et al. (2012) propose a macroscopic traffic model: the S-model. The model is used as a prediction model for MPC control. The S-model uses a sampling time of one cycle time, whereas the model of Van den Berg et al. (2007) uses a sampling time of one second. Therefore, the computation time of the S-model is much lower than the computation time of the model of Van den Berg et al. (2007). The objective function that is minimized is the Total Time Spent (TTS) in the network. Therefore, the optimization problem features a nonlinear, non-convex objective function subject to nonlinear, non-convex constraints.

However, in Lin et al. (2011) the S-model (Lin et al., 2012) is reformulated into a mixed-integer linear model. The resulting Mixed-Integer Linear Programming (MILP) problem can be solved more efficiently than the nonlinear non-convex optimization problem of Lin et al. (2012). The MILP solver used in Lin et al. (2011) can efficiently find a global optimum rather than a local optimum found by Sequential Quadratic Programming (SQP). However, one may argue whether comparison between the SQP solver and the MILP solver is fair in the case of urban traffic control, because the SQP algorithm is not very suitable for discontinuous optimization problems.

Furthermore, the S-model can be reformulated into the S\*-model. In the S\*-model the over-saturated traffic regime is implemented by adding extra constraints. This S\*-model can also be recasted into a mixed-integer linear model. This new model can then be used for a new MILP optimization problem, where the number of auxiliary variables is reduced in half compared to the MILP optimization problem with the S-model. The MPC controller with the S-model and S\*-model tend to perform less in low demand regions than the MPC controller with the SQP algorithm. This is mainly because the free flow travel time is assumed to be constant over time in the S-model and S\*-model.

The MILP problem can be solved very fast by an MILP solver, when compared to an SQP solver. The CPU time is significantly reduced from hundreds of seconds to a few. However, the computation time of MILP still increases exponentially as a function of the problem size.

**Aboudolas et al. (2010)**

The traffic controller proposed by Aboudolas et al. (2010) uses the store-and-forward model to model traffic flow, just like the TUC strategy does. The control problem is formulated into a Quadratic Programming (QP) problem. The QP problem aims at minimizing and balancing the link queues by controlling the green times. The optimization algorithm is embedded in a rolling-horizon scheme for the application in real time. Aboudolas et al. (2010) show that when proper demand knowledge is available, the proposed controller outperforms the TUC strategy and a fixed-time control strategy in every traffic regime. The TUC strategy seems less sensitive to inaccuracies of traffic parameters than the proposed controller. The use of a smaller horizon with the proposed controller will lead to a lower sensitivity to the inaccuracies, because longer model predictions tend to be increasingly less accurate.

**Le et al. (2013)**

The MPC controller proposed by Le et al. (2013) aims at minimizing the sum of all queue lengths, by controlling the green times. The control problem is formulated into a QP problem where the predicted state is penalized quadratically and the control variable is penalized linearly. The model describes the urban traffic network with the use of multi-class queuing networks, where classes relate to different types of network elements. The network state maintains counts of the number of vehicles at each network element. The maximum number of vehicles that can go from one network element to another in an unit of time is to be adjusted by traffic measurements but are assumed to be known. Hence, the model described in Le et al. (2013) is very similar to the CTM of Daganzo (1995), only it does not simulate the shock-wave speed. One could argue that the model described in Le et al. (2013) is just a simplification of the CTM of Daganzo (1995).

**Van de Weg et al. (2016a)**

In Van de Weg et al. (2016a) an MPC controller is proposed that tries to optimize the throughput by minimizing the difference between the cumulative inflow and outflow of every link and origin of the network. The controller does so by controlling the effective fractions of green time. The Link Transmission Model (LTM) of Yperman (2007) is used to model traffic. The proposed traffic model is capable of modeling each traffic regime. It includes the free-flow travel time in the under-saturated regime and shock-wave dynamics in the over-saturated regime.

The performance of the controller is assessed by looking at the total time spent by all vehicles, and at the computation time of the controller. The performance is compared to performance of the controllers of Aboudolas et al. (2010) and Le et al. (2013). The MPC controller of Van de Weg et al. (2016a) can realize a higher throughput than the other two methods. The methods still yield a comparable amount of computation time.

The MPC controller of Van de Weg et al. (2016a) only controls the effective fractions of green time. It does not come up with a signal plan that can directly be implemented. Furthermore, the traffic model is not able to model the fluctuations of flow due to the switching of traffic lights.

## 2-3 Robust traffic control

Uncertainties are common when controlling traffic networks. The controller performance may deteriorate when uncertainties are not included during the controller design. Control strategies that have been applied in practice, obviously are able to take into account uncertainties in some way, regardless of whether the performance deteriorates or not. However, the range of literature dealing with explicit inclusion of uncertainty in the design of urban traffic control is limited. In order to gain more insight into this design problem, the different causes of uncertainty in traffic have to be investigated first.

### 2-3-1 Uncertainties in traffic control

Humans are the main operator when it comes to controlling a vehicle. Every human can act differently to various traffic situations. Thus, traffic can be considered to be a stochastic process; there is a certain chance that a certain scenario occurs. Moreover, not only humans can act differently. Unexpected events may happen, such as a change of weather, road blockages due to road work, and accidents. Traffic controllers should not lose performance when these unexpected events occur. Furthermore, traffic-responsive controllers can make wrong control decisions, because there can be an unknown measurement error. Model-based strategies make use of a traffic model, and this model may represent the reality with an error. Hence, there can be a wide range of uncertainties when controlling traffic.

#### Uncertainty in the demand

Most of the controllers mentioned in Section 2-2 all assume that future predictions of the demand are perfectly known based on historical data and/or current measurement. The use of nominal demand is a reasonable choice, however it is only an approximation of the demand. Clearly, from the nature of traffic it is obvious that in practice fluctuations and unpredictable events are always present.

#### Measurement uncertainty

The traffic-responsive controllers mentioned in Section 2-2 measure the traffic state to make the next control decision. The measurements are commonly made with the use of induction loops or cameras. These sensors can fail, which can result in inappropriate control decisions. These sensors can also have a standard error, because they are not accurate enough.

#### Model uncertainty: Dynamic and Parametric

The model-based controllers discussed in Section 2-2-3 make use of traffic models. In these model-based approaches an optimization procedure is performed based on the predictions of the traffic model. Inaccurate predictions can be made due to a mismatch between the traffic model and the reality.

In model-based approaches the computational complexity of the controllers is one of the main drawbacks. According to Lin et al. (2011) one of the proposed solutions to the computational

complexity is the simplification of the prediction model. A less detailed prediction model should take less computation time to solve than a more detailed model. For instance, aggregated traffic flows can be used in a traffic model. The aggregated traffic flow models deliberately omit some details for the sake of simplicity. Hence, the controllers that use these traffic models choose to have some uncertainty.

The uncertainty due to modeling can be distinguished into dynamic uncertainty and parameter uncertainty. Dynamic uncertainty is uncertainty in the model, that is caused by a difference between the dynamics of the model and the dynamics of the to be controlled process. For instance, some (unknown) non-linear dynamics of the process may be too complicated to model. These dynamics can be omitted by introducing an uncertainty term in the model. Hence, the model becomes an approximation of the process, and therefore there can be uncertainty in the dynamics of the model.

Parameter uncertainty is uncertainty in (some) parameters of the model. When modeling traffic, it is mainly assumed that traffic parameters (e.g. saturation flow and turn ratios) are known and constant. Most of the time these parameters are based on historical data. Therefore, such traffic parameters are an approximation of their real values. Hence, there can be uncertainty in the parameters of the traffic model.

It can be argued whether these uncertainties have a considerable impact on the performance of the controllers. No research has yet been performed on the impact of these uncertainties on the performance.

## Unexpected events

Network flows are influenced by abnormal events that affect the network characteristics and capacity. Traffic networks should be designed to cope with normal fluctuations by allowing alternative routes, but accounting for abnormal events is much more difficult. The potential sources of disruption to transportation networks are numerous, ranging from natural to man-made disasters (e.g. earthquakes, flood, landslides, terrorist attacks, and major accidents). There are also more regular disruptions due to bridge openings, public transport, and emergency transport with priority. The scale, impact, frequency, and predictability of such events vary enormously. The impact of these abnormal events is yet unclear. In order for a controller to handle these abnormal events, the uncertainty has to be described in a mathematical form. There is not yet been any extensive research on the consequences of abnormal events with respect to traffic control.

### 2-3-2 Robust control theory

In the previous section different types of uncertainty were discussed. The main goal of robust control theory is to take these uncertainties into account when designing a controller. Three different conventional robust control strategies are discussed in this section. To assess whether the robust control strategies are suitable for the design of an urban traffic controller, the control strategies in this section are discussed with respect to the following points: 1. Type of uncertainty it accounts for; 2. Real-time feasibility; 3. The use of prediction.

## LQG control

The Linear Quadratic Gaussian (LQG) control problem (see e.g. Anderson and Moore (1990)) tries to find an optimal feedback law for an uncertain linear system that is perturbed by additive Gaussian white noise. The Gaussian white noise is added as a state and output disturbance. The optimal feedback law is found by minimizing a quadratic cost function. The LQG control strategy only makes use of static state feedback control; hence the controller will not be computationally demanding. Furthermore, according to Skogestad and Postlethwaite (2005) the LQG controller has good stability and robustness properties for a Single Input Single Output (SISO) system subjected to white noise. However, the controller does not necessarily provide these properties for a Multiple Input Multiple Output (MIMO) system. A drawback of this approach is that uncertainty cannot always be properly represented by white noise. Furthermore, not all types of uncertainties can be described through a combination of state and output disturbances.

## $H_\infty$ control

In  $H_\infty$  control (see e.g. Skogestad and Postlethwaite (2005)) uncertainty is described in a different way than the uncertainty description of LQG control. In the  $H_\infty$  control problem uncertainty is captured in a matrix of stable perturbations (e.g. by defining a minimum and maximum value for the uncertainty). The  $H_\infty$  control problem tries to minimize the impact of disturbances on the output of a Linear Time Invariant (LTI) system. It does so by finding a feedback controller that minimizes the  $H_\infty$  norm of the transfer function from the disturbance to the output. The resulting feedback controller is not computationally demanding, although the derivation of the gains of the feedback controller can be computationally demanding.  $H_\infty$  control is a control method designed for continuous-time systems, but there exist methods to use it for discrete-time systems as well as shown in Stoorvogel (2000). However, the  $H_\infty$  control problem becomes difficult to solve for discrete-time systems, and analysis and synthesis of the robustness properties becomes hard.

## Robust MPC

The framework of a robust MPC controller is the same as the framework of a nominal MPC controller. However, a robust MPC controller explicitly accounts for uncertainty. Bemporad and Morari (1999) show that different descriptions of uncertainty are used in the literature, which are mainly time domain representations. With robust MPC there can be useful descriptions of measurement and model uncertainty. In both types of uncertainty the actual value is given by a known set of values or plants. According to Xie and Li (2007) the robust MPC can take these uncertainties into account by: (1) using the Min-Max approach, which takes into account the boundaries of uncertainty (e.g. the worst-case scenario) and (2) a chance constrained approach, in which uncertain variables are described as stochastic variables with known probability distribution functions.

According to Bemporad and Morari (1999) the robust analysis of an MPC control strategy is much more difficult than its synthesis. Already in the nominal case, it is nearly impossible to analyze the stability of a closed loop MIMO system with multiple constraints. However, this is possible for the linear case. The synthesis of a robust MPC control strategy can be done

in various ways, but every method will yield extra calculations. Hence, robust MPC will be more computationally demanding than nominal MPC.

### **2-3-3 Robust urban traffic control**

In literature different strategies have been proposed to account for uncertainty in urban traffic controller design. This section provides some of the different types of robust urban traffic control strategies. The strategies can be divided into robust fixed-time control strategies, robust traffic-responsive control strategies, and robust model-base strategies.

#### **Robust fixed-time control**

Robust fixed-time control involves off-line optimization of the cycle time, the split, and the off-set between nearby intersections. The off-line optimization takes the variability of e.g. the demand into account. Therefore, the performance should deteriorate less when this variability is present compared to a fixed-time controller where the variability is not taken into account. Heydecker (1987) shows that if the degree of variability of the demand is significant, optimizing signal plans - with respect to the average demand - may cause additional delays, whereas algorithms that take this variability into account do not have these additional delays. However, the use of the average demand in traffic control will only lead to small losses in average performance when the degree of variability is low.

In Yin (2008) three different approaches are discussed for determining robust optimal signal timings, which minimize the mean of delays per vehicle under (day-to-day) varying demand as well as maintain a stable performance under this varying demand. The major problem for these strategies is that they are optimal for a certain nominal demand, just like nominal fixed-time controllers are. Yin (2008) shows that when the nominal demand shifts, the robust fixed-time controllers are not optimal anymore, although they lose less performance compared to the nominal fixed-time controllers.

#### **Stochastic traffic-responsive control**

Ukkusuri et al. (2010) propose a robust signal control strategy where the future demand is assumed to be uncertain. The uncertain demand is defined by a set demand realizations where each demand has its own probability. Ukkusuri et al. (2010) conclude that introducing uncertainty in the demand has a significant effect on the performance measure. The impact of uncertainty in the demand on the network performance is underestimated when only a nominal demand is used during optimization of the signal timings. The computational complexity of the proposed control method can become a problem, when applied to larger traffic networks. Furthermore, 30 scenarios is the maximum amount of scenarios that could be implemented, due to computational limits. There is no conclusive evidence on the optimal number of scenarios for robust signal design.

#### **Robust traffic-responsive control**

In Tettamanti et al. (2014) a store-and-forward traffic model is extended with a norm-bounded demand and queue uncertainty. The objective function is minimized by finding the optimal

green time sequence for the worst prediction scenario. The worst prediction scenario can be found e.g. by the use of historical data. The same objective function is used as with the TUC strategy. The algorithm works only in saturated and over-saturated conditions, the under-saturated condition is not investigated.

According to Tettamanti et al. (2014) the minimax approach in an MPC framework proposed by Löfberg (2003) is certainly one of the most efficient techniques to deal with the uncertainty problem. A drawback of this method is that the computation time increases exponentially if the size of the network or the prediction horizon increases linearly. Therefore, the problem statement is relaxed into a convex minimization problem and reformulated in a form of linear matrix inequalities. However, in order to obtain this form it is assumed that the uncertainty is unknown but bounded. According to El Ghaoui et al. (1998) these problems can be solved in polynomial time with e.g. primal-dual interior-point methods.

The performance of the robust MPC controller relative to a nominal MPC controller becomes better with more congested and more varying traffic. However, in the situation when there is no uncertainty in the demand, the performance of the robust MPC controller becomes worse compared to the nominal MPC controller, particularly under congested and varying traffic conditions. Hence, this confirms the sensitivity of the robust performance with respect to the estimation of the uncertainty. The robust solution may have worse performance compared to the nominal case if there is no uncertainty in the traffic (e.g. perfect nominal and known conditions).

For the robust MPC controller there is no straightforward improvement of the performance by increasing the prediction horizon, due the uncertainty which leads to uncertain predictions. These uncertain predictions lead to conservatively chosen green times.

## 2-4 Discussions and Conclusions

Literature on traffic controllers has been studied to obtain insight in robust urban traffic control, to form the basis for the remainder of this MSc thesis project. The goal of this MSc thesis to design an urban traffic controller that is able to improve network throughput in all traffic regimes, while remaining real-time feasible and being subjected to uncertainty.

One of the design requirements of an urban traffic controller is to improve network throughput in all traffic regimes. Not every considered nominal urban traffic controller is able to improve the network throughput in all traffic regimes. Some of the model-based control strategies are able to improve network throughput in all traffic regimes. This is due to their ability to predict the future traffic dynamics. However, the main drawback of model-based strategies is their real-time (in)feasibility. By omitting some detail in the traffic model, some model-based approaches (e.g. the approach of Van de Weg et al. (2016a)) are able to become real-time feasible while maintaining a reasonable performance. Although the control strategy proposed by Van de Weg et al. (2016a) shows promising results in terms of performance and computation time, it still needs several assumptions to achieve this performance. Van de Weg et al. (2016a) assume, for instance, that the turn fractions and the demand are known, which may not be the case when the control strategy is implemented in practice.

All discussed nominal urban traffic controllers - except for the model-based approaches - are able to determine their signal timings within the real-time sampling time. Therefore, they are

real-time feasible. However, they are not able to improve throughput in all traffic regimes, which makes them less suitable for the remainder of this research.

In literature there is little research to find on the sensitivity to uncertainty of the considered nominal urban traffic controllers. The only discussed method that is tested with respect to the impact of a specific uncertainty or disturbance is TUC. TUC showed low sensitivity to measurement disturbances according to Diakaki et al. (2003). Despite that, it remains hard to conclude whether the performance of traffic controllers does deteriorate in presence of uncertainty compared to the ideal case. Hence, further investigation should be needed.

It can be agreed that there are a lot different uncertainties in traffic, and therefore it is tried to categorize the uncertainties. However, not all events in traffic may be categorized in a single category of uncertainty. There is not yet been any extensive research on what the impact will be of such an event on the performance of urban traffic controllers.

The presented robust controllers were assessed on three characteristics, the results of the assessment are shown in Table 2-1. Both LQG and  $H_\infty$  control show promising results in terms of computation time. However, both control methods are based on feedback control, and therefore these methods are unable to anticipate on future estimated or predicted disturbances (e.g. the demand). Hence, this makes LQG and  $H_\infty$  control less suitable for the remainder of this research. Robust MPC is able to predict, and is very flexible in terms of choosing different types of uncertainties to account for. However, Robust MPC requires more computations than nominal MPC. This is due to the incorporation of the uncertainty. The computation time is already the main problem of MPC strategies in urban traffic control. Hence, it probably will become more of a problem when robust MPC is used for urban traffic control.

	LQG	$H_\infty$	RMPC
Type of uncertainty		X	X
Computation time	X	X	
Predictive			X

**Table 2-1:** Overview of the requirements for urban traffic control fulfilled by a robust control strategy.

Some of the considered robust urban traffic control strategies show an improvement of the network throughput, while subjected to uncertainty (e.g. in the demand or queue length). However, there still exist several open issues in the field of robust urban traffic control. It is yet unclear what the impact of some uncertainties is on the controllers' performance. Furthermore, the question remains whether the design of a robust urban traffic controller is really necessary. Although, Ukkusuri et al. (2010) and Tettamanti et al. (2014) show that in their particular case it can be relevant to account for uncertainty in traffic controller design. Even though accounting for uncertainty is relevant for urban traffic control, it still remains the question what the optimal way is to account for uncertainty in urban traffic.

The control strategy that will be developed will be based on the linear MPC controller proposed by Van de Weg et al. (2016a). The reason for this is that the controller of Van de Weg et al. (2016a) is real-time feasible and has promising performance in each traffic regime. However, there are also some challenges. Several assumptions are made, which may be relaxed by introducing an uncertainty or disturbance. There are two ways for the controller of Van de

Weg et al. (2016a) to account for uncertainty: (1) using existing robust MPC strategies, and (2) redefining the optimization problem. It is expected that the first option may yield a real-time infeasible controller. Therefore, in this thesis the second option is used to develop a robust urban traffic controller. Note that the definition of robust may not be applicable to this controller anymore.

# The design of the robust urban traffic controller

In this chapter the design of the urban traffic controller is explained. The urban traffic controller tries to optimize throughput in all traffic regimes while remaining real-time feasible and being subjected to uncertainty. The controller is based on the linear Model Predictive Control (MPC) controller of Van de Weg et al. (2016a). First, there is a brief introduction on MPC. After that, the assumptions are introduced. Subsequently, the linear MPC strategy will be elaborated in Section 3-2. In Section 3-3 the main potential sources of uncertainty for the linear MPC strategy are discussed. Subsequently, the redefinition of the optimization problem is proposed in Section 3-4. Finally, this chapter will be concluded in Section 3-5.

### 3-1 Introduction

In the literature survey it is discussed that accounting for uncertainty in urban traffic controller design can be beneficial for the performance. It is also discussed that using MPC in urban traffic control can lead to a controller that optimizes throughput in all traffic regimes while remaining real-time feasible. In this chapter it is tried to integrate these two observations into a new urban traffic controller.

The second observation is already established by the controller proposed by Van de Weg et al. (2016a). It does so by using an aggregated traffic flow model with constant free-flow speed and constant shock wave speed as prediction model. Therefore, the optimization problem becomes a Linear Programming (LP) problem. As a result, the controller is real-time feasible. Hence, the integration with the first observation should also lead to an LP problem. Then the resulting controller is more likely to be real-time feasible.

It is expected that uncertainty has a more negative effect on the throughput of the traffic network in the over-saturated traffic regime than in the under-saturated or saturated regime. In the over-saturated traffic regime there is spill-back, which causes a direct interaction between

intersections. The direct interaction between intersections can cause the uncertainty, which is present at one intersection, to influence neighboring intersections. In the under-saturated and saturated traffic regime there is no spill-back, thus a less direct interaction. Hence, spill-back should be avoided when uncertainty is present.

Thus, the main idea of the approach that is described in this chapter is to avoid the phenomenon of spill-back. It does so by penalizing the number of vehicles on the links of the traffic network. It is expected that this approach yields a more conservative control signal, and realizes better throughput when uncertainty is present in the over-saturated traffic regime.

Note that this work is an extension of the work Van de Weg et al. (2016a) and for completeness some of it is repeated in this chapter. Throughout the chapter it will be indicated what is the extension and what is the work of Van de Weg et al. (2016a). In particular, the theory in Section B-2 and Section 3-2 is repeated from the original linear MPC strategy of Van de Weg et al. (2016a).

### 3-1-1 MPC

The concept of MPC can be exploited in urban traffic control, because using MPC can lead to a controller that optimizes throughput in all traffic regimes while remaining real-time feasible. In this section the framework of an MPC strategy is briefly explained.

The MPC control strategy repeatedly uses a prediction model to optimize the future control actions over a finite time horizon and only implements the first control action. The framework of an MPC controller can be seen in Figure 3-1 and the control process consists of three parts:

1. *Prediction model.* On the basis of a model a prediction of the future evolution of the state is made, which is based on: the current measured state, the predicted future disturbance, and the future control inputs. The prediction is made over a certain time horizon. The predicted state evolution is then used to evaluate the objective function and find the optimal control signal for the future performance by means of optimization.
2. *Optimization.* An optimization algorithm will be applied to compute an optimal control signal that minimizes the performance index over a finite horizon subject to the given constraints. There can be constraints on the control, state, and output signals, motivated by e.g. safety and environmental reasons.
3. *Rolling horizon principle.* When the optimal control input is derived, only the first sample of the control sequence  $u^*(k)$  is implemented. Subsequently, in the next time step the whole procedure is repeated.

### 3-1-2 Assumptions

In the previous section the concept of MPC is briefly explained. Both the controller of Van de Weg et al. (2016a) and the proposed controller with penalty make use of MPC. Furthermore, they also have some of their assumptions in common. The following assumptions, which are based on the work Van de Weg et al. (2016a), are made for both control methods:

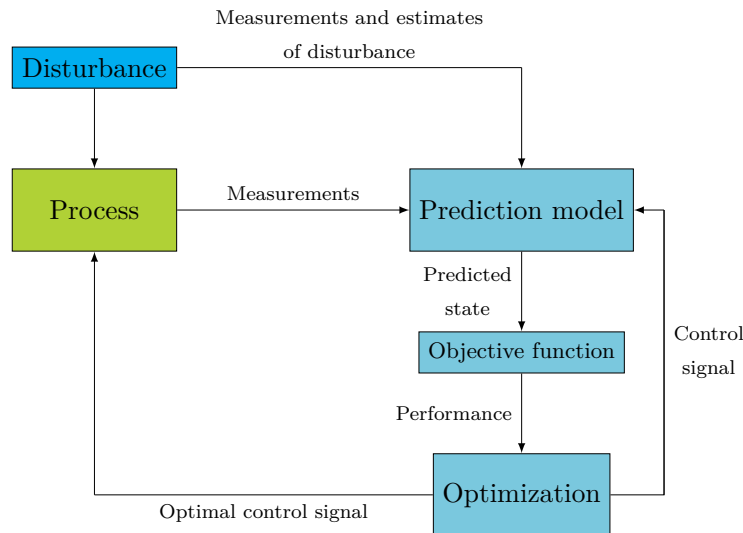


Figure 3-1: Framework MPC controller.

- **Aggregated traffic dynamics** are considered by choosing a sampling time of 10 seconds instead of a sampling time of 1 second. Hereby, the number of time steps for the prediction of traffic dynamics is decreased. Hence, the computation time for the same prediction horizon will be lower for a sampling time of 10 seconds compared to a sampling time of 1 second, because less computations have to be performed.
- **Signal plans** are not considered by the linear MPC strategy, which simplifies the optimization problem. Furthermore, other properties of signal plans, such as minimum green times and maximum red times are not included.
- **Turn fractions** are assumed to be known and constant.
- **Demand and outflow constraints** are assumed to be known with no disturbances or uncertainties.
- **Network parameters**, such as saturation flows, free-flow speeds, shock wave speeds, and maximum link densities are known.
- **Measurements** of the cumulative inflows and outflows are assumed to be available with no errors.

In this thesis the control methods are considered in discrete time. The time step  $k$   $[-]$  and process model sampling time  $T$   $[s]$  refer to the time period  $[Tk, T(k+1))$   $[s]$ . The sampling time of the measurements is assumed to be equal to  $T$ . The prediction model has a time step  $k^c$   $[-]$  and sampling time  $T^c$   $[s]$ , where it holds that  $T^c = \epsilon^c T$  with the factor  $\epsilon^c \in \mathbb{Z}^+$ .

## 3-2 Current control framework

Now the framework of MPC and the assumptions of the linear MPC strategy of Van de Weg et al. (2016a) are described. This section describes how Van de Weg et al. (2016a)

fill in the different parts of their linear MPC strategy: the prediction model and the linear optimization problem formulation. First, the prediction model (Link Transmission Model (LTM)) is explained in Section 3-2-1. Subsequently, in Section 3-2-2 the linear optimization problem is formulated. For completeness it must be noted that the theory of this section is repeated from the work of Van de Weg et al. (2016a).

### 3-2-1 Prediction model: the LTM

The linear MPC strategy that is developed by Van de Weg et al. (2016a) uses the LTM of Yperman (2007) as the prediction model. The LTM is capable of modeling all three traffic regimes. It models free-flow dynamics, saturated dynamics, and shock wave dynamics. The LTM has two more advantages: (1) it can describe the traffic state with only two states, and (2) Van de Weg et al. (2016a) show that it can be used in a linear MPC strategy. From the LTM three elements are used: nodes, links, and origins. All three elements are illustrated in Figure 3-2. As can be seen at link 3 in the figure, there is the possibility to constrain the outflow at exits of the network.

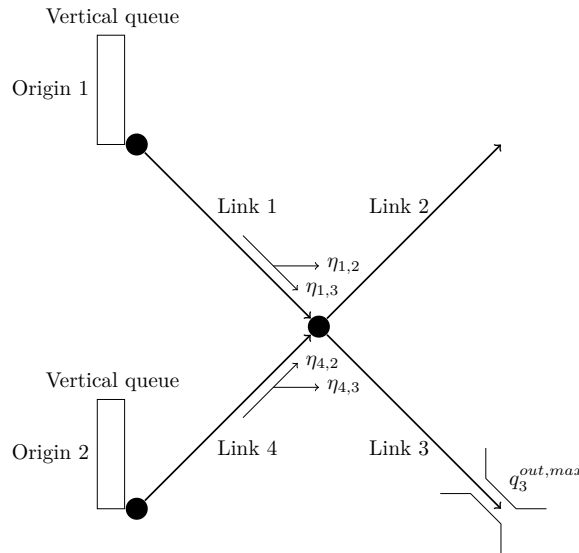


**Figure 3-2:** Network elements of the LTM

### Introduction to LTM

The LTM of Yperman (2007) describes the link dynamics via 2 traffic states: the cumulative inflow  $N_i^{\text{in}}(k^c)$  [veh] and cumulative outflow  $N_i^{\text{out}}(k^c)$  [veh] of every link  $i$  [-] in the network at discrete-time step  $k^c$  [-]. The LTM has two main advantages compared to models that divide the link into segments (e.g. the Cell Transmission Model (CTM)):

- the LTM requires less states than e.g. the CTM. Segment-based approaches divide the link into segments, which requires more traffic states to describe the link dynamics than when the link is considered as one segment;

- The numerical stability of segment-based approaches requires a smaller time step than e.g. the LTM due to the Courant-Friedrichs-Lewy (CFL) condition. The segments of segment-based approaches are usually smaller than with the LTM. Therefore, the simulation often needs to have a smaller time step than the LTM. Hence, the longer the computations will take.

The following assumptions are made for the LTM:

1. the free-flow speed  $v_i^{\text{free}}$  [km/h] for every link  $i$  is known and constant;
2. a vehicle cannot exit the link  $i$  before the time  $t_i^{\text{free}}$  [h] that it requires to travel through link  $i$  with  $v_i^{\text{free}}$  [km/h];
3. in the saturated traffic regime, the link outflow is equal to the saturation outflow  $q_i^{\text{sat}}$  [veh/h], which is known and constant;
4. the shock wave speed  $v_i^{\text{shock}}$  [km/h] for every link  $i$  is known and constant.

Figure 3-3 illustrates the cumulative inflow and outflow of a link with the corresponding vehicle trajectories in the time-space diagram. The vehicles travel from the bottom to the top of the time-space diagram. Through Figure 3-3 the assumptions of the LTM will be explained in more detail. Assumptions 1 and 2 are illustrated by the trajectory of vehicle 6. Assumption 4 can also be seen in Figure 3-3, where the shock wave starts when vehicle 7 exits the link. Subsequently, vehicle 13 can only enter the link after the shock wave travel time  $t_i^{\text{shock}}$  [h]. Hence, it can be concluded that the maximum link outflow depends on the link inflow in the past, due to the first two assumptions. Assumption 4 implies that the maximum link inflow depends on the outflow of the link in the past. The next section will use these observations to formulate the LTM into linear state equations and constraints.

### Linear state equations of the LTM

The dynamics of the LTM are modeled using linear state equations of the cumulative curves and linear constraints. This is possible due to the use of effective fractions of green time. The control variables are the effective fractions of green time  $b_i^{\text{L,eff}}(k^c)$  [-] and  $b_j^{\text{O,eff}}(k^c)$  [-], respectively for every link  $i$  and for every origin  $j$ . The effective fraction of green time for a link is defined as the realized link outflow  $q_i^{\text{realized}}(k^c)$  [veh/h] divided by the link saturation flow:

$$b_i^{\text{L,eff}}(k^c) = \frac{q_i^{\text{realized}}(k^c)}{q_i^{\text{sat}}}. \quad (3-1)$$

The cumulative outflow of link  $i$  is updated as follows:

$$N_i^{\text{L,out}}(k^c + 1) = N_i^{\text{L,out}}(k^c) + b_i^{\text{L,eff}}(k^c) q_i^{\text{sat}} T^c, \quad (3-2)$$

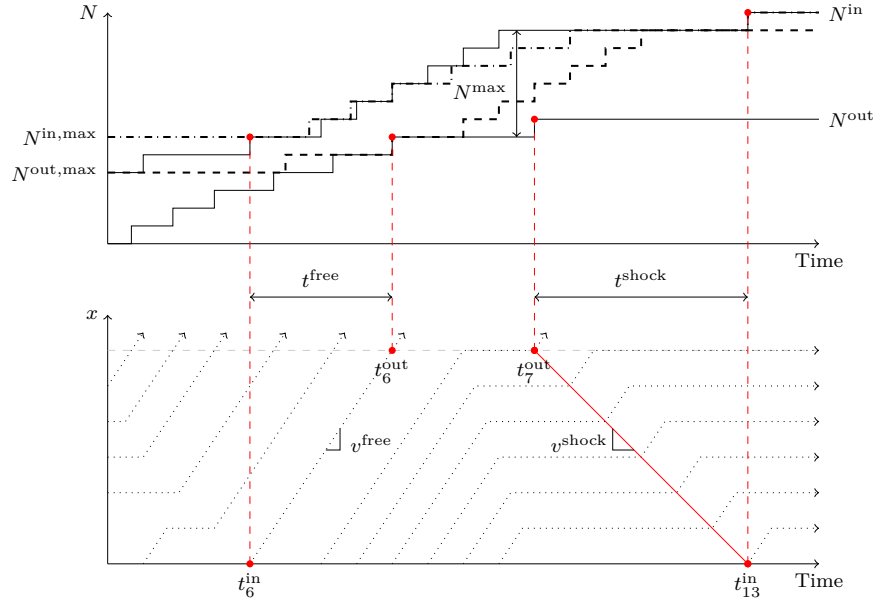


**Figure 3-3:** Time-space diagram (bottom) and plot of the cumulative curves (top).

where  $b_i^{L,\text{eff}}(k^c)$  is used to limit the outflow when there is no queue. Furthermore, the free-flow dynamics can be modeled using the following inequality constraint:

$$N_i^{L,\text{out}}(k^c + 1) \leq \gamma_i^{c,\text{fr}} N_i^{L,\text{in}}(k^c - k_i^{c,\text{free}} + 2) + (1 - \gamma_i^{c,\text{fr}}) N_i^{L,\text{in}}(k^c - k_i^{c,\text{free}} + 1), \quad (3-3)$$

where  $k_i^{c,\text{free}} = \lceil t_i^{\text{free}}/T^c \rceil [-]$  is the discrete free-flow travel time, and the fraction  $\gamma_i^{c,\text{fr}} = k_i^{c,\text{free}} - t_i^{\text{free}}/T^c [-]$  the residual of a sampling time step that the free-flow travel time is exceeded by  $k_i^{c,\text{free}}$ . The mathematical operator  $\lceil \cdot \rceil$  rounds the argument to the next larger integer. This constraint causes the cumulative outflow curve to lie below the cumulative inflow curve shifted by the free-flow travel time. The cumulative inflow curve shifted by the free-flow travel time is illustrated the dashed line in the cumulative curves plot of Figure 3-3. Note that  $k_i^{c,\text{free}} \geq 2$  to guarantee CFL conditions.

The maximum outflow of a link is modeled as an external process disturbance. Therefore, a (temporal) bottleneck can be included in the framework. To implement a bottleneck at an exit link of the network, the outflow of that link is constrained by the maximum outflow  $q_i^{\text{out,max}}(k^c)$  [veh/h]:

$$b_i^{L,\text{eff}}(k^c) q_i^{\text{sat}} \leq q_i^{\text{out,max}}(k^c) \quad \forall i \in I^{\text{Exit}}, \quad (3-4)$$

where  $I^{\text{Exit}}$  is the set of exits links. The cumulative inflow of link  $i$  is updated as follows:

$$\begin{aligned}
N_i^{L,\text{in}}(k^c + 1) = & N_i^{L,\text{in}}(k^c) + \sum_{i^{\text{us}} \in I_i^{\text{in}}} \left( \eta_{i^{\text{us}},i}(k^c) b_i^{L,\text{eff}}(k^c) q_i^{\text{sat}} T^c \right) \\
& + \sum_{j \in J_i^{\text{in}}} \left( \eta_{j,i}(k^c) b_j^{O,\text{eff}}(k^c) q_j^{\text{sat}} T^c \right),
\end{aligned} \tag{3-5}$$

where  $I_i^{\text{in}}$  is the set of all links directly upstream of link  $i$  and  $J_i^{\text{in}}$  is the set of all origins directly upstream of link  $i$ . The turn fraction from link  $i^{\text{us}}$  to  $i$  is indicated by  $\eta_{i^{\text{us}},i}(k^c)$  [-], and the turn fraction from origin  $j$  to link  $i$  is indicated by  $\eta_{j,i}(k^c)$  [-]. The shock wave dynamics are included by a constraint on the cumulative inflow of link  $i$ :

$$\begin{aligned}
N_i^{L,\text{in}}(k^c + 1) \leq & \gamma_i^{c,\text{sh}} N_i^{L,\text{out}}(k^c - k_i^{\text{shock}} + 2) \\
& + (1 - \gamma_i^{c,\text{sh}}) N_i^{L,\text{out}}(k^c - k_i^{\text{shock}} + 1) + N_i^{\text{max}},
\end{aligned} \tag{3-6}$$

where  $k_i^{c,\text{shock}} = \lceil t_i^{\text{shock}} / T^c \rceil$  [-] is the discrete shock wave time, and the fraction  $\gamma_i^{c,\text{sh}} = k_i^{c,\text{shock}} - t_i^{\text{shock}} / T^c$  [-] the residual of a sampling time step that the shock wave time is exceeded by  $k_i^{c,\text{shock}}$ . This constraint causes the cumulative inflow curve to lie below the cumulative outflow curve shifted by the shock wave travel time. The cumulative outflow curve shifted by the shock wave travel time is illustrated the dotted line in the cumulative curves plot of Figure 3-3. Note that  $k_i^{c,\text{shock}} \geq 2$  to guarantee CFL conditions. The origins are modeled using a vertical queue model. In a vertical queue model the queue occupies no space. The cumulative outflow of origin  $j$  is updated as follows:

$$N_j^{O,\text{out}}(k^c + 1) = N_j^{O,\text{out}}(k^c) + b_j^{O,\text{eff}}(k^c) q_j^{\text{sat}} T^c, \tag{3-7}$$

which is bounded by:

$$N_j^{O,\text{out}}(k^c + 1) \leq N_j^{O,\text{in}}(k^c + 1), \tag{3-8}$$

where is  $N_j^{O,\text{in}}(k^c + 1)$  is the cumulative inflow of origin  $j$  and is updated as follows:

$$N_j^{O,\text{in}}(k^c + 1) = N_j^{O,\text{in}}(k^c) + q_j^{\text{in}}(k^c) T^c. \tag{3-9}$$

The control variables  $b_i^{L,\text{eff}}(k^c)$  [-] and  $b_j^{O,\text{eff}}(k^c)$  [-] should be constrained to represent splits:

$$0 \leq b_i^{L,\text{eff}}(k^c) \leq 1, \tag{3-10}$$

$$0 \leq b_j^{O,\text{eff}}(k^c) \leq 1, \tag{3-11}$$

$$\sum_{i \in I_y^{\text{conflict}}} b_i^{L,\text{eff}}(k^c) \leq 1, \tag{3-12}$$

where  $I_y^{\text{conflict}}$  is the set of signals which are in conflict with each other. The first two constraints cause the effective fractions of green times to vary between 0 and 1. The third constraint causes the sum of effective fractions of green times of each intersection to be equal or less than 0. Hence, the effective green times are distributed over the conflicting links.

### 3-2-2 Linear optimization problem formulation

The linear MPC strategy tries to maximize the network throughput over the prediction horizon  $K_p T^c$  [s]. Maximizing the network throughput is realized by minimizing the Total Time Spent (TTS) of the network, while it is assumed that the network inflow is not affected by the control actions. The TTS of the network is minimized by optimizing the effective green times used by the traffic streams in the network. This optimization problem can be formulated into an LP problem. In order to do so, the linear dynamic traffic equations of the previous section have to be rewritten into state space form:

$$x(k^c + 1) = Ax(k^c) + B(k^c)u(k^c) + Cd(k^c), \quad (3-13)$$

where the state  $x(k^c) \in \mathbb{R}^{n^{\text{states}} \times 1}$  given by:

$$x(k^c) = \left[ \left( x_1^L(k^c) \right)^\top \quad \dots \quad \left( x_{n^L}^L(k^c) \right)^\top \quad \left( x_1^O(k^c) \right)^\top \quad \dots \quad \left( x_{n^O}^O(k^c) \right)^\top \right]^\top, \quad (3-14)$$

and where the state  $x_i^L(k^c) \in \mathbb{R}^{n_i^{L,s} \times 1}$  of link  $i$  has the following structure:

$$x_i^{c,L}(k^c) = \left[ N_i^{L,\text{out}}(k^c) \quad \dots \quad N_i^{L,\text{out}}(k^c - k_i^{c,\text{shock}}) \quad N_i^{L,\text{in}}(k^c) \quad \dots \quad N_i^{L,\text{in}}(k^c - k_i^{c,\text{free}}) \right]^\top. \quad (3-15)$$

The number  $n_i^{L,s} = k_i^{c,\text{shock}} + k_i^{c,\text{free}} + 2$  denotes the length of the vector. Similar to the state of each link  $i$ , the state  $x_j^{c,O}(k^c) \in \mathbb{R}^{n_j^{O,s} \times 1}$  of an origin  $j$  has the following structure:

$$x_j^{c,O}(k^c) = \left[ N_j^{O,\text{out}}(k^c) \quad N_j^{O,\text{in}}(k^c) \right]^\top. \quad (3-16)$$

The number  $n_j^{O,s} = 2$  denotes the length of this vector, and the number  $n^{\text{states}} = \sum_{i \in i^L} n_i^{L,s} +$

$\sum_{j \in j^O} n_j^{O,s}$  denotes the length of the state vector  $x(k^c)$ .

The input vector  $u(k^c) \in \mathbb{R}^{n^{\text{inputs}} \times 1}$  is given by:

$$u(k^c) = \left[ b_1^{L,\text{eff}}(k^c) \quad \dots \quad b_{n^L}^{L,\text{eff}}(k^c) \quad b_1^{O,\text{eff}}(k^c) \quad \dots \quad b_{n^O}^{O,\text{eff}}(k^c) \right]^\top, \quad (3-17)$$

where  $n^{\text{inputs}} = n^L + n^O$  is the number of inputs. Finally, the disturbance vector  $d(k^c) \in \mathbb{R}^{n^O \times 1}$  is given by:

$$d(k^c) = \left[ q_1^{\text{in}}(k^c) \quad \cdots \quad q_{n^O}^{\text{in}}(k^c) \right]^\top. \quad (3-18)$$

The objective function of the linear MPC strategy is:

$$J(x) = \sum_{k_0=k^c}^{k^c+K_p} T^c \left\{ \sum_{i \in I^L} \left( N_i^{L,\text{in}}(k^c) - N_i^{L,\text{out}}(k^c) \right) + \sum_{j \in I^O} \left( N_j^{O,\text{in}}(k^c) - N_j^{O,\text{out}}(k^c) \right) \right\}. \quad (3-19)$$

The minimization of the objective function with respect to  $x$  can be formulated as an LP problem of the following form:

$$\begin{aligned} \min_{\bar{u}(k^c)} \quad & Z \tilde{B} \bar{u}(k^c) + Z(\tilde{A}x(k^c) + \tilde{C} \bar{d}(k^c)) \\ \text{s.t.} \quad & M^{\text{ineq}} \bar{u}(k^c) \leq V^{\text{ineq}}, \end{aligned} \quad (3-20)$$

where the vector  $\bar{u}(k^c)$  contains all the inputs that should be optimized, and the vector  $\bar{d}(k^c)$  contains the prediction of the demand over the prediction horizon. The vector  $Z \in \mathbb{R}^{1 \times K_p n^{\text{states}}}$  is used to compute the value of the objective function by multiplication with the future predicted state. The matrix  $\tilde{B}(k^c)$ , initial state matrix  $\tilde{A}(k^c)$ , and initial disturbance matrix  $\tilde{C}(k_0^c)$  are used to compute the prediction of the states  $\bar{x}(k^c)$ . The matrix  $M^{\text{ineq}}$  and the vector  $V^{\text{ineq}}$  contain the inequality constraints of the optimization problem e.g. (3-3), and (3-6).

The state  $x(k^c + n)$  for an arbitrary time step  $k^c + n$  is given by:

$$x(k^c + n) = A^n x(k^c) + \sum_{i=1}^n A^{n-1} (B(k^c + i - 1)u(k^c + i - 1) + Cd(k^c + i - 1)). \quad (3-21)$$

The vector  $\bar{u}(k^c) \in \mathbb{R}^{n^{\text{in,tot}} \times 1}$  – with  $n^{\text{in,tot}} = K_p(n^L + n^O)$  – is defined as:

$$\bar{u}(k^c) = \left[ \left( u(k_0^c) \right)^\top \quad \cdots \quad \left( u(k_0^c + K_p - 1) \right)^\top \right]^\top, \quad (3-22)$$

and the vector  $\bar{d}(k^c) \in \mathbb{R}^{K_p n^O \times 1}$  is defined as:

$$\bar{d}(k^c) = \left[ \left( d(k_0^c) \right)^\top \quad \cdots \quad \left( d(k_0^c + K_p - 1) \right)^\top \right]^\top. \quad (3-23)$$

By defining the matrix  $\tilde{A} \in \mathbb{R}^{n^{\text{states}} K_p \times n^{\text{states}}}$  as:

$$\tilde{A} = \begin{bmatrix} A & A^2 & \cdots & A^{K_p} \end{bmatrix}^\top, \quad (3-24)$$

and the matrix  $\tilde{B}(k^c) \in \mathbb{R}^{n^{\text{states}} K_p \times n^{\text{in,tot}}}$  as:

$$\tilde{B}(k^c) = \begin{bmatrix} B(k^c) & 0 & \cdots & 0 \\ AB(k^c) & B(k^c + 1) & \cdots & 0 \\ \vdots & \vdots & \ddots & \vdots \\ A^{K_p-1}B(k^c) & A^{K_p-2}B(k^c + 1) & \cdots & B(k^c + K_p - 1) \end{bmatrix}, \quad (3-25)$$

and the matrix  $\tilde{C} \in \mathbb{R}^{n^{\text{states}} K_p \times K_p n^o}$  as:

$$\tilde{C} = \begin{bmatrix} C & 0 & \cdots & 0 \\ AC & C & \cdots & 0 \\ \vdots & \vdots & \ddots & \vdots \\ A^{K_p-1}C & A^{K_p-2}C & \cdots & C \end{bmatrix}, \quad (3-26)$$

a prediction of the evolution of the states is given by the following linear equation:

$$\bar{x}(k^c) = \tilde{A}x(k_0^c) + \tilde{B}\bar{u}(k^c) + \tilde{C}\bar{d}(k^c), \quad (3-27)$$

with the vector  $\bar{x}(k^c) \in \mathbb{R}^{K_p n^{\text{states}} \times 1}$  containing the extended traffic states at every time step  $x(k^c + n)$  from time step  $k_0^c$  to  $k_0^c + K_p$  defined as:

$$\bar{x}(k^c) = \left[ \left( x(k_0^c + 1) \right)^\top \cdots \left( x(k_0^c + K_p) \right)^\top \right]^\top. \quad (3-28)$$

### Linear inequality constraints

All the constraints of the optimization problem in (3-20) are included in the matrix  $M^{\text{ineq}}$  and vector  $V^{\text{ineq}}$ . The constraints make sure that the traffic flow modeling is in accordance with the LTM, which is specified in Section 3-2-1. The inequality matrix  $M^{\text{ineq}}$  and vector  $V^{\text{ineq}}$  consists of various parts:

$$\begin{aligned} M^{\text{ineq}} &= \begin{bmatrix} M_1^{\text{ineq}} & \cdots & M_7^{\text{ineq}} \end{bmatrix}^\top, \\ V^{\text{ineq}} &= \begin{bmatrix} V_1^{\text{ineq}} & \cdots & V_7^{\text{ineq}} \end{bmatrix}^\top. \end{aligned} \quad (3-29)$$

These parts are used to model the following:

- The first part is used to model the free-flow dynamics according to (3-3).
- The second part is used to the spill back dynamics according to (3-6).
- The third part is used to constrain the outflow out of an origin according to (3-8).
- The fourth part is used to include the constraints (3-4) on the maximum outflow of the number  $n^E$  of exits in the network
- The fifth and sixth part are used to limit the control signals according to (3-10) and (3-11).
- The seventh part takes care of the conflicts (3-12).

### Dimension of optimization problem

The computation time, i.e. the time it takes to solve the optimization problem, is influenced by the size of the optimization problem. The size is dependent on the size of the input vector and on the number of constraints. For linear programming the worst-case CPU time is of the form  $O(n^m)$ , where  $n$  is the size of the input vector and  $m$  is the number of equality constraints. The input vector  $\bar{u}(k^c)$  contains  $(n^L + n^O)K_p$  elements. Furthermore, there are  $(4n^L + 3n^O + n^E + n^{\text{con}})K_p$  inequality constraints are required, where  $n^{\text{con}}$  is the number of conflicts in the network.

## 3-3 Analysis of uncertainty in the current control framework

The previous section showed the structure of the control framework proposed by Van de Weg et al. (2016a). The framework is built upon certain assumptions, which may not hold in reality. With future implementation in mind some of these assumptions may be relaxed by introducing an uncertainty, e.g. the assumption of a known demand can be relaxed into an unknown disturbance on the demand. The unknown disturbance on the demand can be a better representation of the demand in reality. This section points out the different sources of uncertainty. It does so by dividing the sources into different groups and discussing the different groups one by one.

In Figure 3-4 the framework of the MPC controller of Van de Weg et al. (2016a) is shown. The potential sources of uncertainty have a dashed line: uncertainty in the measurement of the state, uncertainty in the measurement of the disturbance, and uncertainty in the prediction model.

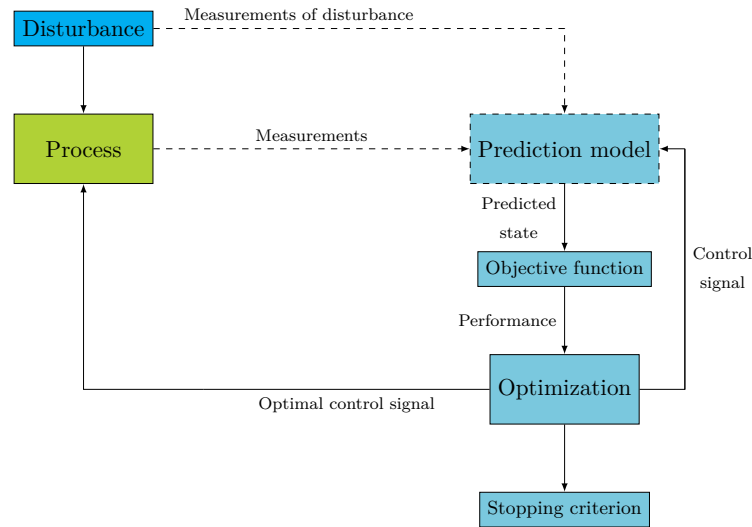


**Figure 3-4:** Framework MPC controller with sources of uncertainty have or are encircled with a dashed line.

The various uncertainties/disturbances are summarized below:

- Model uncertainty
- Parameter uncertainty
  - Saturation flow
  - Free-flow travel time
  - Shock wave travel time
  - Maximum density
- Measurement error
  - Cumulative inflow
  - Cumulative outflow
- Disturbance
  - Turn fractions
  - Demand
  - Outflow constraint

### 3-3-1 Uncertainty in the measurement of the state

The measurement of the state consists in measuring the cumulative inflow and outflow of every link and origin of the network. When there is an error in the estimation of the state, the MPC strategy will not yield an optimal solution. It is expected that an error in the measurement of the state will have a direct effect on the performance of the controller, since the measurement of the state is used as the initial value for the prediction of future states.

### 3-3-2 Uncertainty in the measurement of the disturbances

The measurement of the disturbances consists in measuring the demand at the origins, the maximum outflow at the exits, and the turn fractions. The turn fractions are assumed to be known, and therefore the linear optimization problem is an LP problem. Furthermore, the demand and outflow constraint are assumed to be known.

It is expected that uncertainty in the demand has the least significant effect on the performance of the controller of Van de Weg et al. (2016a). Uncertainty in the demand has a direct effect on the cumulative inflow and outflows of the origins, from where the effect will propagate through the rest of the network. It is expected that through the receding horizon principle the controller of Van de Weg et al. (2016a) is able to notice the fluctuations in the demand, because the propagation of the demand uncertainty will take some time. Note that, it is assumed that there are no internal origins (e.g. a parking area). Internal origins can affect the flows within the network.

On the contrary, it is expected that uncertainty in the turn fractions has a more significant effect on the performance than demand uncertainty. Uncertainty in the turn fractions will have a direct effect on the cumulative inflows and outflows of a link and on the cumulative inflow of downstream links and on the cumulative outflow of upstream links. This effect will be present throughout the network. Therefore, the controller of Van de Weg et al. (2016a) is less able to notice the fluctuations in the turn fractions, because the uncertainty in the turn fractions has a more direct effect than the demand uncertainty.

It is expected that uncertainty in the outflow constraint (e.g. a bottleneck) has a higher impact on the performance than demand uncertainty. The uncertainty is now originated at the exits instead of the origins, and therefore will have a direct effect on the cumulative inflow and outflow of the exits. The throughput of a traffic network is directly related to the cumulative outflow of the exits. Hence, the uncertainty in the outflow constraint is expected to influence the throughput more than demand uncertainty.

### 3-3-3 Uncertainty in the prediction model

A prediction of the state over a certain time horizon is made on the basis of a traffic model, which is based on: the current measured state, the predicted future disturbance, and the future control inputs. The predicted state is then used to evaluate the objective function and to find the optimal control actions for the future through optimization. Uncertainty in the prediction model can be further distinguished in model uncertainty and parameter uncertainty.

A model-based controller bases its control decisions on the prediction of the prediction model. Uncertainty in the prediction model can have the effect that the controller makes the wrong control decision, which can result in a significant decrease in performance.

#### Model uncertainty

In the linear MPC strategy of Van de Weg et al. (2016a) a linear traffic model (LTM) with green fractions and aggregated traffic flows is used for prediction. The linearity of the model is an advantage, because of its low computation time. The linearity of the traffic model is partly obtained by introducing green fractions and aggregated traffic flows. However, the green fractions and aggregated traffic flows are a simplification of the situation in reality. The control of intersections by traffic lights is actually a non-linear process, due to the signal plans and switching between red, yellow, and green light. The traffic flows are simulated with aggregated traffic flows by interpolating the cumulative inflows and outflows of every

link with a sampling time of 10 seconds. The cumulative flows do not capture the interaction between individual vehicles in a link. Hence, the controller of Van de Weg et al. (2016a) has a model-reality mismatch when implemented in practice. This model-reality mismatch can be seen as a model uncertainty.

### Parameter uncertainty

The linear traffic model uses certain parameters that are assumed to be known and constant for every link of the network: saturation flow, free-flow travel time, shock wave travel time, and the maximum density. The assumptions that these parameters are constant and known may not hold in reality. The free-flow travel time may vary for individual vehicles. One may argue whether an average value for these parameters may be sufficient for accurate prediction of the future state.

## 3-4 Extension of the control framework

In this section the optimization problem of the control strategy of Van de Weg et al. (2016a) will be redefined. The proposed adjustment should yield a real-time feasible controller, which optimizes throughput in all traffic regimes, while accounting for uncertainty. In order to keep the controller real-time feasible the optimization problem is kept linear. Furthermore, it is expected that uncertainty has greater impact on the performance in a more saturated situation than a less saturated situation. Therefore, it is tried to avoid phenomena, such as spill-back, to minimize the impact of the uncertainty.

### 3-4-1 General idea

The general idea of the proposed extensions is to let the MPC strategy find a more conservative control decision. To realize this more conservative control decision, a penalty is introduced in the objective function. The value of the penalty depends on the number of vehicles that can fit in a link. The number of vehicles that can fit in a link is a function of the link capacity minus the cumulative inflow and plus the cumulative outflow delayed by the shock wave travel time.

In the LTM the cumulative inflow  $N_i^{L,in}(k^c)$  [veh] is constrained by the maximum cumulative inflow  $N_i^{in,max}(k^c)$  [veh]:

$$N_i^{in,max}(k^c) = N_i^{max} + \gamma_i^{c,sh} N_i^{L,out}(k^c - k_i^{shock} + 1) + (1 - \gamma_i^{c,sh}) N_i^{L,out}(k^c - k_i^{shock}). \quad (3-6)$$

In the saturated and over-saturated traffic regimes the MPC strategy will fully utilize the constraint (3-6), in other words:  $N_i^{L,in}(k^c) = N_i^{in,max}(k^c)$ . However, this may cause the uncertainty to have a greater impact on the performance, because spill-back is more likely to occur. To make sure that uncertainty does not cause any spill-back, a safety margin  $N_i^{safety}(k^c)$  [veh] can be introduced:  $N_i^{L,in}(k^c) = N_i^{in,max}(k^c) - N_i^{safety}(k^c)$ . In Figure 3-5 the effect of a safety margin on the maximum cumulative inflow is shown with corresponding

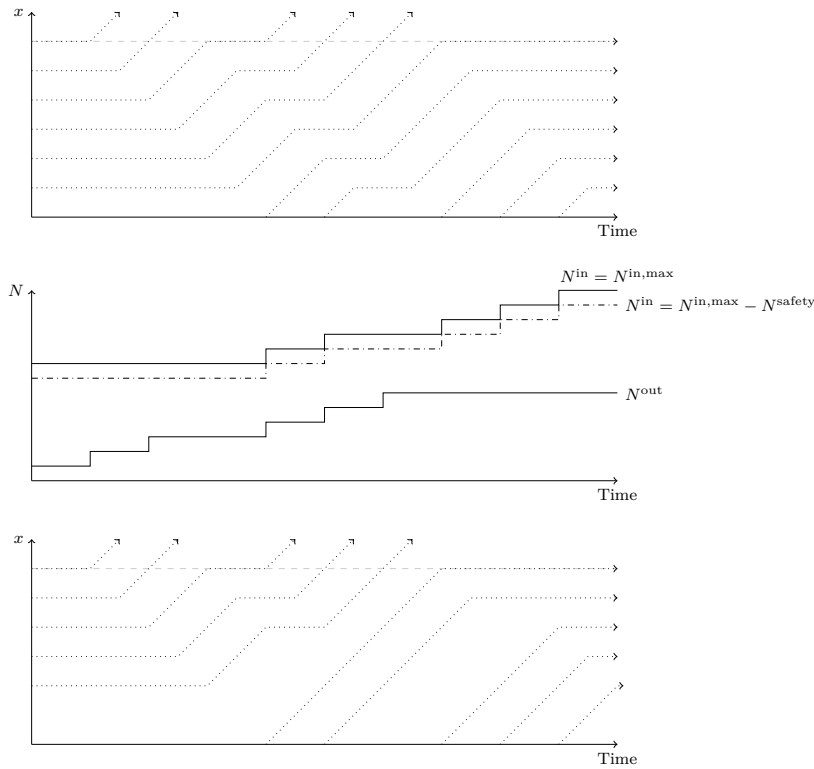


**Figure 3-5:** Plot of the cumulative curves with and without safety margin (middle), space-time diagram without safety margin (top), and space-diagram with safety margin (bottom).

space-time diagram with and without safety margin. The effect is that less vehicles are allowed onto the link.

There can be two ways of introducing such a safety margin: either by implementing a constraint or by implementing a penalty. A drawback of using a constraint is that the optimization problem can become infeasible, because the controlled process may violate this constraint. Another drawback is that a constraint is less flexible than a penalty, because the importance of the penalty can be indicated in the objective function. The penalty can be weighted relative to the other performance index (e.g. throughput). This cannot be done for a hard constraint. Note that a hard constraint can be relaxed into a soft constraint by using a penalty function. Hence, it is chosen to introduce a penalty  $P_i(k^c)$  [–] to represent the safety margin for every link  $i \in I^L$ , where  $I^L$  is the set of all link indices.

How does this penalty represent the safety margin? The penalty is equal to zero when the number of vehicles in a link is below a certain threshold. If the number of vehicles surpasses the threshold, the penalty will increase constantly until the number of vehicles reaches its maximum. The penalty is at its maximum when the number of vehicles is at its maximum. The penalty of every link is accumulated and minimized via the objective function. Thus, the MPC strategy tries to maximize throughput and minimize the penalty simultaneously. Hence, the proposed extension tries to avoid the links of the network of getting too full, while not losing too much throughput.

In the remainder of this section the proposed extension of the control framework of Van de

Weg et al. (2016a) is explained in further detail by by deriving the mathematical formulation of the penalty, introducing some assumptions, and by presenting the extended optimization formulation.

### 3-4-2 Mathematical formulation

The mathematical formulation of the extension is explained in this section. The extension is a function of the state and two control parameters. The state consists of the cumulative inflows and outflow of every link plus the cumulative inflow and outflow of every origin.

The value of  $P_i(k^c)$  depends on the additional number of vehicles that can fit in link  $i$  at discrete time step  $k^c$  [-]. Given  $N_i^{L,\text{in}}(k^c)$  and  $N_i^{\text{in,max}}(k^c)$ , the additional number of vehicles  $N_i^{\text{remaining}}(k^c)$  [veh] that can fit in link  $i$  at time step  $k^c$  is represented by:

$$N_i^{\text{remaining}}(k^c) = N_i^{\text{in,max}}(k^c) - N_i^{L,\text{in}}(k^c). \quad (3-30)$$

The value of  $P_i(k^c) \in [0, \beta_i]$  is calculated in the following way:

$$P_i(k^c) = \max \left( 0, \beta_i - \frac{\beta_i N_i^{\text{remaining}}(k^c)}{\alpha_i N_i^{\text{max}}} \right), \quad (3-31)$$

where the threshold  $\alpha_i \in [0, 1]$  is a tuning parameter for each link  $i$  and  $\beta_i \in \mathbb{R}$  is the maximum value of the penalty. In Figure 3-6 a graph of  $P_i(k^c)$  can be seen as function of  $N_i^{\text{remaining}}$ .

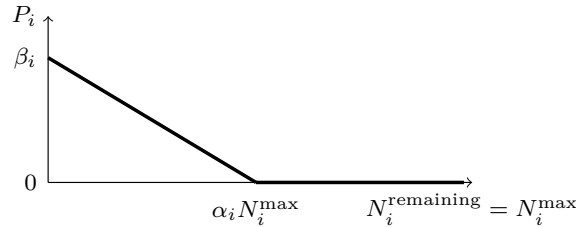


**Figure 3-6:** The penalty  $P_i$  as function of  $N_i^{\text{remaining}}$ .

Combining all the state variables from (3-30), the following is defined:

$$\Delta N_i(k^c) = N_i^{L,\text{in}}(k^c) - \gamma_i^{\text{c,sh}} N_i^{L,\text{out}}(k^c - k_i^{\text{shock}} + 1) - (1 - \gamma_i^{\text{c,sh}}) N_i^{L,\text{out}}(k^c - k_i^{\text{shock}}). \quad (3-32)$$

The physical interpretation of  $\Delta N_i(k^c)$  can be seen in Figure 3-7. When  $\Delta N = N^{\text{max}}$ , the space of a link is fully utilized. So then there is either a shock wave passing through the link, or the link is at its maximum density. By filling in (3-30) in (3-31),  $P_i(k^c)$  can also be expressed as a function of  $\Delta N_i(k^c)$ ,  $N_i^{\text{max}}$ ,  $\beta_i$ , and  $\alpha_i$ :

$$P_i(k^c) = \max \left( 0, \frac{\beta_i \Delta N_i(k^c)}{\alpha_i N_i^{\text{max}}} + \frac{\beta_i (\alpha_i - 1)}{\alpha_i} \right). \quad (3-33)$$

In Figure 3-8 a graph of  $P_i(k^c)$  can be seen as function  $\Delta N_i$ .

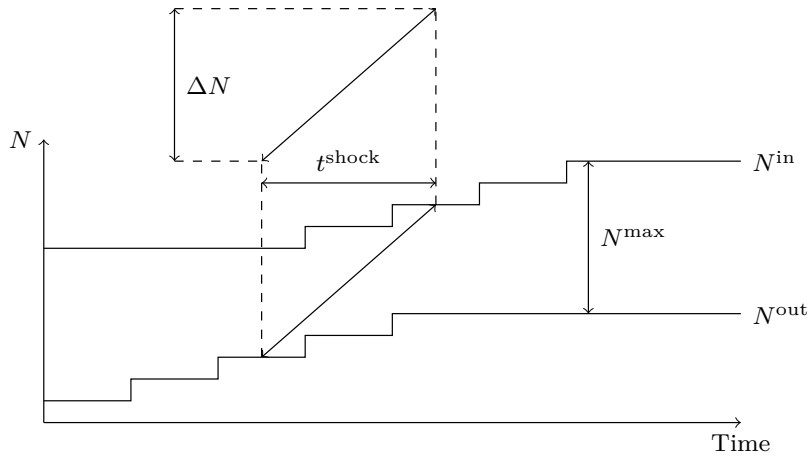


**Figure 3-7:** Plot of cumulative flows with  $\Delta N$  pointed out.

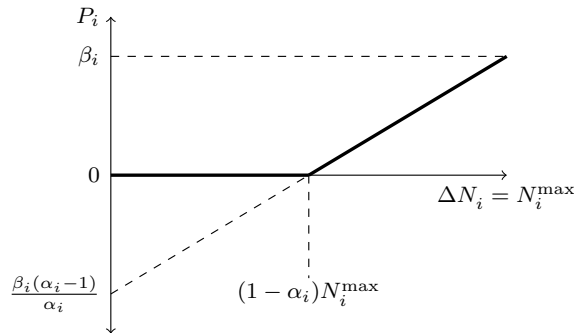


**Figure 3-8:** The penalty  $P_i$  as function of  $\Delta N_i$ .

### 3-4-3 Additional Assumptions

For the extended control method the assumptions of Section B-2 also hold. Nevertheless, there are some additional assumptions compared to the control method of Van de Weg et al. (2016a). The assumptions apply to the control parameters  $\alpha_i$  [-] and  $\beta_i$  [-] of the extended control method. The control parameter  $\alpha_i$  is chosen to be constant over time for the sake of simplicity. The physical interpretation of  $\alpha_i$  causes  $\alpha_i \in [0, 1]$ . Furthermore, the control parameter  $\beta_i \in \mathbb{R}$  is chosen to be constant.

### 3-4-4 Linear optimization formulation

#### Objective function

Minimizing the penalty  $P_i(k^c)$  may lead to a more conservative reference. Therefore,  $P_i(k^c)$  is included in the original objective function of the MPC strategy. The original objective function has the aim of minimizing the TTS of all vehicles in the network over the prediction horizon  $K_p t^c$  [h]. By including the penalty, the extended objective function becomes:

$$\begin{aligned}
J_{\text{ext}}(x) = \sum_{k_0=k^c}^{k^c+K_p} T^c \left\{ \sum_{i \in I^L} \left( N_i^{L,\text{in}}(k^c) - N_i^{L,\text{out}}(k^c) \right) + \sum_{i \in I^L} \left( \frac{P_i(k^c)}{T^c} \right) \right. \\
\left. + \sum_{j \in I^O} \left( N_j^{O,\text{in}}(k^c) - N_j^{O,\text{out}}(k^c) \right) \right\}.
\end{aligned} \tag{3-34}$$

Note that when  $P_i(k^c, \beta_i = 0) = 0 \forall k^c, \forall i \in I^L$  the linear optimization problem remains the original linear optimization problem of Van de Weg et al. (2016a). However, it does have an extra state per link. The objective function can be formulated as a linear optimization problem of the following form:

$$\begin{aligned}
\min_{\hat{u}(k^c)} Z_{\text{ext}} \tilde{B}_{\text{ext}} \hat{u}(k^c) + Z_{\text{ext}} (\tilde{A}_{\text{ext}} x_{\text{ext}}(k^c) + \tilde{C}_{\text{ext}} \bar{d}(k^c)) \\
\text{s.t. } M_{\text{ext}}^{\text{ineq}} \hat{u}(k^c) \leq V_{\text{ext}}^{\text{ineq}},
\end{aligned} \tag{3-35}$$

where the vector  $\hat{u}(k^c)$  contains all the inputs that should be optimized. The vector  $Z_{\text{ext}}$  is used to compute the value of the objective function by multiplication with the future predicted extended state. The matrices  $\tilde{A}_{\text{ext}}$ ,  $\tilde{B}_{\text{ext}}$ ,  $\tilde{C}_{\text{ext}}$ , and disturbance vector  $\bar{d}(k^c)$  and initial state vector  $x_{\text{ext}}(k^c)$  are used to compute the prediction of the states  $\bar{x}_{\text{ext}}(k^c)$ . The matrix  $M_{\text{ext}}^{\text{ineq}}$  and the vector  $V_{\text{ext}}^{\text{ineq}}$  contain the inequality constraints of the extended optimization problem.

## State

The original state  $x_i^{c,L}(k^c)$  of link  $i$  has the following structure:

$$\begin{aligned}
x_i^{c,L}(k^c) &= \left[ N_i^{L,\text{out}}(k^c) \quad \dots \quad N_i^{L,\text{out}}(k^c - k_i^{c,\text{shock}}) \quad N_i^{L,\text{in}}(k^c) \quad \dots \quad N_i^{L,\text{in}}(k^c - k_i^{c,\text{free}}) \right]^\top, \\
x_i^{c,L}(k^c) &\in \mathbb{R}^{n_i^{L,s} \times 1},
\end{aligned} \tag{3-36}$$

where  $n_i^{L,s} = k_i^{c,\text{shock}} + k_i^{c,\text{free}} + 3$  is the length of the vector. To implement  $P_i(k^c)$  for each link  $i$  the penalty is added to the state, and then the extended state becomes:

$$\begin{aligned}
x_{i,\text{ext}}^{c,L}(k^c) &= \left[ \left( x_i^{c,L}(k^c) \right)^\top \quad P_i(k^c) \right]^\top, \\
x_{i,\text{ext}}^{c,L}(k^c) &\in \mathbb{R}^{n_{i,\text{ext}}^{L,s} \times 1},
\end{aligned} \tag{3-37}$$

where  $n_{i,\text{ext}}^{L,s} = k_i^{c,\text{shock}} + k_i^{c,\text{free}} + 3$  becomes the length of the vector.

### System matrices

By creating a vector  $\hat{u}(k^c) \in \mathbb{R}^{n^{\text{in,tot}} \times 1}$  – with  $n^{\text{in,tot}} = K_p(n^L + n^O)$  – defined as:

$$\hat{u}(k^c) = \left[ \left( \tilde{u}(k^c) \right)^\top \quad \cdots \quad \left( \tilde{u}(k^c + K_p - 1) \right)^\top \right]^\top, \quad (3-38)$$

and defining the matrix  $\tilde{A}_{\text{ext}} \in \mathbb{R}^{n^{\text{states}} K_p \times n^{\text{states}}}$ ,  $\tilde{B}_{\text{ext}} \in \mathbb{R}^{n^{\text{states}} K_p \times n^{\text{in,tot}}}$ , and  $\tilde{C}_{\text{ext}} \in \mathbb{R}^{n^{\text{states}} K_p \times n^O}$  as:

$$\begin{aligned} \tilde{A}_{\text{ext}} &= \begin{bmatrix} A_{\text{ext}} & A_{\text{ext}}^2 & \cdots & A_{\text{ext}}^{K_p} \end{bmatrix}^\top, \\ \tilde{B}_{\text{ext}}(k^c) &= \begin{bmatrix} B_{\text{ext}}(k^c) & 0 & \cdots & 0 \\ A_{\text{ext}} B_{\text{ext}}(k^c) & B_{\text{ext}}(k^c + 1) & \cdots & 0 \\ \vdots & \vdots & \ddots & \vdots \\ A_{\text{ext}}^{K_p-1} B_{\text{ext}}(k^c) & A_{\text{ext}}^{K_p-2} B_{\text{ext}}(k^c + 1) & \cdots & B_{\text{ext}}(k^c + K_p - 1) \end{bmatrix}, \\ \tilde{C}_{\text{ext}} &= \begin{bmatrix} C_{\text{ext}} & 0 & \cdots & 0 \\ A_{\text{ext}} C_{\text{ext}} & C_{\text{ext}} & \cdots & 0 \\ \vdots & \vdots & \ddots & \vdots \\ A_{\text{ext}}^{K_p-1} C_{\text{ext}} & A_{\text{ext}}^{K_p-2} C_{\text{ext}} & \cdots & C_{\text{ext}} \end{bmatrix}, \end{aligned} \quad (3-39)$$

a prediction of the evolution of the states is given by the following linear equation:

$$\bar{x}_{\text{ext}}(k^c) = \tilde{B}_{\text{ext}}(k^c) \bar{u}(k^c) + \tilde{A}_{\text{ext}} x_{\text{ext}}(k^c) + \tilde{C}_{\text{ext}} \bar{d}(k^c), \quad (3-40)$$

with the vector  $\bar{x}_{\text{ext}}(k^c) \in \mathbb{R}^{K_p n^{\text{states}} \times 1}$  containing the extended traffic states at every time step  $x_{\text{ext}}(k^c + n)$  from time step  $k_0^c$  to  $k_0^c + K_p$  defined as:

$$\bar{x}_{\text{ext}}(k^c) = \left[ \left( x_{\text{ext}}(k_0^c + 1) \right)^\top \quad \cdots \quad \left( x_{\text{ext}}(k_0^c + K_p) \right)^\top \right]^\top. \quad (3-41)$$

### Constraints

The constraints of the original optimization problem have to be altered to make them compatible with the extended state  $x_{i,\text{ext}}^{c,L}(k^c)$ . Furthermore, the max operator in (3-33) can be replaced by two inequality constraints:

$$P_i(k^c) \geq \frac{\beta_i \Delta N_i(k^c)}{\alpha_i N_i^{\text{max}}} + \frac{\beta_i (\alpha_i - 1)}{\alpha_i}, \quad (3-42)$$

$$P_i(k^c) \geq 0. \quad (3-43)$$

This is only allowed since  $P_i$  is minimized through the objective function (3-34). These inequality constraints are added to the optimization problem. The first constraint can be rewritten into standard form:

$$M_8^{\text{ineq}} \hat{u}_{\text{ext}}(k^c) \leq V_8^{\text{ineq}}, \quad (3-44)$$

with the matrix  $M_8^{\text{ineq}} \in \mathbb{R}^{n^L K_p \times n^{\text{in,tot}}}$  and vector  $V_8^{\text{ineq}} \in \mathbb{R}^{n^L K_p \times 1}$  given as:

$$\begin{aligned} M_8^{\text{ineq}} &= \bar{M}_8^{\text{ineq}} \tilde{B}, \\ V_8^{\text{ineq}} &= \bar{V}_8^{\text{ineq}} - \bar{M}_8^{\text{ineq}} (\tilde{A}x(k^c) + \tilde{C}\bar{d}(k^c)), \end{aligned} \quad (3-45)$$

where the matrix  $\bar{V}_8^{\text{ineq}} \in \mathbb{R}^{n^L K_p \times 1}$  is given by:

$$\bar{V}_8^{\text{ineq}} = \left[ \frac{\beta_1(1-\alpha_1)}{\alpha_1} \quad \dots \quad \frac{\beta_i(1-\alpha_i)}{\alpha_i} \right]^\top. \quad (3-46)$$

The matrix  $\bar{M}_8^{\text{ineq}} \in \mathbb{R}^{n^L K_p \times n^{\text{states}} K_p}$  is given as:

$$\bar{M}_8^{\text{ineq}} = \begin{bmatrix} \ddots & & 0 \\ & M_8 & \\ 0 & & \ddots \end{bmatrix}, \quad (3-47)$$

with the matrix  $M_8 \in \mathbb{R}^{n^L \times n^{\text{states}}}$  given as:

$$M_8 = \begin{bmatrix} \ddots & & & & & & & & & & 0 \\ & 0 & \dots & 0 & -\frac{\gamma_i^{\text{c,sh}} \beta_i}{\alpha_i N_i^{\text{max}}} & -\frac{(1-\gamma_i^{\text{c,sh}}) \beta_i}{\alpha_i N_i^{\text{max}}} & \frac{\beta_i}{\alpha_i N_i^{\text{max}}} & 0 & \dots & 0 & -1 \\ & 0 & & & & & & & & & \ddots \end{bmatrix}. \quad (3-48)$$

The second constraint can be rewritten into standard form:

$$M_9^{\text{ineq}} \hat{u}_{\text{ext}}(k^c) \leq V_9^{\text{ineq}}, \quad (3-49)$$

with the matrix  $M_9^{\text{ineq}} \in \mathbb{R}^{n^L K_p \times n^{\text{in,tot}}}$  and vector  $V_9^{\text{ineq}} \in \mathbb{R}^{n^L K_p \times 1}$  given as:

$$\begin{aligned} M_9^{\text{ineq}} &= \bar{M}_9^{\text{ineq}} \tilde{B}, \\ V_9^{\text{ineq}} &= -\bar{M}_9^{\text{ineq}} (\tilde{A}x(k^c) + \tilde{C}\bar{d}(k^c)). \end{aligned} \quad (3-50)$$

Here, the matrix  $\bar{M}_9^{\text{ineq}} \in \mathbb{R}^{n^L K_p \times n^{\text{states}} K_p}$  is given as:

$$\bar{M}_9^{\text{ineq}} = \begin{bmatrix} \ddots & & 0 \\ & M_9 & \\ 0 & & \ddots \end{bmatrix}, \quad (3-51)$$

with the matrix  $M_9 \in \mathbb{R}^{n^L \times n^{\text{states}}}$  given as:

$$M_9 = \begin{bmatrix} \ddots & & & & 0 \\ & [0 \ \dots \ 0 \ -1] & & & \\ & & & & \\ 0 & & & & \ddots \end{bmatrix}. \quad (3-52)$$

### 3-5 Conclusions and discussions

This chapter has introduced an extension to the work of Van de Weg et al. (2016a). The theory behind the proposed extension is described in this chapter. The MPC controller of Van de Weg et al. (2016a) consists of three main parts: the prediction model, the objective function, and the optimization algorithm. The proposed extension adjusted the objective function by introducing an extra term. The extra term is a penalty applied to each link. The penalty is a function of the number of vehicles that can fit in a link and the control parameters  $\alpha_i$  and  $\beta_i$ .

The proposed extension should yield a better controller performance than the controller of Van de Weg et al. (2016a) when uncertainty is present. The uncertainty is expected to have a greater impact on the performance in the saturated and over-saturated traffic regime, because spill-back is more likely to occur. A safety margin can be introduced to avoid spill-back. The safety margin is established by finding a more conservative control decision. This control decision is made more conservative by introducing a penalty.

The proposed extension does not require any additional measurements compared to the controller of Van de Weg et al. (2016a). However, the implementation of the penalty does require an extra state variable per link, and two extra constraints. Thus, the optimization problem has become bigger than the optimization problem of Van de Weg et al. (2016a). Nevertheless, the optimization problem is still a linear programming problem. Hence, it is expected that the proposed extension is real-time feasible. However, it should be investigated whether the grown size of the optimization problem has a significant impact on the computation time.

The control parameters  $\alpha_i$  and  $\beta_i$  respectively represent the threshold and the maximum value of the penalty respectively for link  $i$ . The parameters should be chosen in such a way that the highest throughput is realized. It is expected that the optimal values for these parameters may vary for various demands, different types and magnitude of uncertainty. For future field implementation the values for  $\alpha_i$  and  $\beta_i$  should be determined by deterministic rules or by simulation. It is recommended to derive the values gradually during field implementation

to improve the performance, since there are not yet any deterministic rules to determine (sub)optimal  $\alpha_i$  and  $\beta_i$ . In this research  $\alpha_i$  and  $\beta_i$  are assumed to be constant over time. However, this may not be optimal for the performance of the controller.

In the under-saturated regime it is expected that the proposed controller does not have any effect on the performance when  $\alpha_i$  is assumed to be small enough. The traffic network remains on the free-flow branch of the macroscopic fundamental diagram, when it operates in the under-saturated traffic regime. On the free-flow branch of the macroscopic fundamental diagram the vehicles density is relatively low. Hence, the number of vehicles in a link will probably not pass the threshold value of the penalty function. The threshold value, which is a function of  $\alpha_i$ , will be high when the value of  $\alpha_i$  is low. Hence, the proposed controller is expected to not influence the performance in the under-saturated traffic regime.

# Evaluation of the robust urban traffic controller

In this chapter the proposed urban traffic controller will be evaluated by means of simulation. First, the different case studies are introduced. After that, the common features of the simulation set-up are described. Subsequently, the case specific simulation set-up and results of each case study will be presented. The results will be divided into quantitative findings and qualitative findings. Finally, this chapter will be concluded. In the remainder of this chapter the controller of Van de Weg et al. (2016a) is denoted as the LP (Linear Programming) controller, and the proposed extension is denoted as the LPP (Linear Programming with Penalty) controller.

## 4-1 Introduction

The goal of this chapter is the evaluation of the proposed extension on the work of Van de Weg et al. (2016a). The evaluation consists of two parts: (1) the quantitative analysis, which is based on the Total Time Spent (TTS) and the computation time of the LPP controller, and (2) the qualitative analysis, which is based on the behavior of the LPP controller. The desired behavior of the LPP controller consists of two tasks:

1. Perform better than the LP controller when uncertainty is present in the over-saturated and saturated traffic regime;
2. Do not perform worse than the LP controller when uncertainty is present in the under-saturated regime

It is expected that different types of uncertainty have different impacts. Therefore, the different types of uncertainty, which were discussed in Section 3-3, should be investigated separately. For the sake of simplicity only uncertainty in the disturbances and the model are evaluated.

The evaluation of uncertainty in the state is expected to be much more complex, because the proposed controller makes use of the state to determine the penalty. Hence, the following cases are considered:

- **case study 1** evaluates the impact of the LPP controller on the TTS by comparing it to the LP controller when the traffic network is subjected to a demand with noise. The LPP controller is only provided with the average value of this demand;
- **case study 2** evaluates the impact of the LPP controller on the TTS by comparing it to the LP controller when the traffic network is subjected to turn fractions with noise. The LPP controller is only provided with the average value of these turn fractions;
- **case study 3** evaluates the impact of the LPP controller on the TTS by comparing it to the LP controller when the exits of the traffic network are subjected to outflow constraints with noise. The LPP controller is only provided with the average value of these outflow constraints;
- **case study 4** evaluates the impact of the LPP controller on the TTS by comparing it to the controller of Van de Weg et al. (2016b) for different demands when model uncertainty is present. The model uncertainty is explained in more detail in Section 4-6.

## 4-2 Simulation set-up

The simulation set-up for the first three cases can be seen in Figure 4-1. The Link Transmission Model (LTM) of Yperman (2007) is chosen as the process model (i.e. it represents the “real” world) and as the prediction model. However, the simulation sampling time step of the process model is set to 1 second while the sampling time step of the prediction model is set to 10 seconds. The process model and prediction model are chosen to be the same, because the evaluations should show the effect of the LPP controller while only one specific type of uncertainty is present. This is the case when the process model and the prediction model are the same. Note that the prediction model and the process model are not the same in case study 4, due to a nonlinearity in the process model. This will be elaborated in the case-specific simulation set-up of case study 4.

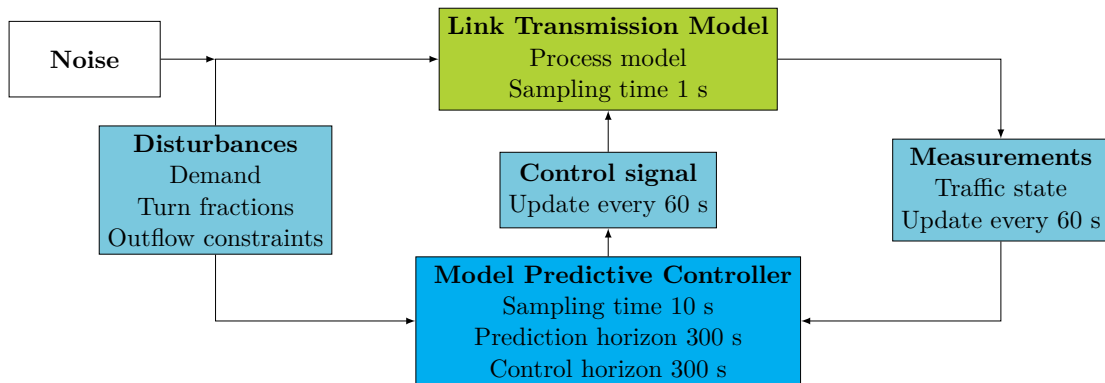


Figure 4-1: Overview of the simulation set-up

In every case study another type of uncertainty is investigated. It is assumed that during a case study the controller performance is not affected by the remaining potential sources of uncertainty. Thus, the controller has no exact predictions of the future demand available in case study 1. The controller has no exact prediction of the turn fractions available in case study 2. Furthermore, the controller has no exact prediction of the outflow constraints available in case study 3. Finally, in case study 4 the optimized green fractions are not directly applied to the “real world” as in the first three case studies but are translated to signal timings, which then are implemented to the “real” world. In every case study it is assumed that the controller has perfect measurements of the traffic states available.

The simulations are carried out using Matlab R2015b on a computer with a 3.1 GHz processor and 8 GB RAM. The standard linear optimization function `linprog` of Matlab implemented with the ‘dual-simplex’ algorithm is used to solve the linear optimization problem. The computation time required by the optimization problem at every time step and the time needed to formulate the optimization problem at every time step are used for comparison between the different cases.

#### 4-2-1 Timing parameters

The timings parameters that are used in the case studies are summarized in Table 4-1 and are based on results found by Van de Weg et al. (2016a). Their work shows that a controller sampling time between 2 seconds and 20 seconds does not influence the TTS for a prediction horizon of 300 seconds. Furthermore, they show that a controller update interval larger than 60 seconds has a negative effect on the TTS. Throughout the work of Van de Weg et al. (2016a) the control horizon is set the same as the prediction horizon. Thus, for the case studies it is chosen to have a controller update interval of 60 seconds, and a prediction and control horizon of 300 seconds, which corresponds to 5 steps with a control sampling time of 60 seconds. The timing parameters for case study 4 are based on results found by Van de Weg et al. (2016b) and are presented in Section 4-6-1.

Parameter	Value	Parameter	Value
Simulation sample time	1 s	Prediction horizon	300 s
Control sample time	10 s	Control horizon	300 s
		Update interval MPC	60 s

**Table 4-1:** Timing parameters of case study 1, 2, and 3.

#### 4-2-2 Network

The traffic network as illustrated in Figure 4-2 is used for evaluation. It consists of 2 intersections, with 3 origins and 3 destinations in total. Link 7 is one of the destinations and it is modeled as a bottleneck, which is introduced to model all traffic regimes. It is chosen to use a small network, because it is expected that a small network can give better understanding of the qualitative behavior of the controller.

The network consists of 15 links, each of which represents a one-lane road. Every main road (e.g. link 1, 4, 8, and 12) splits into a left or right-turning link and a through-going link. The

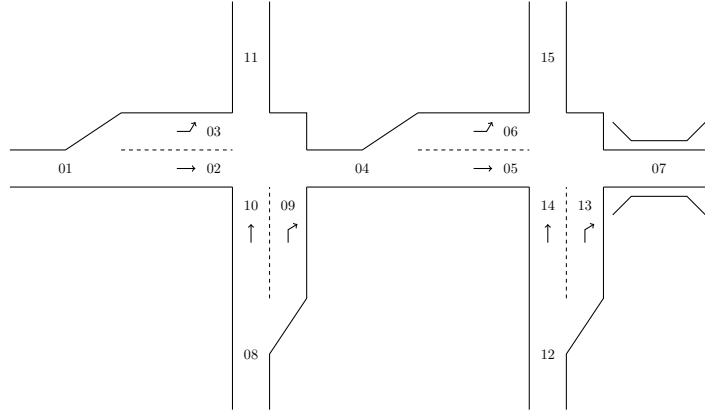


**Figure 4-2:** Network of two intersections considered in the case studies.

links 1, 8, and 12 represent the origins of the network, and links 7, 11, and 15 represent the exits, where link 7 has an outflow constraint of 1000 veh/h. The saturation flow  $q_i^{\text{sat}}$  [veh/h] of every link is set to 2000 veh/h. Furthermore, the maximum density and length of every link are set to 0.4 veh/m and to 200 m respectively. Thus, the maximum number of vehicles  $N^{\text{max}}$  of every link is 80 vehicles. The free-flow speed  $v^{\text{free}}$  is set at 10 m/s, which yields a free-flow travel time  $t^{\text{free}}$  of 20 seconds. The shock wave speed  $v^{\text{shock}}$  is set at 5 m/s, which yields a shock wave travel time  $t^{\text{shock}}$  of 40 seconds. The characteristics of every link are summarized in Table 4-2.

Parameter	Value	Parameter	Value
Maximum density	0.4 veh/m	Length	200 m
Saturation flow	2000 veh/h	Maximum number of vehicles	80 veh
Free-flow speed	10 m/s	Free-flow travel time	20 s
Shock wave speed	5 m/s	Shock wave travel time	40 s

**Table 4-2:** Link characteristics of the network considered in every case study.

The turn fractions of the network are shown in Table 4-3. When the same demand is applied to every origin of the network, the turn fractions will yield the same demand at the bottleneck as the demand at the origins. For example, if a demand of 1100 veh/h is applied to every origin (link 1, 8, and 12), the demand with a destination into link 7 is 1100 veh/h. The simulation time of every simulation is set to 3600 seconds.

Turn fractions			
$\eta_{1,2} = 0.4$	$\eta_{4,5} = 0.67$	$\eta_{8,9} = 0.6$	$\eta_{12,13} = 0.33$
$\eta_{1,3} = 0.6$	$\eta_{4,6} = 0.33$	$\eta_{8,10} = 0.4$	$\eta_{12,14} = 0.67$
$\eta_{2,4} = 1$	$\eta_{5,7} = 1$	$\eta_{9,4} = 1$	$\eta_{13,7} = 1$
$\eta_{3,11} = 1$	$\eta_{6,15} = 1$	$\eta_{10,11} = 1$	$\eta_{14,15} = 1$

**Table 4-3:** Turn fractions of the network

## 4-3 Case Study 1: Uncertainty in the demand

This section presents the results of evaluating the impact of demand uncertainty on the performance of the LPP controller. The resulting performance is compared with the performance of the LP controller. In Section 4-3-1 the set-up of the simulations is presented. After that, Section 4-3-2 presents the quantitative results and Section 4-3-3 the qualitative results.

### 4-3-1 Case study 1 - evaluation set-up

Case study 1 consists of two parts, namely, 1A and 1B. The first part (1A) consists of evaluating the TTS of the LP controller for different demands and for different levels of uncertainty in the demand. The second part (1B) consists of evaluating the performance of the LPP controller for different demands for a significant level of uncertainty. The level of the uncertainty is determined in case study 1A.

The uncertainty in the demand is created by a difference between the actual demand  $q^{\text{in,act}}(k)$  [veh/h] and the nominal demand  $q^{\text{in,nom}}(k)$  [veh/h], with a maximum difference of  $\gamma^{\text{q}^{\text{in}}}$  percent of  $q^{\text{in,nom}}(k)$ . The actual demand is applied to the traffic network, while the nominal demand is used for prediction of future traffic dynamics. The actual demand is determined as follows:

$$q^{\text{in,act}}(k) = [1 + \gamma^{\text{q}^{\text{in}}} \Delta^{\text{q}^{\text{in}}}(k)] q^{\text{in,nom}}(k), \quad (4-1)$$

where  $\Delta^{\text{q}^{\text{in}}}(k)$  is a random variable between -1 and 1 with a uniform distribution. Hence, the actual demand fluctuates around the nominal demand every 10 seconds with a uniform distribution. The nominal demand is taken to be constant over time and the same for every origin.

Case 1A and 1B are both evaluated for 16 different demands varying between 100 veh/h and 1600 veh/h with intermediate steps of 100 veh/h. Furthermore, the various levels of the uncertainty are according to Table 4-4. Hence, there are 224 simulations, which are all repeated ten times with a different random seed. The values of the TTS for each demand and level of uncertainty will be averaged over these ten experiments.

Case 1A	1	2	3	4	5	6	7	8	9	10	11	12	13	14
$\gamma^{\text{q}^{\text{in}}}$	0	0.02	0.05	0.1	0.15	0.2	0.3	0.4	0.5	0.6	0.7	0.8	0.9	1

**Table 4-4:** Case 1A: different levels of the uncertainty.

For the second part (1B) of case 1 the performance of the LPP controller will be evaluated. The LPP controller has two control variables: the threshold for the penalty  $\alpha$  and the height of the penalty  $\beta$ . It is not clear how to choose  $\alpha$  and  $\beta$  in order to find an optimal performance. Therefore, the performance of the LPP controller is evaluated for various combinations of  $\alpha$  and  $\beta$ . It is expected that this will lead to additional insights on the behavior of the LPP controller. The penalty is applied to every link. The values for  $\alpha$  and  $\beta$  vary between 0 and 1 with intermediate steps of 0.1. The level for the uncertainty is determined at case 1A.

In case 1A the LP controller is subjected to demand uncertainty. The demand uncertainty will influence the accuracy of the prediction, and therefore the demand uncertainty will have an impact on the TTS. It is expected that for increasing  $\gamma^{q^{in}}$  the TTS increases. However, it is expected that the increase will be less significant for the saturated and over-saturated traffic regime. In the under-saturated traffic regime the vehicles in the network will drive with the free-flow speed. In the network the origins and intersections are two links apart. Thus, a vehicle will take twice the free-flow travel time of a link, which is 20 seconds and 40 seconds in total, to travel from an origin to an intersection. In the saturated and over-saturated regime this origin to intersection travel time will even be longer. Furthermore, the update interval of the control signal is set to 60 seconds. Hence, the demand uncertainty will propagate relatively slowly through the network compared to the update interval. Therefore, the LP controller is likely to notice the uncertainty in the demand due to the receding horizon principle. Hence, the LP controller is expected to lose less of its performance in the saturated and over-saturated traffic regime compared to the under-saturated traffic regime when demand uncertainty is present.

In case 1B the LPP controller is subjected to demand uncertainty for various combinations of  $\alpha$  and  $\beta$ . The demand uncertainty and the various combinations will influence the TTS. The performance of the LPP controller is compared to the performance of the LP controller. It is expected that the LPP controller will only lead to little or no decrease in TTS in every traffic regime, compared to the LP controller. This is expected because the LP controller is likely to be able to anticipate to the demand uncertainty due to the receding horizon principle. The update frequency of the control signal is set to 60 s. The uncertainty in the demand has to travel at least 40 s - twice the free-flow travel time of one link - to reach the nearest intersection. Hence, the controller is likely to be able to anticipate to the demand uncertainty.

### 4-3-2 Case study 1 - quantitative results

Figure 4-3 presents the performance of the LP controller for three different demands with different levels of uncertainty. The performance is expressed as a percentage of the performance when the demand is fully known and no uncertainty is present. As expected it can be seen that the relative impact of uncertainty is more significant for lower demands. For example, the relative impact for a demand of 1100 veh/h and 1200 veh/h is less significant than for a demand of 500 veh/h or 1000 veh/h. The reason for this is that for demands higher than 1000 veh/h the traffic network becomes congested, and the uncertainty propagates slower through the network. Hence, the LP controller is able to lose less performance due the receding horizon principle.

For the second part (1B) of the first case the level for the uncertainty is set at  $\gamma^{q^{in}} = 0.4$ . This is the lowest level of uncertainty where the impact of the uncertainty on the performance reaches 1 % for a demand of 900 veh/h and 1000 veh/h. The absolute values for the TTS are summarized in Table 4-5.

Figure 4-4 presents a part of the quantitative results of the first case study. Four demand scenarios are considered here: 900 veh/h, 1000 veh/h, 1100 veh/h, and 1200 veh/h. Although sixteen different demand scenarios have been evaluated, the most significant scenarios are discussed here. These scenarios are the most significant, because they illustrate the transition from the under-saturated traffic regime to the over-saturated traffic regime.

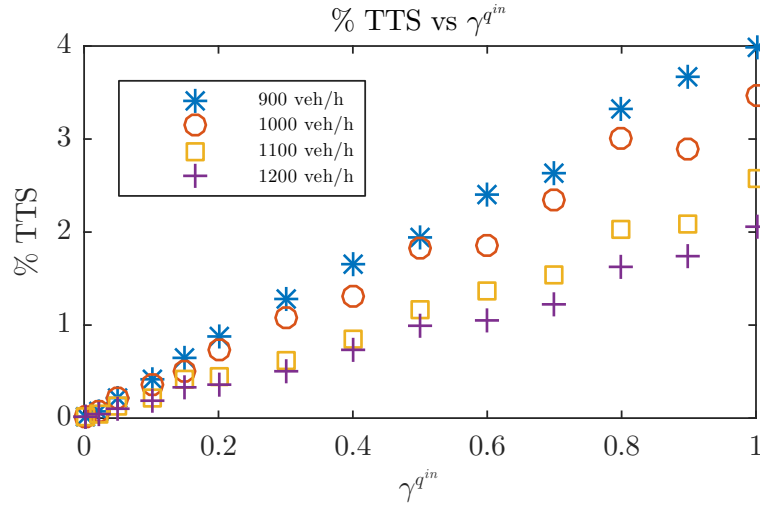


**Figure 4-3:** Case 1A: % TTS increase compared to no uncertainty situation vs  $\gamma^{q^{in}}$  for the demands 900, 1000, 1100, and 1200 veh/h.

Demand [veh/h]	Perfect knowledge	Without perfect knowledge	
	TTS [veh·h]	TTS [veh·h]	% of perfect knowledge
900	54.4	55.3	1.6%
1000	64.7	65.5	1.3%
1100	112.9	113.8	0.8%
1200	165.8	167.0	0.7%

**Table 4-5:** Overview of the TTS of the LP controller with and without perfect demand knowledge for four demand patterns at  $\gamma^{q^{in}} = 0.4$ .

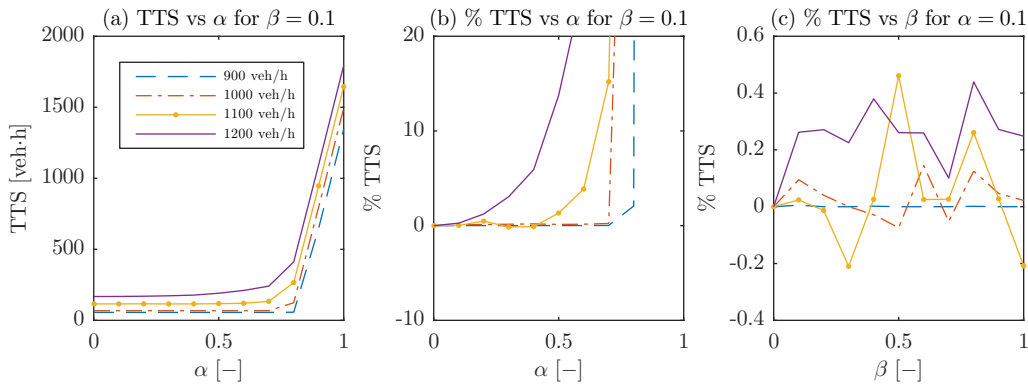


**Figure 4-4:** Case 1B: TTS vs  $\alpha$  and  $\beta$  for the demands 900, 1000, 1100, and 1200 veh/h.

Figure 4-4 shows that, as expected, for demands lower than the bottleneck capacity, the LPP controller has little to no effect on the TTS for low values of  $\alpha$  (e.g.  $\alpha \in [0, 0.7]$ ). For increasing demands that exceed the bottleneck capacity, the LPP controller has an increasingly negative effect on the performance. This effect becomes less negative when the values of  $\alpha$  decreases. Furthermore, it can be observed that different values for  $\beta$  have no different effect on the

performance.

### 4-3-3 Case study 1 - qualitative results

The purpose of the qualitative results is to get insight in the behavior of the controller when demand uncertainty is present. In order to assess the behavior of the LPP controller, this section looks at how the vehicle flows propagate through the traffic network. In this section the focus lies on two specific cases: (1) a case that shows that the behavior of the LPP controller is the same as the LP controller in the under-saturated traffic regime and (2) a case that shows that the behavior of the LPP controller is not the same as the LP controller in the saturated and over-saturated traffic regime.

During the quantitative analysis it is observed that for demands lower than the bottleneck capacity, the LPP controller has almost no effect on the TTS for low values of  $\alpha$ . Furthermore, it is also observed that for increasing demands that exceed the bottleneck capacity, the LPP controller has an increasingly negative effect on the performance. To analyze these phenomena and the corresponding behavior of the LP controller, a closer look is taken into the movement of the vehicle streams. For the first case the demand is set at 1000 veh/h and  $\alpha$  and  $\beta$  are set to 0.5 and 0.1, respectively. For the second case the demand is set at 1200 veh/h and  $\alpha$  and  $\beta$  are set to 0.5 and 0.1 respectively. According to Figure 4-4 the LPP controller yields a 0.1% and 13.8 % increase in TTS for the first and second case, respectively. Figure 4-5 shows the number of vehicles in several links for the first case. Figure 4-6 shows the number of vehicles in several links for the second case.

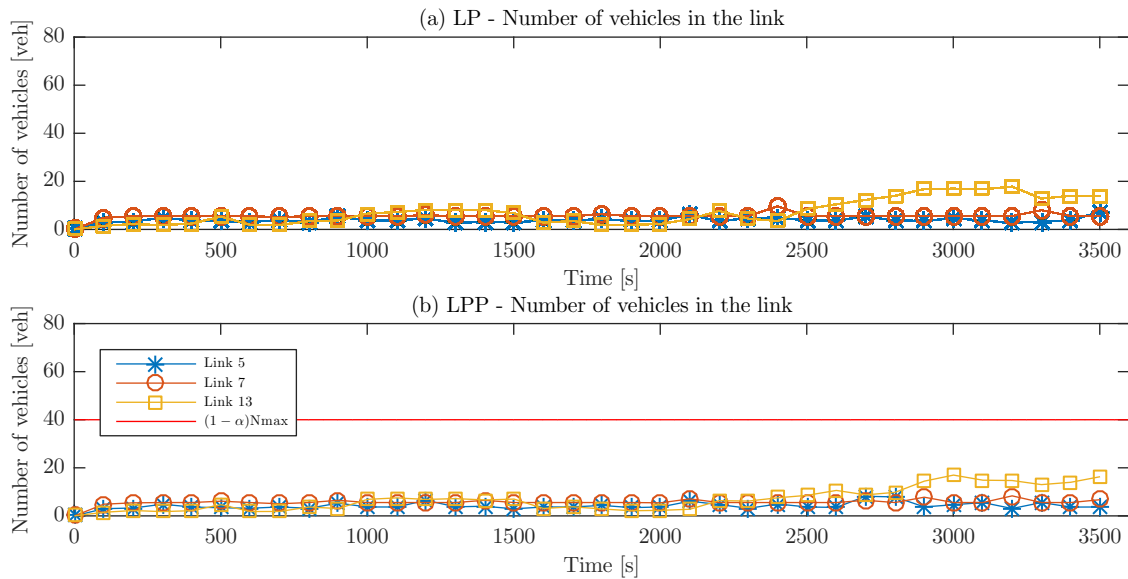


**Figure 4-5:** Case 1B: Number of vehicles in the link over time for the LP controller (a) and the LPP controller (b) for a demand of 1000 veh/h and  $(\alpha, \beta) = (0.5, 0.1)$

The first case has a demand of 1000 veh/h that is applied to every origin. Due to the topology of the network (e.g. placement of origins and turn fractions) the demand with a destination to link 7 is also 1000 veh/h. Hence, the capacity of the bottleneck link 7, which is 1000 veh/h, is not exceeded. There is almost no queue build up during the whole simulation time of 3600 s,

except for link 13. This is due to the random demand fluctuations, which cause the demand to exceed the bottleneck capacity for some time. The behavior of both controllers is almost the same, because the number of vehicles does not exceed the threshold. However, there are some small fluctuations in the build up of the queue of link 13, 5, and 7. This is probably due to the fact that the linear optimization problem has multiple solutions. Hence, there are a variety of ways that lead to the same TTS.

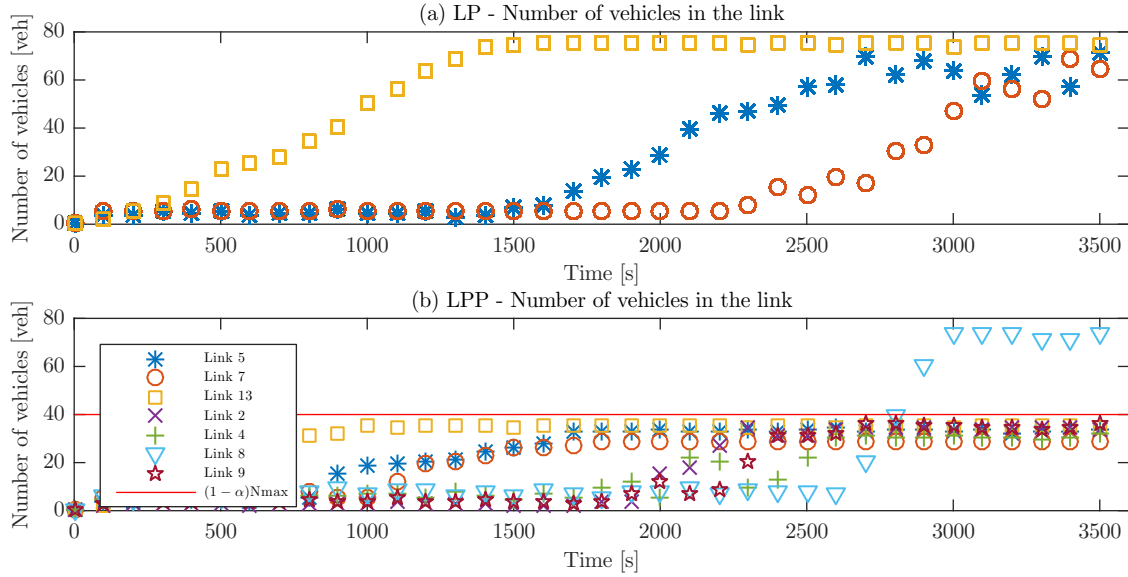


**Figure 4-6:** Case 1B: Number of vehicles in the link over time for the LP controller (a) and the LPP controller (b) for a demand of 1200 veh/h and  $(\alpha, \beta) = (0.5, 0.1)$

The second case has a demand of 1200 veh/h that is applied to every origin. Due to the topology of the network (e.g. placement of origins and turn fractions) the demand with a destination to link 7 is also 1200 veh/h. Hence, the capacity of the bottleneck link 7, which is 1000 veh/h, is exceeded. Since the demands at link 4 and 12 are equal and the turn fraction from link 12 to 13 is smaller compared to the turn fraction from link 4 to 5, the LP controller gives priority to link 5 and lets the number of vehicles increase in link 13.

Around time 1500 s link 13 is almost full and the controller starts to increase the number of vehicles in link 5. At time 2500 s link 5 is almost full, and the controller starts to increase the number of vehicles in link 7 until it is almost full too at 3600 s, which is where the simulation stops.

The penalty of the LPP controller starts for  $N_i^{\text{in}}(k) - N_i^{\text{out}}(k - k^{\text{shock}}) \geq N_i^{\text{max}}(1 - \alpha_i)$  for each link  $i$ . The LPP controller tries to minimize the penalty, and therefore it tries to keep the number of vehicles in the link below the threshold. As expected the LPP controller starts to increase the number of vehicles in the links in the same order as the LP controller (e.g. first link 13, then link 5 and 7). However, the LPP controller does not increase the number of vehicles until the link is almost full, but it increases the number of vehicles to almost  $(1 - \alpha_i)N_i^{\text{max}}$ . The number of vehicles increases not exactly to  $(1 - \alpha_i)N_i^{\text{max}}$ , because  $N_i^{\text{out}}(k - k^{\text{shock}})$  is used to calculate the number of vehicles in the link instead of  $N_i^{\text{out}}(k)$ . The main advantage of using  $N_i^{\text{out}}(k - k^{\text{shock}})$  is that the penalty also takes into account the shock wave dynamics.

After the LPP controller has filled link 13, 5, and 7, it starts filling other links, such as link 2, 4, and 9. Even link 8 is filled, which results in the queue spilling back to the origin. Hence, the LPP controller distributes the vehicle throughput due to the penalty and the high value of  $\alpha_i$ .

Summarizing, the evaluation shows that the LPP controller acts as expected. The behavior of the LP and LPP controller is almost the same in the under-saturated traffic regime. The small difference in behavior is probably due to the fact that the linear optimization problem has multiple solutions. Hence, there are a variety of ways that lead to the same TTS. However, more investigation is needed to proof this statement. In the saturated and over-saturated traffic regime the LPP controller is able to reduce the number of vehicles in every link up to the threshold. However, this causes the vehicles to be placed somewhere else in the network, which even results in spill-back to one of the origins.

## 4-4 Case Study 2: Uncertainty in the turn fractions

This section presents the results of evaluating the impact of uncertainty in the turn fractions on the performance of the LPP controller. The resulting performance is compared with the performance of the LP controller. In Section 4-4-1 the set-up of the simulations is presented. After that, Section 4-4-2 presents the quantitative results and Section 4-4-3 the qualitative results.

### 4-4-1 Case study 2 - Evaluation set-up

Case study 2 consists of two parts, namely, 2A and 2B. The first part (2A) consists in evaluating the TTS of the LP controller for different demands and for different levels of uncertainty in the turn fractions. The second part (2B) consists in evaluating the performance of the LPP controller for different demands for a significant level of uncertainty in the turn fractions. The level of the uncertainty in the turn fractions is determined in case study 2A.

The uncertainty in the turn fractions is created by a difference between the actual turn fraction  $\eta^{\text{act}}(k)$  [-] and the nominal turn fraction  $\eta^{\text{nom}}(k)$  [-], with a maximum difference of  $\gamma^\eta$  percent of  $\eta^{\text{nom}}(k)$ . The actual turn fractions are applied to the traffic network, while the nominal turn fractions are used for prediction of future traffic dynamics. The calculation of the turn fractions for link 1 to link 2 and 3 are shown as an example to illustrate how the actual turn fractions are determined:

$$\begin{aligned}\eta_{1,2}^{\text{act}}(k) &= \max(\min([1 + \gamma^\eta \Delta_{1,2}(k)]\eta_{1,2}^{\text{nom}}(k), 1), 0) \\ \eta_{1,3}^{\text{act}}(k) &= 1 - \eta_{1,2}^{\text{act}}(k),\end{aligned}\tag{4-2}$$

where  $\Delta_{1,2}(k)$  is a random variable between -1 and 1 with a uniform distribution. The min and max operator are there to ensure that the physical constraint  $0 \leq \eta \leq 1$  is satisfied. The nominal turn fractions are constant over time. Note that for high values of  $\gamma^\eta$  the distribution is not uniform anymore, due to the min and max operator.

Case 2A and 2B are both evaluated for 16 different demand patterns varying between 100 veh/h and 1600 veh/h with intermediate steps of 100 veh/h and 14 different levels of uncertainty as indicated in Table 4-4. Hence, there are 224 simulations, which are all repeated ten times with a different random seed. The values of the TTS for each demand and level of uncertainty will be averaged over these ten runs.

For the second part (2B) of case 2 the performance of the LPP controller will be evaluated. Just as case 1B the performance of the LPP controller is evaluated for various combinations of  $\alpha$  and  $\beta$ . The penalty is applied to every link. The values for  $\alpha$  and  $\beta$  vary between 0 and 1 with intermediate steps of 0.1. The level for the uncertainty is determined at case 2A.

In case 2A the LP controller is subjected to uncertainty in the turn fractions. The uncertainty in the turn fractions will influence the accuracy of the prediction, and therefore the uncertainty in the turn fractions will have an impact on the TTS. It is expected that for increasing  $\gamma^n$  the TTS increases. Moreover, in contrast to case 1A, it is expected that the increase will be more significant for the saturated and over-saturated regime. The uncertainty in the turn fractions will probably have a more direct effect on the performance than demand uncertainty. The uncertainty in the turn fractions is applied to every turn fraction in the network. Therefore, it will affect the whole network directly. Hence, the LP controller is expected to lose more performance for uncertainty in the turn fractions in each traffic regime than for demand uncertainty. Furthermore, the impact is expected to be more significant in the saturated and over-saturated traffic regime than in the under-saturated traffic regime.

In case 2B the LPP controller is subjected to uncertainty in the turn fractions for various combinations of  $\alpha$  and  $\beta$ , which will influence the TTS. The performance of the LPP controller is compared to the performance of the LP controller. It is expected that the LPP controller will lead to a decrease in TTS in the saturated and over-saturated traffic regime. The LPP controller is designed so that it will not act differently than the LP controller in the under-saturated traffic regime. Hence, in general it is expected that the more conservative control signal provided by the LPP controller will yield a better performance than the LP controller in the saturated and over-saturated traffic regime.

#### 4-4-2 Case study 2 - quantitative results

Figure 4-7 presents the performance of the LP controller for four different demand patterns when uncertainty in the turn fractions is present. The performance is expressed as a percentage of the performance when the turn fractions are fully known and no uncertainty is present. It can be seen that there is a small relative impact of uncertainty on the TTS in the under-saturated regime. When the demand at the bottleneck reaches the capacity, the impact of the uncertainty increases significantly with the highest impact around  $\gamma^n = 0.7$ . The impact of the uncertainty increases when the demand increases further after it has exceeded the capacity. The reason for this is that the fluctuations of the flows in the network become larger when the demand increases. The controller is not able to anticipate on the fluctuations, because they are unknown. However, after approximately  $\gamma^n = 0.6$  the impact of the uncertainty starts decreasing for a demand of 1100 veh/h and 1200 veh/h. This is probably due to the physical constraint on the turn fractions (e.g. the min and max operator), which causes the distribution of the uncertainty to lack uniformity for  $\gamma^n \geq 0.5$ . For example, a turn fraction of 0.6 loses its uniform distribution for  $\gamma^n > 2/3$ , because for those values of  $\gamma^n$

turn fractions higher than 1 can be generated. The turn fractions that are higher than 1 are then altered to 1 due to the physical constraint (e.g. the min operator).

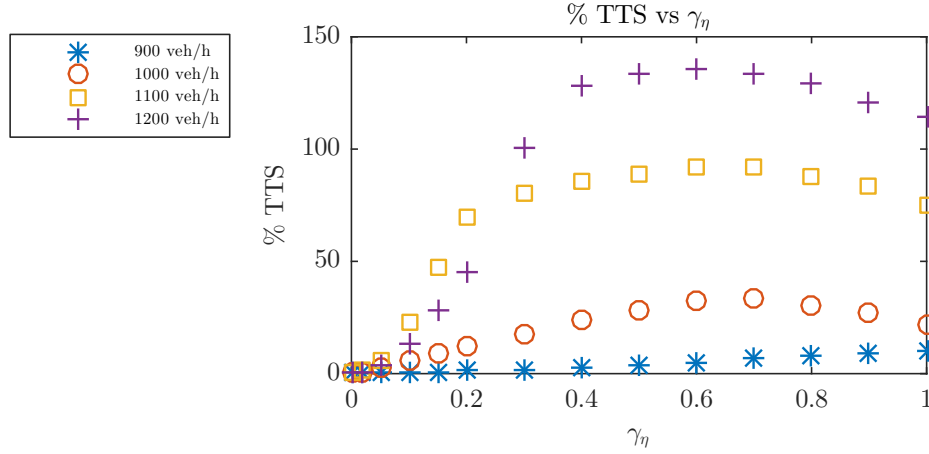


**Figure 4-7:** Case 2A: % TTS increase compared to no uncertainty situation vs  $\gamma^\eta$  for the demands 900, 1000, 1100, and 1200 veh/h.

For part 2B two different levels of uncertainty are evaluated: (1)  $\gamma^\eta = 0.4$ , and (2)  $\gamma^\eta = 0.2$ . Both levels do not cause any deterioration of the uniformity. The absolute values for the TTS are summarized in Table 4-6.

Demand [veh/h]	$\gamma^\eta = 0.2$		$\gamma^\eta = 0.4$	
	TTS [veh·h]	% of FK	TTS [veh·h]	% of FK
900	55.1	1.2%	55.9	2.7%
1000	68.0	11.8%	75.3	24.0%
1100	119.8	69.3%	125.3	85.4%
1200	171.4	45.7%	174.3	127.8%

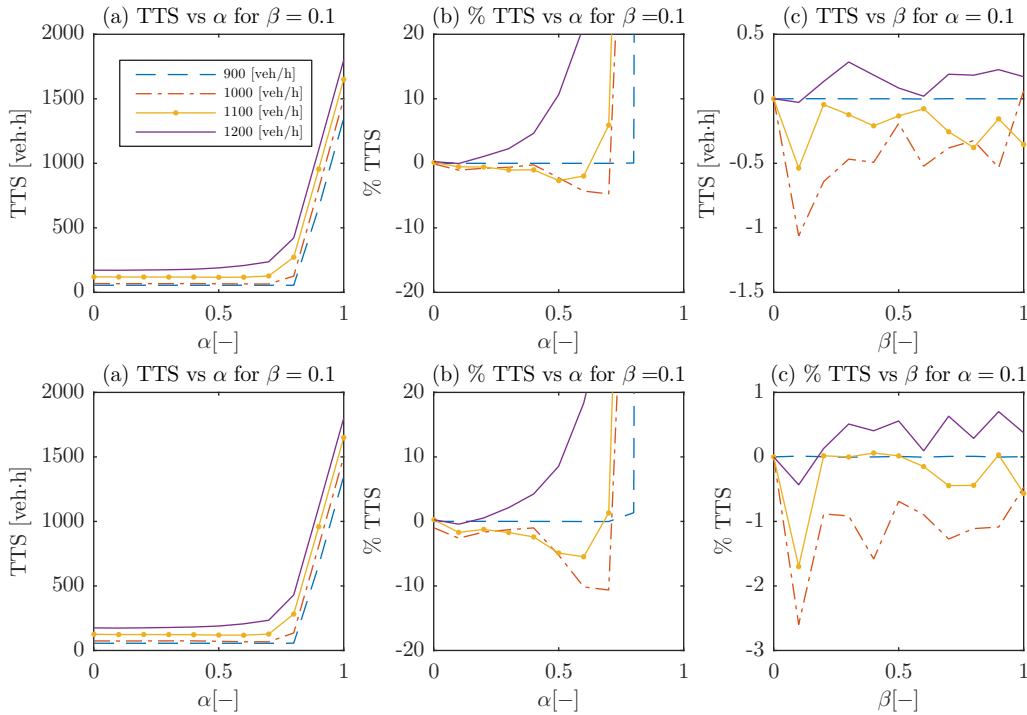
**Table 4-6:** Overview of the TTS of the LP controller without full knowledge of the actual turn fractions for  $\gamma^\eta = 0.2$  and  $\gamma^\eta = 0.4$  and four demand patterns. The percentages show the increase of the TTS compared to the LP controller with full knowledge (FK) of the actual turn fractions for the given  $\gamma^\eta$ .

Figure 4-8 presents the evaluation results of the quantitative analysis of the second case study for  $\gamma^\eta = 0.2$  and  $\gamma^\eta = 0.4$ , respectively. In Table 4-7 the most optimal settings for the LPP controller are shown. As in the previous case, four demand scenarios are considered here: 900 veh/h, 1000 veh/h, 1100 veh/h, and 1200 veh/h. Although sixteen different demand scenarios have been evaluated, the most significant scenarios are presented here. These scenarios are the most significant, because they illustrate the transition from the under-saturated traffic regime to the over-saturated traffic regime.

Figure 4-8 shows that, as expected, for demands lower than the bottleneck capacity, the LPP controller has no effect on the TTS for low values of  $\alpha$ . When the value of  $\alpha$  increases it will eventually affect the TTS. At a demand of 1000 veh/h the impact of the uncertainty is the greatest. Therefore, the LPP controller is able to reach the highest performance increase at this demand. This effect weakens when the demand is increased further.

For a demand of 1200 veh/h there is a relatively high negative impact on the performance for higher values of  $\alpha$ . At  $\gamma^n = 0.2$  and  $\gamma^n = 0.4$  the impact is almost exclusively negative. However, at  $\gamma^n = 0.4$  a slight TTS decrease of 0.4% can be obtained for  $\alpha = 0.1$ .

It can also be observed that the LPP controller can perform relatively better for  $\gamma^n = 0.4$  than for  $\gamma^n = 0.2$ . This is probably due to the higher impact of  $\gamma^n = 0.4$  on the performance of the LP controller as can be seen in Table 4-7.



**Figure 4-8:** Case 2B: TTS vs  $\alpha$  and  $\beta$  for  $\gamma^n = 0.2$  (top) and  $\gamma^n = 0.4$  (bottom) for the demands 900, 1000, 1100, and 1200 veh/h.

Demand [veh/h]	$\gamma^n$	LP	LPP, $\beta = 0.1$		
		TTS [veh·h]	TTS [veh·h]	% of LP	$\alpha$ [-]
900	0.2	55.1	55.1	0.0%	[0.1;0.8]
1000	0.2	68.0	64.8	-4.7%	0.7
1100	0.2	119.8	116.6	-2.7%	0.5
1200	0.2	171.3	171.3	0.0%	0.1
900	0.4	55.9	55.9	0.0%	[0.1;0.7]
1000	0.4	75.1	67.1	-10.6%	0.7
1100	0.4	125.1	118.2	-5.5%	0.6
1200	0.4	174.4	173.6	-0.4%	0.1

**Table 4-7:** Overview of four demand patterns with their minimum TTS with corresponding value of  $\alpha$  at  $\gamma^n = 0.2$  and  $\gamma^n = 0.4$ , with and without demand uncertainty respectively.

### 4-4-3 Case study 2 - qualitative results

The purpose of the qualitative results is to get insight in the behavior of the controller when uncertainty in the turn fractions is present. In order to assess the behavior of the LPP controller, this section looks at how vehicle flows propagate through the traffic network. Table 4-7 shows the optimal settings for the LPP controller. It would be interesting to determine where the performance increase for a demand of 1000 veh/h and 1100 veh/h comes from. This performance increase at high values of  $\alpha$  is not as expected. However, the performance increase at  $\alpha = 0.1$  is as expected. Therefore, in this section the focus lies on two specific cases:

1. A case that shows the behavior of the LPP controller compared to the LP controller for  $\alpha = 0.1$  for a demand of 1000 veh/h and 1100 veh/h;
2. A case that shows the behavior of the LPP controller compared to the LP controller for the optimal values of  $\alpha$  for a demand of 1000 veh/h.

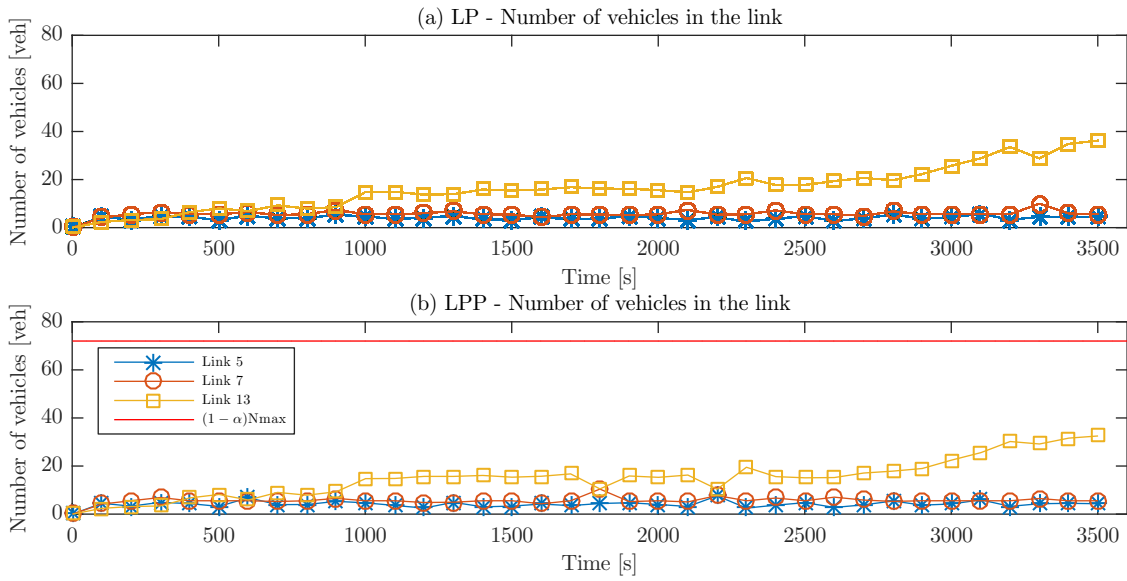
For the first case the demand is set at 1000 veh/h and at 1100 veh/h;  $\alpha$  and  $\beta$  are set to 0.1 and 0.1, respectively. According to Figure 4-8 the LPP controller yields a 1.7% decrease in TTS for a demand of 1000 veh/h and a 2.6 % decrease in TTS for a demand of 1100 veh/h.

Figure 4-9 shows the number of vehicles in several links for a demand of 1000 veh/h. The threshold for the penalty is not reached during the simulation time of 3600 s. This implies that the controllers should yield the same TTS, however this is not the case. The reason for this is that the LPP controller places more vehicles in link 7 than in link 13 compared to the LP controller, because the linear optimization problem probably has multiple solutions. However, more investigation is needed to proof this statement. Due to the extra number of vehicles in link 7, the outflow of link 7 is less affected by the fluctuations of the turn fractions. Hence, the LPP controller is able to maintain a slight higher flow in the bottleneck, which results in a better performance than the LP controller.

Figure 4-10 shows the number of vehicles in several links at a demand of 1100 veh/h. The demand of 1100 veh/h exceeds the bottleneck capacity. Thus, the LP controller starts to increase the number of vehicles again in link 13. At around 2300 s link 13 is full, and the LP controller starts to build a queue in link 5. It can also be observed that around 2300 s, 3100 s, and 3400 s there is some spill-back from link 13 to link 12.

The LPP controller also starts to increase the number of vehicles in link 13. At around 2200 s the threshold of the penalty is reached for link 13 and the LPP controller starts to increase the number of vehicles in link 5. The queue in link 5 starts to build up earlier than it does with the LP controller. The LPP controller also stores some vehicles in link 7 at approximately 2300 s and 3100 s. It can also be observed that there is no spill-back from link 3 to link 12, which leads to better throughput in link 12. Hence, the better throughput of link 12 and the larger number of vehicles in link 7 lead to an increase in performance for the LPP controller.

For the second case the demand is set at 1000 veh/h. According to Table 4-7 the optimal value for  $\alpha$  for a demand of 1000 veh/h is 0.7, where the LPP controller yields a 10.6% increase in TTS compared to the LP controller. Figure 4-11 shows the number of vehicles in several links. It can be observed that the LP controller starts to increase the number of vehicles in link 13 due to the fluctuations of the turn fractions, whereas the LPP controller increases the



**Figure 4-9:** Case 2B: Number of vehicles in the link over time for the LP controller (a) and the LPP controller (b) for a demand of 1000 veh/h and  $(\alpha, \beta) = (0.1, 0.1)$

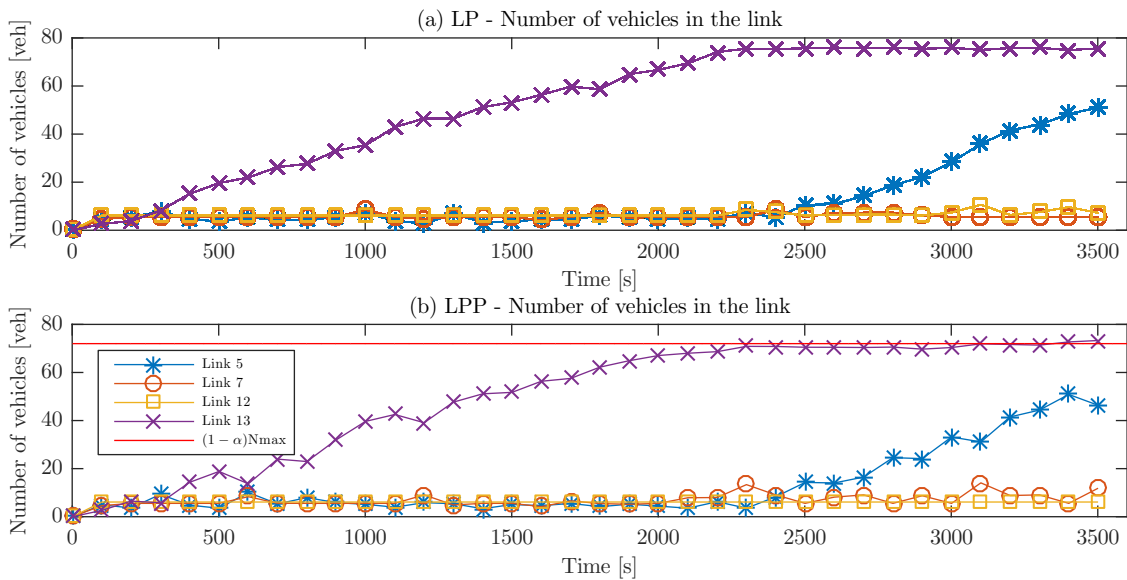


**Figure 4-10:** Case 2B: Number of vehicles in the link over time for the LP controller (a) and the LPP controller (b) for a demand of 1100 veh/h and  $(\alpha, \beta) = (0.1, 0.1)$

number of vehicles in link 5, 7, and 13. Hence, the outflow in link 7 is again affected less by the uncertainty in the turn fractions, which results in an increase in performance for the LPP controller.

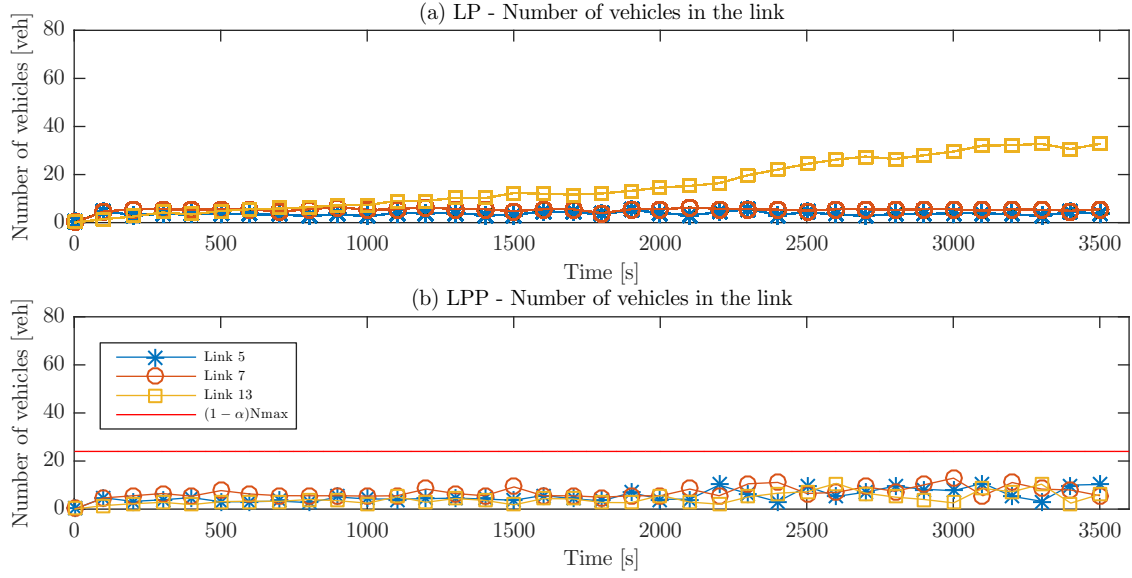


**Figure 4-11:** Case 2B: Number of vehicles in the link over time for the LP controller (a) and the LPP controller (b) for a demand of 1000 veh/h and  $(\alpha, \beta) = (0.7, 0.1)$

## 4-5 Case Study 3: Uncertainty in the outflow constraint

This section presents the results of evaluating the impact of uncertainty on the outflow constraint on the performance of the LPP controller. The resulting performance is compared with the performance of the LP controller. In Section 4-5-1 the set-up of the simulations is presented. After that, Section 4-5-2 presents the quantitative results and Section 4-5-3 the qualitative results.

### 4-5-1 Case study 3 - Evaluation set-up

Case study 3 consists of two parts, namely, 3A and 3B. The first part (3A) consists of evaluating the TTS of the LP controller for different demands and for different levels of uncertainty in the outflow constraint. The second part (3B) consists of evaluating the performance of the LPP controller for different demands for a significant level of uncertainty. The level of the uncertainty is determined in case study 3A.

The uncertainty in the outflow constraint is only applied to link 7, which is the bottleneck of the network. The uncertainty is created by a difference between the actual bottleneck capacity  $q^{\text{bn,act}}(k)$  [veh/h] and the nominal bottleneck capacity  $q^{\text{bn,nom}}(k)$  [veh/h], with a maximum difference of  $\gamma^{\text{q}^{\text{BN}}}$  percent of  $q^{\text{bn,nom}}(k)$ . The actual bottleneck capacity is applied to the traffic network, while the nominal bottleneck capacity is used for prediction of future traffic dynamics. The actual bottleneck capacity is determined as follows:

$$q^{\text{bn,act}}(k) = [1 + \gamma^{\text{q}^{\text{BN}}} \Delta^{\text{q}^{\text{BN}}}(k)] q^{\text{bn,nom}}(k), \quad (4-3)$$

where  $\Delta^{q^{BN}}(k)$  is random variable between -1 and 1 with a uniform distribution. Hence, the actual bottleneck capacity fluctuates around the nominal bottleneck capacity every 10 seconds with a uniform distribution. Link 7 is the only link with a bottleneck. The nominal bottleneck capacity at every simulation is constant over time and is only applied to link 7.

Case 3A and 3B are both evaluated for 16 different demands varying between 100 veh/h and 1600 veh/h with intermediate steps of 100 veh/h. and 14 different levels of uncertainty as repeated in Table 4-4. Hence, there are 224 simulations, which are all repeated ten times with a different random seed. The values of the TTS for each demand and level of uncertainty will be averaged over these ten experiments.

For the second part (3B) of case 3 the performance of the LPP controller will be evaluated. Just as case 1B and 2B the performance of the LPP controller is evaluated for various combinations of  $\alpha$  and  $\beta$ . The penalty is applied on every link. The values for  $\alpha$  and  $\beta$  vary between 0 and 1 with intermediate steps of 0.1. The level for the uncertainty is determined in case 3A.

In case 3A the LP controller is subjected to uncertainty in the bottleneck capacity. The uncertainty in the bottleneck capacity will influence the accuracy of the prediction, and it will therefore have an impact on the TTS. It is expected that there is no impact of the uncertainty in the under-saturated traffic regime, because the uncertainty in the bottleneck capacity has no effect on situations where the demand is lower than the bottleneck capacity. Furthermore, the impact is expected to be more significant in the saturated and over-saturated traffic regime than in the under-saturated traffic regime. It is also expected that the impact of the uncertainty is the highest when the demand is equal to the bottleneck capacity and that for increasing  $\gamma^{q^{BN}}$  the impact on the TTS increases. This is the case for a demand of 1000 veh/h, where there is no congestion in the network without uncertainty. When  $\gamma^{q^{BN}}$  is increased, the fluctuating actual demand will exceed the bottleneck capacity and therefore create congestion, which causes an increase in the TTS. It is expected that the impact will be less for demands patterns where the nominal demand already exceeds the bottleneck capacity, because congestion is already present then.

In case 3B the LPP controller is subjected to uncertainty in the turn fractions for various combinations of  $\alpha$  and  $\beta$ , which will influence the TTS. The performance of the LPP controller is compared to the performance of the LP controller. It is expected that the LPP controller will lead to a decrease in TTS in the saturated and over-saturated traffic regime and that there will be no effect on the TTS in the under-saturated traffic regime.

#### 4-5-2 Case study 3 - quantitative results

Figure 4-12 presents the performance of the LP controller for four different demand patterns when uncertainty in the bottleneck capacity is present. The performance is expressed in a percentage of the performance when the bottleneck capacity is fully known and no uncertainty is present. It seems that there is a linear relation between the relative impact and the level of the uncertainty. Furthermore, it can be seen that the impact is the highest for a demand of 1000 veh/h. The reason for this is that the bottleneck capacity is equal to 1000 veh/h. So the demand of 1000 veh/h can still be served by the bottleneck without causing congestion. However, a tiny disturbance can cause the traffic to break down, which cannot be solved because there is no capacity left. Figure 4-12 also shows that the impact is lower for a

demand of 1100 veh/h and 1200 veh/h compared to the impact for a demand of 1000 veh/h. In both situations the traffic is already broken down, and therefore the uncertainty in the bottleneck has less effect on the TTS.

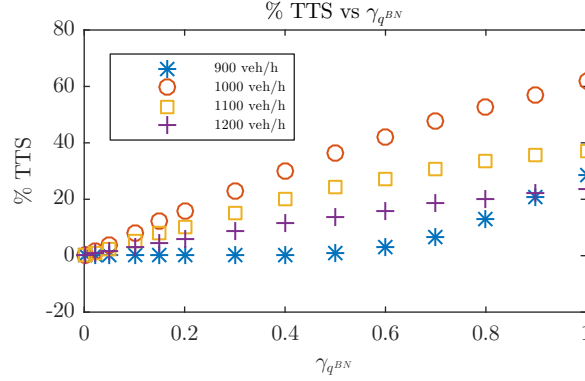


**Figure 4-12:** Case 3A: % TTS increase compared to no uncertainty situation vs  $\gamma^{q^{BN}}$  for the demands 900, 1000, 1100, and 1200 veh/h.

Another observation can be made from Figure 4-12. It can be seen that for a demand of 900 veh/h there is almost no impact of uncertainty on the TTS for  $\gamma^{q^{BN}} \leq 0.5$ . For  $\gamma^{q^{BN}} \geq 0.5$  there is an increase in impact on the TTS. The reason for this is that the fluctuations in the bottleneck capacity become so high that the demand exceeds the bottleneck capacity too often, which causes a breakdown. This will result in an increasing number of vehicles in the links, and therefore an increase in the TTS.

For part 3B two different weights of uncertainty are evaluated: (1)  $\gamma^{q^{BN}} = 0.2$ , and (2)  $\gamma^{q^{BN}} = 0.4$ . The absolute values for the TTS and relative impact are listed in Table 4-8 for these values of  $\gamma^{q^{BN}}$ .

Demand [veh/h]	$\gamma^{q^{BN}} = 0.2$		$\gamma^{q^{BN}} = 0.4$	
	TTS [veh·h]	% of FK	TTS [veh·h]	% of FK
900	54.5	0.0%	55.0	0.2%
1000	73.9	15.7%	87.3	29.8%
1100	126.6	10.3%	139.1	19.9%
1200	178.2	6.0%	188.6	11.5%

**Table 4-8:** Overview of the TTS of the LP controller without full knowledge of the bottleneck capacity for  $\gamma^{q^{BN}} = 0.2$  and  $\gamma^{q^{BN}} = 0.4$  and four demand patterns. The percentages show the increase of the TTS compared to the LP controller with full knowledge (FK) of the actual bottleneck capacity for the given  $\gamma^{q^{BN}}$ .

Figure 4-13 presents the evaluation results of the quantitative analysis of the third case study for  $\gamma^{q^{BN}} = 0.2$  and  $\gamma^{q^{BN}} = 0.4$ . In Table 4-9 the most optimal settings for the LPP controller are shown. As in the previous cases, only four demand scenarios are considered here: 900 veh/h, 1000 veh/h, 1100 veh/h, and 1200 veh/h. Although sixteen different demand scenarios have been evaluated, the most significant demand scenarios are discussed here. These scenarios are the most significant, because they illustrate the transition from the under-

saturated traffic regime to the over-saturated traffic regime.

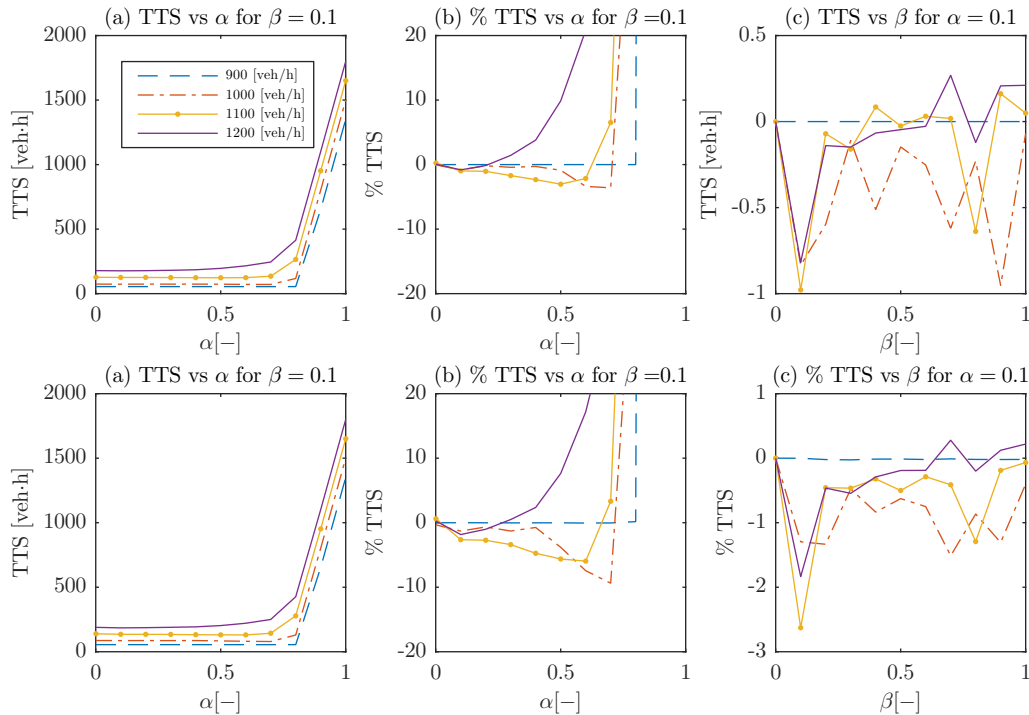


**Figure 4-13:** Case 3B: TTS vs  $\alpha$  and  $\beta$  for  $\gamma^n = 0.2$  (top) and  $\gamma^n = 0.4$  (bottom) for the demands 900, 1000, 1100, and 1200 veh/h.

Figure 4-13 shows that, as expected, for demands lower than the bottleneck capacity, the LPP controller has no effect on the TTS for low values of  $\alpha$ . When the value of  $\alpha$  increases it will eventually affect the TTS. At a demand of 1000 veh/h the impact of the uncertainty is the greatest. Therefore, the LPP controller is able to reach the highest performance increase at this demand. This effect weakens when the demand is increased further.

Demand [veh/h]	$\gamma^n$	LP	LPP, $\beta = 0.1$		
		TTS [veh·h]	TTS [veh·h]	% of LP	$\alpha$ [-]
900	0.2	54.5	54.5	0.0%	[0.1;0.8]
1000	0.2	73.9	71.2	-3.6%	0.7
1100	0.2	127.0	122.8	-3.0%	0.5
1200	0.2	178.4	176.8	-0.8%	0.1
900	0.4	55.0	55.0	0.0%	[0.1;0.8]
1000	0.4	87.1	79.2	-9.3%	0.7
1100	0.4	139.6	130.5	-6.0%	0.6
1200	0.4	189.0	185.0	-1.8%	0.1

**Table 4-9:** Overview of four demand patterns with their minimum TTS with corresponding value of  $\alpha$  at  $\gamma^n = 0.2$  and  $\gamma^n = 0.4$ , with and without demand uncertainty respectively.

For a demand of 1200 veh/h there is relatively high negative impact on the performance for higher values of  $\alpha$ . At  $\gamma^n = 0.2$  and  $\gamma^n = 0.4$  the impact is almost exclusively negative.

However, at  $\gamma^n = 0.4$  a slight TTS decrease of 1.8% and 0.8% for  $\gamma^n = 0.2$  can be obtained for  $\alpha = 0.1$ .

It can also be observed that the LPP controller can perform relatively better for  $\gamma^n = 0.4$  than for  $\gamma^n = 0.2$ . This is probably due to the higher impact of  $\gamma^n = 0.4$  on the performance of the LP controller as can be seen in Table 4-7.

### 4-5-3 Case study 3 - qualitative results

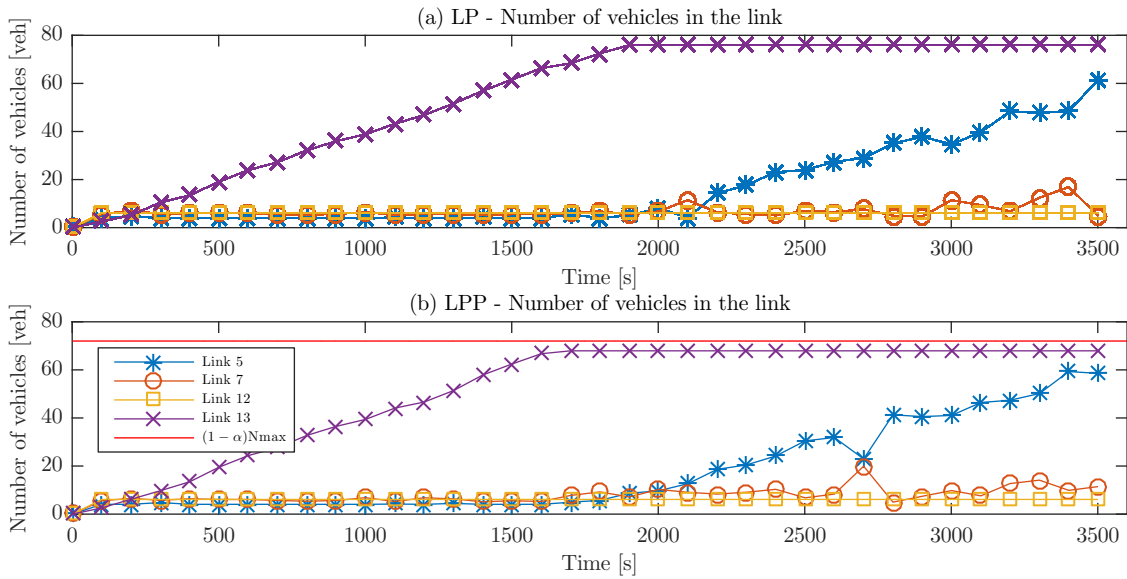
The purpose of the qualitative results is to get insight into the behavior of the controller when uncertainty in the bottleneck capacity is present. In order to assess the behavior of the LPP controller, this section investigates at how vehicle flows propagate through the traffic network. Table 4-9 shows the optimal settings for the LPP controller. It would be interesting to determine where the performance increase for a demand of 1000 veh/h, 1100 veh/h, and 1200 veh/h comes from. This performance increase at high values of  $\alpha$  is not as expected. However, the performance increase at  $\alpha = 0.1$  is as expected. Therefore, in the following section two specific cases are investigated:

1. A case that shows the behavior of the LPP controller compared to the LP controller for  $\alpha = 0.1$  for a demand of 1100 veh/h and 1200 veh/h;
2. A case that shows the behavior of the LPP controller compared to the LP controller for the optimal values of  $\alpha$  for a demand of 1000 veh/h and 1100 veh/h.

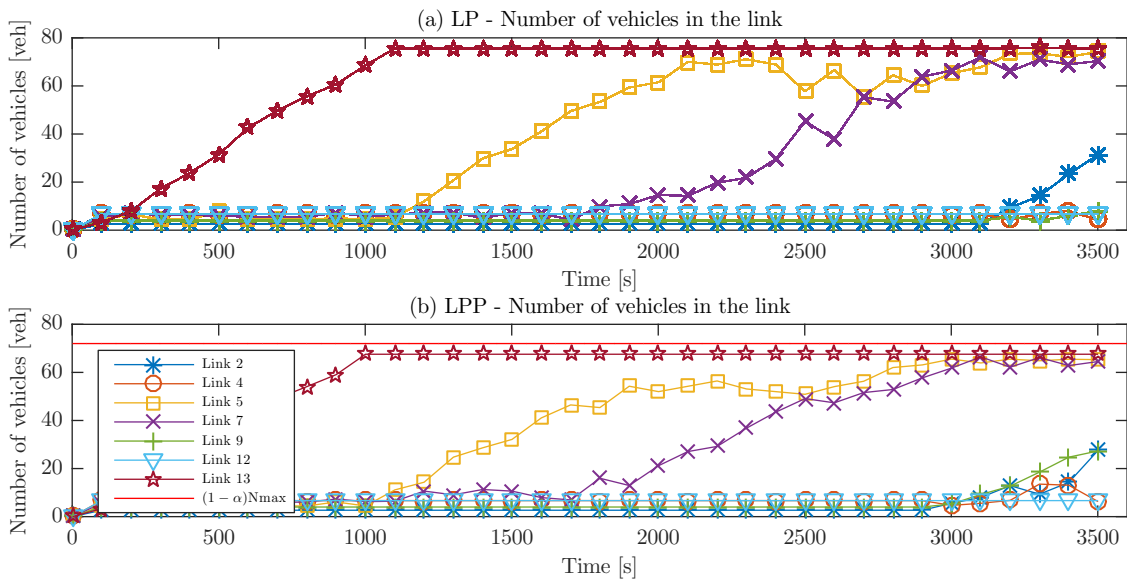
For the first case the demand is set at 1100 veh/h and at 1200 veh/h;  $\alpha$  and  $\beta$  are set to 0.1 and 0.1, respectively. According to Figure 4-13 the LPP controller yields a 2.6% decrease in TTS for a demand of 1100 veh/h and a 1.8 % decrease in the TTS for a demand of 1200 veh/h.

Figure 4-14 shows the number of vehicles in several links for a demand of 1100 veh/h. The demand of 1100 veh/h exceeds the bottleneck capacity. Hence, both controllers start increasing the number of vehicles in links 13 and 5. The LPP controller starts to increase the number of vehicles earlier in link 5 than the LP controller. It also increases the number of vehicles more in link 7 than the LP controller, which is the reason for the performance increase of the LPP controller. Thus, the LPP controller is able take advantage of the unknown fluctuations of the bottleneck capacity.

Figure 4-15 shows the number of vehicles in several links for a demand of 1200 veh/h. The demand of 1200 veh/h exceeds the bottleneck capacity. Hence, both controllers start increasing the number of vehicles in links 13, 5, and 7. The reason for the performance increase of the LPP controller is that it increases the number of vehicles in link 7 earlier than the LP controller. Therefore, the LPP controller is able take advantage of the unknown fluctuations of the bottleneck capacity. However, the performance increase of the LPP controller is lower for a demand of 1200 veh/h than for a demand of 1100 veh/h. The reason for this is that the LPP controller causes spill-back from link 5 to link 4. In the figure there is a small increase in the number of vehicles in link 4 for the LPP controller, which results in a decrease of flow from link 4 towards link 6. Hence, the performance increase of the LPP controller becomes less.



**Figure 4-14:** Case 3B: Number of vehicles in the links over time for the LP controller (a) and the LPP controller (b) for a demand of 1100 veh/h and  $(\alpha, \beta) = (0.1, 0.1)$



**Figure 4-15:** Case 3B: Number of vehicles in the link over time for the LP controller (a) and the LPP controller (b) for a demand of 1200 veh/h and  $(\alpha, \beta) = (0.1, 0.1)$

Figure 4-16 shows the number of vehicles in several links for a demand of 1100 veh/h. The reason for the performance increase of the LPP controller is the same as the previously discussed cases. The LPP controller places more vehicles in link 7, and therefore it is able to take advantage of the bottleneck capacity fluctuations.

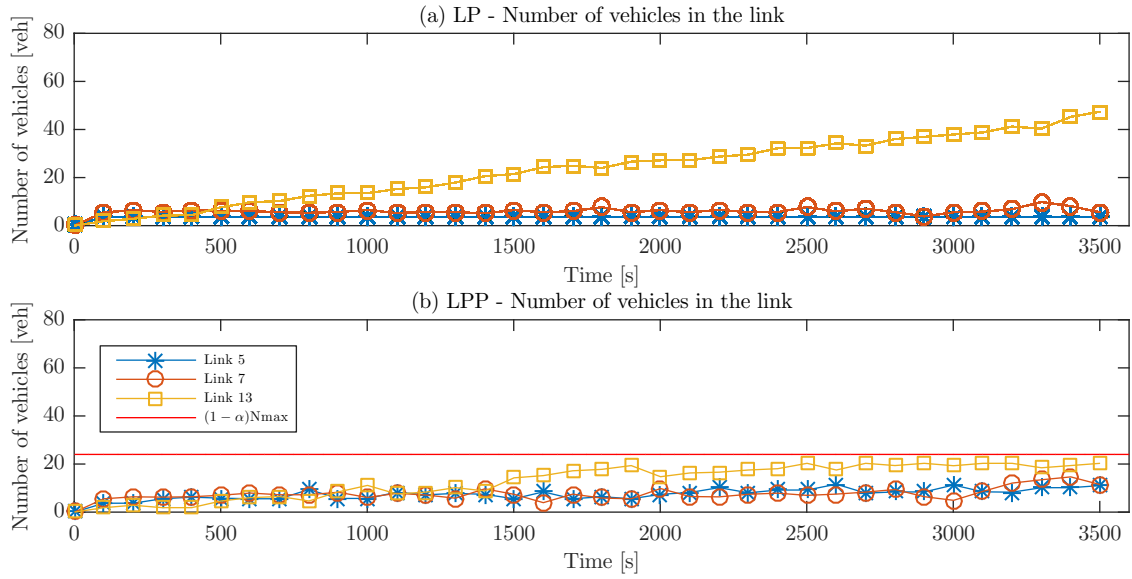


**Figure 4-16:** Case 3B: Number of vehicles in the link over time for the LP controller (a) and the LPP controller (b) for a demand of 1000 veh/h and  $(\alpha, \beta) = (0.7, 0.1)$

## 4-6 Case Study 4: Model uncertainty

This section presents the results of evaluating the impact of model uncertainty on the performance of the LPP controller. The resulting performance is compared with the performance of the LPP controller. In Section 4-6-1 the set-up of the simulations is presented. After that, Section 4-6-2 presents the quantitative results and Section 4-6-3 the qualitative results.

### 4-6-1 Case study 4 - Evaluation set-up

Van de Weg et al. (2016a) propose a linear Model Predictive Control (MPC) framework, where a simplified traffic model (LTM) is used. The proposed control strategy tries to optimize the TTS of the network, by controlling the fractions of green time. In order for the control strategy to be implemented in practice, the fractions have to be translated into red and green times. Van de Weg et al. (2016b) propose a two-layer control framework, which can be seen in Figure 4-17. The first layer (network layer with MPC) generates an optimal cumulative outflow reference for each controlled link. The second layer (local layer) tries to follow the reference, by minimizing the error between the realized cumulative outflow and the reference at each individual intersection. Note that the MPC controller used for the first layer is the same as the LP controller. The error between the realized outflow and the reference is inevitable. The error depends on several parameters and variables, and may have a significant impact on the controller performance.

The prediction model does not model the local layer. Hence, there is some mismatch between what is predicted by the prediction model and what actually happens in the simulation model (e.g. reality). Case study 4 consists in evaluating the performance of the LPP controller for different demands when subjected to this model uncertainty.

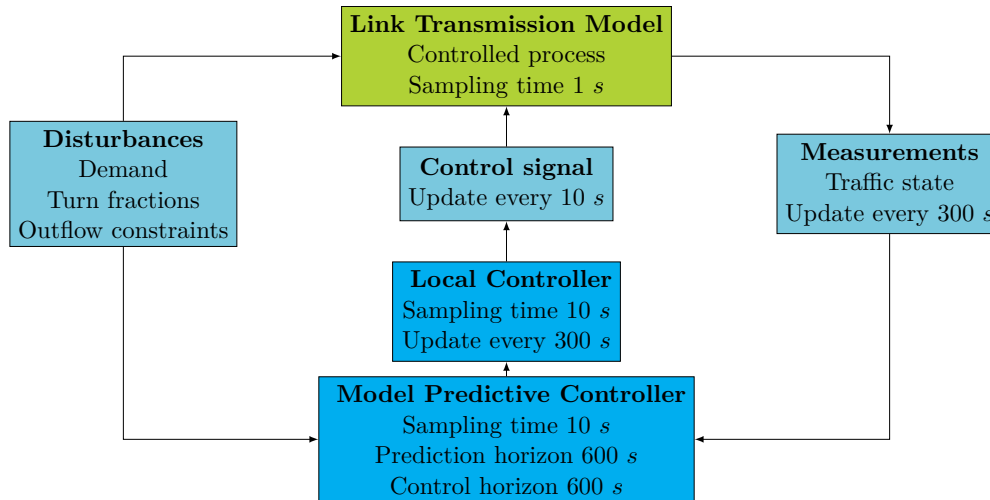


**Figure 4-17:** Overview of the simulation set-up for case study 4

The timing parameters that are used in case study 4 are summarized in Table 4-10 and are based on results found by Van de Weg et al. (2016b). Their work shows that an update interval of the MPC controller of 60 seconds has a negative effect on the TTS. Therefore, the update interval of the MPC controller is set at 300 seconds. Furthermore, they show that the prediction horizon should then be increased to 600 seconds.

Parameter	Value	Parameter	Value
Simulation sample time	1 s	Prediction horizon	600 s
Control sample time	10 s	Control horizon	600 s
Update interval local control	10 s	Update interval MPC	300 s

**Table 4-10:** Timing parameters of case study 4.

Figure 4-18 shows the performance of the controller of Van de Weg et al. (2016b) compared to the performance of the LP controller. It can be observed that the impact of the local layer is the most significant for a demand equal to the bottleneck capacity. The reason for this is that the local layer makes an error in the tracking of the outflow reference, which is provided by the LP controller. The tracking error causes the traffic to break down at a demand of 1000 veh/h, whereas the LP controller itself was able to prevent breakdown. This tracking error is caused by the fluctuations in traffic flow, due to the switching from red to green light and vice versa.

Another observation can be made from Figure 4-18. It seems that there is a linear relation between the demand and the TTS. However, the gradient of this relation differs for demands that do not exceed the bottleneck capacity and for demands that do exceed the capacity. Furthermore, it can be seen that the impact has a slight increase for an increasing demand that does not exceed the bottleneck capacity. Moreover, the impact seems to decrease towards 0% for an increasing demand that does exceed the bottleneck capacity. The reason for this is that the tracking error has less effect on the outflow of the network, because the congestion in the network causes the tracking error to propagate more slowly through the network.

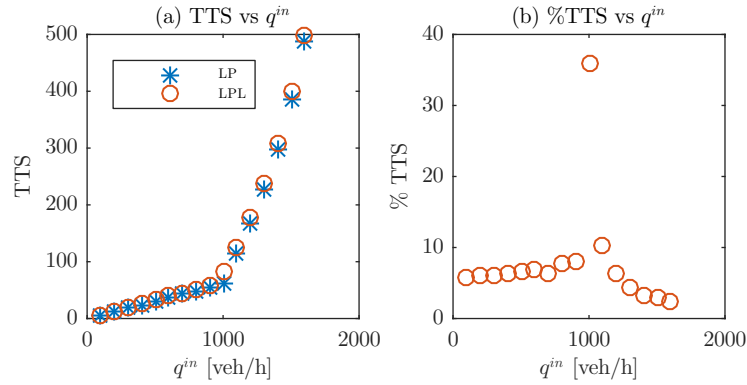
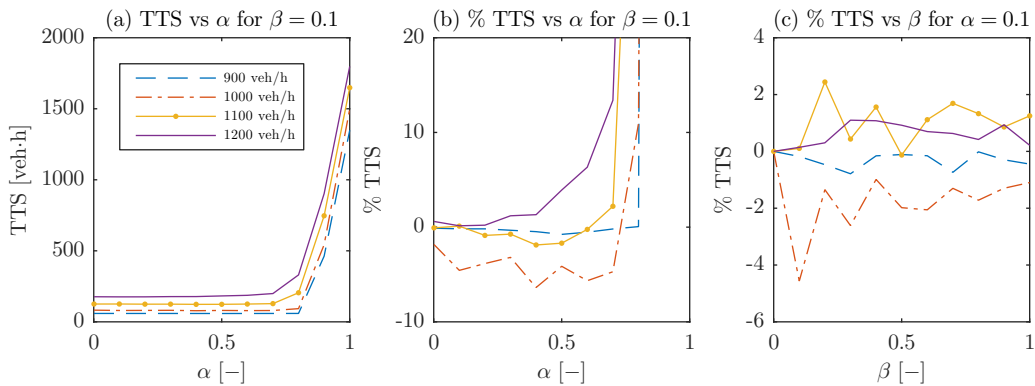


**Figure 4-18:** Case 4: TTS comparison between no uncertainty (LP) and model uncertainty (LPL). In (a) the absolute values of the two situations can be seen for different demands. In (b) the % TTS increase of the uncertainty situation compared to the no uncertainty situation is plotted. It can be observed that the most significant impact occurs where the demand is equal to the bottleneck capacity.

In the remainder of case study 4 the focus lies on assessing the performance and behavior of the LPP controller for demands that are around the bottleneck capacity. It is expected that the LPP controller is able to increase performance in the saturated and over-saturated traffic regime. However, for high demands there may be less improvement because there is less impact by the local control layer.

#### 4-6-2 Case study 4 - quantitative results

Figure 4-19 presents the evaluation results of the quantitative analysis. As in the previous cases, only four demand scenarios are considered here: 900 veh/h, 1000 veh/h, 1100 veh/h, and 1200 veh/h. Although sixteen different demand scenarios have been evaluated, the most significant demand scenarios are discussed here. These scenarios are the most significant, because they illustrate the transition from the under-saturated traffic regime to the over-saturated traffic regime.



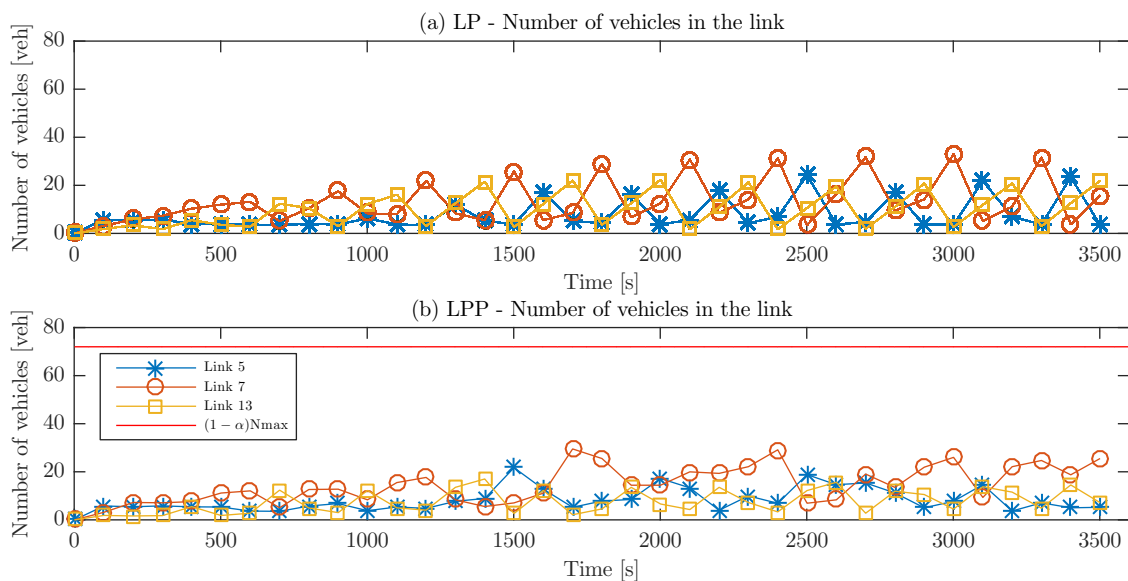
**Figure 4-19:** Case 4B: TTS vs  $\alpha$  and  $\beta$  for  $T^{local} = 10$  s for the demands 900, 1000, 1100, and 1200 veh/h.

Figure 4-19 shows that, as expected, for demands lower than the bottleneck capacity, the LPP controller has little to no effect on the TTS for low values of  $\alpha$ . When the value of  $\alpha$  increases it will eventually affect the TTS. At a demand of 1000 veh/h the impact of the uncertainty is the greatest. Therefore, the LPP controller is able to reach the highest performance increase at this demand. This effect weakens when the demand is increased further.

For a demand of 1200 veh/h there is a relatively high negative impact on the performance for higher values of  $\alpha$ . The impact is exclusively negative. It can also be observed that there is no significant improvement in the performance for a demand of 1100 veh/h.

### 4-6-3 Case study 4 - qualitative results

Figure 4-20 shows the number of vehicles in several links for a demand of 1000 veh/h when  $\alpha$  and  $\beta$  are both set to 0.1. The threshold for the penalty is not reached during the simulation time of 3600 s. This implies that the controllers should yield the same TTS, however this is not the case. The LPP controller yields a decrease of 1.6% in the TTS. The reason for this is that the LPP controller places more vehicles in link 7 compared to the LP controller, because the linear optimization problem probably has multiple solutions. Due to the extra vehicles in link 7, the outflow of link 7 is less affected by the local control layer. Hence, the LPP controller is able to maintain a slightly higher flow in the bottleneck, which results in a better performance than the LP controller.



**Figure 4-20:** Case 4B: Number of vehicles in the links over time for the LP controller (a) and the LPP controller (b) for a demand of 1000 veh/h and  $(\alpha, \beta) = (0.1, 0.1)$

## 4-7 Computation time

In the first 3 case studies the computation time of the LPP controller and the LP controller is tracked. The computation time reported here consists of the computation time required

	Demand		
	100 veh/h	1000 veh/h	1600 veh/h
ACPU [s] of LP controller	0.108	0.096	0.104
ACPU [s] of LPP controller	0.116 (+7.0%)	0.114 (+17.9%)	0.120 (+15.3%)

**Table 4-11:** Overview of the average CPU time used by the optimization algorithm of the LP controller and LPP controller for different demands.

by the linear optimization problem at every time step and the time needed to formulate the optimization problem at every time step. In Table 4-11 the average CPU time is presented for  $(\alpha, \beta) = (0.1, 0.1)$ . It can be observed that every computation time of the LPP controller is higher than that of the LP controller.

## 4-8 Conclusions and recommendations

This section presents the conclusions and recommendations for the cases studies.

- Conclusions regarding the impact of the various uncertainties on the TTS of the LP controller:
  1. The impact of demand uncertainty is the highest for low demands that do not exceed the bottleneck capacity. The impact decreases for an increasing demand that exceeds the bottleneck capacity. The reason for this is that the uncertainty propagates slower through the network if there is congestion;
  2. Uncertainty in the turn fractions has a more direct effect on the traffic dynamics compared to demand uncertainty. The impact of uncertainty in the turn fractions is the highest for high demands that exceed the bottleneck capacity. The reason for this is that higher demand causes higher fluctuations in flow. The controller is not able to correct for these fluctuations, resulting in a worse performance;
  3. The impact of uncertainty in the bottleneck capacity is the highest for a demand that is equal to the bottleneck capacity. The uncertainty causes a breakdown that cannot be solved because there is no capacity left, whereas without the uncertainty the traffic will not break down in the first place. This also explains why there is less impact for demands that exceed the bottleneck capacity, because traffic already has undergone a breakdown due to the higher demand;
  4. The impact of the model uncertainty is the highest for a demand that is equal to the bottleneck capacity. For low demands the impact is almost constant. For an increasing demand that exceeds the bottleneck capacity, the impact decreases because the relative share of TTS due to the uncertainty decreases compared to the TTS caused by the higher demand.
- Conclusions regarding the quantitative results of the LPP controller on the various uncertainties:

1. The LPP controller is able to improve performance for every type of uncertainty, except for the demand uncertainty;
  2. Higher uncertainty levels result in an increased improvement, but also result in a higher absolute value for the TTS;
  3. The controller parameter  $\beta$  does not have a significant effect on the TTS when demand uncertainty is present. For the other uncertainties there is a small decrease in TTS for  $\beta = 0.1$ . Higher values of  $\beta$  have very little effect on the performance.
  4. The controller parameter  $\alpha$  has a significant effect on the TTS. For demands that do not exceed the bottleneck capacity  $\alpha$  has no effect on the performance, except for high values of  $\alpha$ .
  5. The LPP controller can reach the highest performance improvement for a demand that is equal to the bottleneck capacity.
  6. For a demand that exceeds the bottleneck capacity, the LPP controller yields little to no positive impact on the performance;
  7. The LPP controller needs up to 18% more computation time than the LP controller.
- Conclusions regarding the qualitative results of the LPP controller on the various uncertainties:
    1. The LPP controller yields a more conservative control signal. It makes the links in the network less full, and therefore distributes the traffic more evenly over the network.
    2. Additional case studies should be developed to check whether the LPP controller can prevent spill-back and therefore cause less delay.
    3. The performance improvement of the LPP controller is mainly due to the placement of more vehicles in the bottleneck link. Therefore, the outflow of the bottleneck link is less influenced by the uncertainties.
  - The network that is used in the case studies consists of 2 intersections and is provided with a constant demand. The problem with the constant demand is that there is only a small region for which the controller is able to increase performance. For the simulations where the demand is higher than the bottleneck capacity the phenomenon of spill-back is inevitable. Thus, spill-back will not be avoided, and therefore the LPP controller is not able to reach its full potential. Hence, the following changes may improve the case studies for additional evaluation of the LPP controller:
    1. use a different demand pattern, such as a time varying demand pattern rather than a demand pattern that is constant over time;
    2. apply the bottleneck only for a certain period of time.
  - The following points could be used for further evaluation of the LPP controller:
    1. not every source of uncertainty is considered during the evaluation, for instance uncertainty in the state. The uncertainties that were not considered during this evaluation should also be investigated in the future;

2. it should be verified what most realistic types of uncertainty are and they should be implemented in the simulations;
3. in the case studies it is assumed that there is only one source of uncertainty present. However, in the “real” world it is likely that there are multiple sources of uncertainty present at once. Hence, the controller should be evaluated for multiple sources of uncertainty at once;
4. for the case studies the same timing parameters (e.g. the prediction horizon, control horizon, and update frequency) were used, and they were based on the work of Van de Weg et al. (2016a). Due to uncertainty and differences in case study the optimal values for these parameters may have changed, and therefore it should be investigated whether these optimal values have changed and could be adjusted for the given situations.

# Conclusions and recommendations

A linear robust Model Predictive Control (MPC) strategy is developed for urban traffic that is specifically designed to avoid the phenomenon of spill-back. The controller is designed so that it only accounts for uncertainty in the saturated and over-saturated traffic regime. It is shown by simulation that this control strategy can improve the network throughput when uncertainty is present. This holds for uncertainty in the turn fractions, uncertainty in the bottleneck capacity, and model uncertainty. In this chapter the conclusions of this research are presented first. After that, the recommendations for further research will be presented.

## 5-1 Conclusions

The conclusions on the MSc thesis project will be presented according to the three design steps presented in Section 1-2:

- **Analyze** where the major opportunities lie in the field of robust urban traffic control;
- **Develop** a linear robust MPC strategy that improves the traffic network throughput when subjected to uncertainty and remaining real-time feasible;
- **Evaluate** the impact of the different uncertainties on the performance for not accounting for uncertainty, and assess the proposed controller on its ability to improve the throughput.

### 5-1-1 Conclusions on the literature survey

Literature on traffic controllers has been studied to obtain insights in robust urban traffic control. Chapter 2 presents the findings on this literature. These findings will be briefly summarized here.

One of the goals of an urban traffic controller is to improve network throughput in all traffic regimes. However, not every urban traffic controller that is considered in the literature survey

is able to improve the network throughput in all traffic regimes. Some of the model-based control strategies are able to improve network throughput in all traffic regimes. This is due to their ability to predict future traffic dynamics. However, before these types of controllers can be implemented, there are some challenges to overcome. One of these challenges is that the controllers are not always real-time feasible. The approach of Van de Weg et al. (2016a) is able to become real-time feasible while maintaining a reasonable performance. It does so by omitting some detail in the prediction model of traffic. However, by omitting some detail Van de Weg et al. (2016a) choose to have some model-reality mismatch. Furthermore, they assume that perfect knowledge is available of the measurements and disturbances.

There are various control approaches that can handle uncertainties. Both Linear Quadratic Gaussian (LQG) and  $H_\infty$  control are considered and show promising results in terms of computation time. However, both control methods are based on feedback control only, and therefore these methods are unable to anticipate on future estimated or predicted disturbances (e.g. the demand). In contrast, robust MPC is also considered and it can anticipate on the future. Robust MPC shows promising results in term of performance when uncertainty is present. However, one of the challenges of robust MPC is the computation time.

Some of the considered robust urban traffic control strategies show an improvement of the network throughput when subject to uncertainty (e.g. in the demand or queue length). However, there still exist several open issues in the field of robust urban traffic control, such as it is yet unclear what the impact of some uncertainties is on the controllers' performance and the question whether the design of a robust urban traffic controller is really necessary remains.

## 5-1-2 Conclusions on the development of the control strategy

Based on the findings of the literature survey a control strategy is developed in Chapter 3 based on the linear MPC controller of Van de Weg et al. (2016a). The goal of the controller is that it should be robust and real-time feasible. Van de Weg et al. (2016a) assume that the measurement of the state and the disturbances are fully known. These assumptions may not hold in the "real" world, thus these assumptions may have to be relaxed. This could be done by introducing noise or an uncertainty. In this thesis the MPC strategy is redefined to come up with a linear robust urban traffic controller.

The proposed robust controller only accounts for uncertainty in the saturated and over-saturated traffic regime by avoiding spill-back, where other robust urban traffic controllers focus on every traffic regime. The reason for this is that it is expected that the impact of uncertainty is significantly higher in the saturated and over-saturated traffic regime than in the under-saturated traffic regime. Thus, the controller is designed so that in the under-saturated traffic regime it does not account for uncertainty. Accounting for uncertainty

This should result avoid a too conservative input resulting in a too high decrease in performance. Hence, the proposed controller differs from other robust traffic controllers. In the under-saturated regime the proposed controller should yield the same behavior as the controller of Van de Weg et al. (2016a).

From traffic flow theoretical considerations it is expected that uncertainty has a greater impact on the performance in the saturated and over-saturated traffic regime. The reason for this is that spill-back is more likely to occur in those regimes and spill-back causes additional

delays. The uncertainty causes controllers to make less optimal control decisions because the controller is misinformed. Hence, this increases the likelihood of spill-back. A safety margin can be introduced to avoid spill-back. The safety margin is established by penalizing the number of vehicles that violate this safety margin. The penalty describes the number of vehicles for each link at every time step that exceed a given threshold multiplied by a given constant. The value of the penalty increases with an increasing number of vehicles when the threshold is exceeded. By minimizing the penalty the controller tries to avoid that the number of vehicles in a link exceeds this threshold, and therefore the controller incorporates a safety margin in every link.

The proposed extension does not require any additional measurements compared to the controller of Van de Weg et al. (2016a). However, the implementation of the penalty does require an extra state variable per link, and two extra constraints. Thus, the size of the optimization problem is larger than the optimization problem of Van de Weg et al. (2016a). Nevertheless, the optimization problem is still a linear programming problem. Hence, it is expected that the proposed extension is real-time feasible.

### 5-1-3 Conclusions on the evaluation of the control strategy

In Chapter 4 the control strategy is evaluated for different sources of uncertainty by means of simulation. For every uncertainty category, different case studies are conducted. The controller of Van de Weg et al. (2016a) has three potential types of uncertainty: uncertainty in the prediction or estimation of the disturbances, uncertainty in the measurement of the state, and uncertainty in the prediction model. In this thesis only the uncertainty in the disturbances and in the prediction model are considered. The evaluation of uncertainty in the state is expected to be much more complex, because the proposed controller makes use of the the state to determine the penalty. Section 4-8 provides an extensive overview of the conclusions, the most important findings will be repeated here:

- accounting for uncertainty is necessary, because almost every considered uncertainty has a significant effect on the performance of the traffic controller;
- the proposed controller is able to improve performance when subject to uncertainty in the turn fractions, uncertainty in the bottleneck capacity, and uncertainty in the prediction model when compared to the controller of Van de Weg et al. (2016a). However, the controller is not able to improve the performance when subject to demand uncertainty. As expected the performance increase is mainly reached in a small demand region;
- the impact of uncertainty is the most significant on the performance of the controller of Van de Weg et al. (2016a) when the flow into the bottleneck is equal to the capacity of the bottleneck. However, this is not the case for uncertainty in the turn fractions;
- the qualitative behavior of the control strategy is similar to the behavior of the controller of Van de Weg et al. (2016a), in the sense that it has a similar impact on the evolution of the traffic dynamics;
- the value of the threshold of the penalty can have a significant effect on the performance. For low demands in combination with low values for the threshold there is no effect on

the performance. However as expected, for high demands there is a significant negative effect on the performance for low values of the threshold;

- the value of the maximum height of the penalty does not have a significant effect on the performance. For one particular value of the maximum height of the penalty there is a small increase in performance. For higher values of the maximum height there is very little effect on the performance;
- the performance improvement is mainly due to the placement of more vehicles in the bottleneck link and not by preventing spill-back as the controller is intended. Therefore, the outflow is less influenced by the uncertainties;
- the cases could be improved to check whether the proposed controller can prevent spill-back, and therefore cause less delay;
- As expected, the computation time of the proposed controller is higher than for the controller of Van de Weg et al. (2016a). Evaluations show that the increase is 20% at maximum for every considered case study.

## 5-2 Recommendations

There is still a lot to improve in the control strategy that is proposed in this MSc thesis. Moreover, the concept of using a penalty will have to be evaluated in more detail by defining additional case studies. Section 5-2-1 will give some recommendations regarding more extensive case studies. After that, recommendations are presented in Section 5-2-2 on how the control strategy can be extended and improved in order to obtain a better performance. Concluding, some directions will be presented in Section 5-2-3 for further research in the field of robust urban traffic control.

### 5-2-1 Further research - extension of the case study

The network that is used in the case studies consists of 2 intersections and is provided with a constant demand. The problem with the constant demand is that there is only a small demand region for which the controller is able to increase the performance. For the simulations where the demand is higher than the bottleneck capacity the phenomenon of spill-back is inevitable. Thus, spill-back will not be avoided, and therefore the proposed controller is not able to reach its full potential. Hence, the following points could be used to define additional case studies:

- use a different demand pattern (e.g. a time varying demand pattern) rather than a demand pattern that is constant over time;
- apply the bottleneck only for a certain period of time;

The following points could also be used to extend the case studies:

- In the case studies it was assumed that there is only one source of uncertainty present. In reality there will be multiple sources of uncertainty. Hence, the controllers should be evaluated for multiple sources of uncertainty at once;
- It should be verified what the most realistic types of uncertainty are and they should be implemented in the simulations;

### 5-2-2 Further research - improvements and extensions on the control strategy

The following can be investigated to extend the control strategy or to improve its performance in terms of computation time and Total Time Spent (TTS):

- The optimal values for the control parameters could be dependent on the demand or on other traffic parameters. Since the demand and some traffic parameters are different for every link, the values of the control parameters could be adjusted for individual links to increase the performance of the controller;
- To reach the full potential of the proposed controller the optimal values for the threshold and the maximum value of the penalty should be found. A brute force grid search would not be suitable for that. Hence, it is recommended to use a more sophisticated method,. Furthermore, it is expected that the threshold is a function of some traffic parameters, such as the demand, shock wave speed, and so forth. This function may be found by analytic or numerical derivation, or the function may be empirically determined with experiments.
- It should be investigated whether accounting for uncertainty by avoiding spill-back is more beneficial than accounting for uncertainty by different approaches, such as the approach of Tettamanti et al. (2014);
- For the case studies the same timing parameters (e.g. the prediction horizon, control horizon, and update frequency) were used, and they were based on the work of Van de Weg et al. (2016a). Due to the uncertainty and the differences in case study the optimal values for these parameters may have changed, and therefore could be adjusted in the given situation;
- It should be investigated whether the increased size of the optimization problem of the proposed controller has a significant impact on the computation time.
- For the improvement of the computation time the penalty could be imposed only on the links that are influenced by uncertainty instead of imposing the penalty on every link. Note that for each link not imposed with a penalty this would save  $K_p$  variables and  $2K_p$  inequality constraints in the optimization problem;

### 5-2-3 Further research - regarding robust urban traffic control

The following can be investigated to obtain more insights into the field of robust urban traffic control:

- This thesis showed that almost every considered uncertainty has a significant effect on the performance of the traffic controller. Hence, accounting for uncertainty is necessary;
- It is shown that the performance increase is mainly due to the distribution of vehicles to other links. This may also be realized by minimizing the relative occupancy of links as is done by Aboudolas et al. (2010). Combining this together with maximizing the throughput, could lead to better controller performance. However, this turns the linear programming problem into a quadratic programming problem, which costs more computation time. It is expected that the computation time is still doable as the computation time would increase polynomially with respect to the size of the optimization problem, since a quadratic programming problem is also convex;
- The proposed control strategy may not be the most optimal strategy for accounting for uncertainty. Therefore, the performance - in terms of throughput and computation time - of the proposed controller should be extensively compared with other robust urban traffic controllers;
- In future research the introduction of more incidental sources of uncertainty should be introduced such emergency vehicles, priority vehicles, accidents, and unexpected road work.
- Eventually urban traffic controllers are designed to be implemented in the “real” world. Microscopic simulation models can provide us with more realistic traffic scenarios. In future research these models can then be used to show whether robust control is still necessary for urban traffic control.

#### 5-2-4 Further research - regarding urban traffic control

In Section 1-2 it is mentioned that the traffic control problem is a very complex problem, because the traffic controller has to satisfy several requirements when implemented in practice. The linear robust urban traffic controller does not satisfy all these requirements, thus there are still some challenges. These challenges will be listed below. Note that Van de Weg et al. (2016a) also indicate various challenges which have some overlap with the recommendations listed below.

- Robust urban traffic control could in further research be extended to heterogeneous traffic. It should be investigated to what extent heterogeneous traffic will affect the performance of the controller. Furthermore, it should be studied whether there are other uncertainties present for the different traffic participants.
- The proposed control strategy does not consider cycle times, clearance times, minimum green times, and offsets. These variables should be included in future work. These variables could be included but at the cost of a more complex optimization problem. However, these variables may also be introduced by translating the aggregated traffic flows to signal plans.
- Due to the proliferation of in-vehicle technologies, information of individual vehicles may be used to determine traffic parameters, such as turn fractions, demands, and speed of

individual vehicles. Future research could consist of using this information to make more accurate predictions of the future traffic dynamics.

- In this thesis only the improvement of the throughput is studied. In future research other objective functions may be studied. Furthermore, the various sources of uncertainties could have different impacts for other objective functions. Further research is required to study other objective functions and their relation to uncertainty.







$$B_{i,2}^L(k^c) = \begin{bmatrix} 0 & \cdots & 0 \\ \vdots & \ddots & \vdots \\ \eta_{(w,1),i}(k^c)q_{w,i}^{\text{cap}}T^c & \cdots & \eta_{(w,n^O),i}(k^c)q_{w,i}^{\text{cap}}T^c \\ 0 & \cdots & 0 \\ \vdots & \ddots & \vdots \\ 0 & \cdots & 0 \end{bmatrix}. \quad (\text{A-7})$$

The matrix  $B_j^O(k^c) \in \mathbb{R}^{n_j^{O,s} \times (n^L + n^O)}$  of origin  $j$  is given by:

$$B_j^O(k^c) = \begin{bmatrix} B_{j,1}^O(k^c) & B_{j,2}^O(k^c) \end{bmatrix}, \quad (\text{A-8})$$

with  $B_{j,1}^O(k^c) \in \mathbb{R}^{n_j^{O,s} \times n^L}$  is given by:

$$B_{j,1}^O(k^c) = 0, \quad (\text{A-9})$$

and  $B_{j,2}^O(k^c) \in \mathbb{R}^{n_j^{O,s} \times n^O}$  is given by:

$$B_{j,2}^O(k^c) = \begin{bmatrix} 0 & \cdots & 0 & q_{w,j}^{\text{cap}}(k^c)T^c & 0 & \cdots & 0 \\ 0 & \cdots & 0 & 0 & 0 & \cdots & 0 \end{bmatrix}. \quad (\text{A-10})$$

The matrix  $C \in \mathbb{R}^{n^{\text{states}} \times n^O}$  is given by:

$$C = \begin{bmatrix} C_1^L & \cdots & C_{n^L}^L & C_1^O & \cdots & C_{n^O}^O \end{bmatrix}^\top, \quad (\text{A-11})$$

where the matrix  $C_i^L \in \mathbb{R}^{n_i^{L,s} \times n^O}$  of link  $i$  is given by:

$$C_i^L = 0, \quad (\text{A-12})$$

and the matrix  $C_j^O \in \mathbb{R}^{n_j^{O,s} \times n^O}$  of origin  $j$  is given by:

$$C_j^O = \begin{bmatrix} 0 & \cdots & 0 & 0 & 0 & \cdots & 0 \\ 0 & \cdots & 0 & T^c & 0 & \cdots & 0 \end{bmatrix}. \quad (\text{A-13})$$

The vector  $Z \in \mathbb{R}^{1 \times K_p n^{\text{states}}}$  is used to compute the value of the objective function by multiplication with  $\bar{x}(k^c)$ . The vector  $Z$  is defined as:

$$\begin{aligned} Z &= T^c \begin{bmatrix} Z_k & \cdots & Z_k \end{bmatrix} \\ Z_k &= T^c \begin{bmatrix} Z_1^L & \cdots & Z_{n^L}^L & Z_1^O & \cdots & Z_{n^O}^O \end{bmatrix}, \end{aligned} \quad (\text{A-14})$$

with the vector  $Z_i^L \in \mathbb{R}^{1 \times n_i^{L,s}}$  of link  $i$  defined as:

$$Z_i^L = \begin{bmatrix} -1 & 0 & \cdots & 0 & 1 & 0 & \cdots & 0 \end{bmatrix}, \quad (\text{A-15})$$

and the vector  $Z_j^O \in \mathbb{R}^{1 \times 2}$  of origin  $j$  defined as:

$$Z_j^O = \begin{bmatrix} -1 & 1 \end{bmatrix}. \quad (\text{A-16})$$

### A-1-2 Specification of the inequality constraints

The first matrix  $M_1^{\text{ineq}} \in \mathbb{R}^{n^L K_p \times n^{\text{in,tot}}}$  and vector  $V_1^{\text{ineq}} \in \mathbb{R}^{n^L K_p \times 1}$  are used to model the free-flow dynamics according to (3-3). This constraint is applied to the predicted state  $\bar{x}(k^c)$ :

$$\begin{aligned} \bar{M}_1^{\text{ineq}} \bar{x}(k^c) &\leq 0, \\ \bar{M}_1^{\text{ineq}} (\tilde{A}x(k^c) + \tilde{B}\bar{u}(k^c) + \tilde{C}\bar{d}(k^c)) &\leq 0, \\ \bar{M}_1^{\text{ineq}} \tilde{B}\bar{u}(k^c) &\leq -\bar{M}_1^{\text{ineq}} (\tilde{A}x(k^c) + \tilde{C}\bar{d}(k^c)), \end{aligned} \quad (\text{A-17})$$

which can be represented in the standard form:

$$\begin{aligned} M_1^{\text{ineq}} &= \bar{M}_1^{\text{ineq}} \tilde{B}, \\ V_1^{\text{ineq}} &= -\bar{M}_1^{\text{ineq}} (\tilde{A}x(k^c) + \tilde{C}\bar{d}(k^c)), \end{aligned} \quad (\text{A-18})$$

here, the matrix  $\bar{M}_1^{\text{ineq}} \in \mathbb{R}^{n^L K_p \times n^{\text{states}} K_p}$  is given as:

$$\bar{M}_1^{\text{ineq}} = \begin{bmatrix} \ddots & & 0 \\ & M_1 & \\ 0 & & \ddots \end{bmatrix}, \quad (\text{A-19})$$

with the matrix  $M_1 \in \mathbb{R}^{n^L \times n^{\text{states}}}$  given as:









---

# Appendix B

---

## Local control strategy

In this appendix a detailed description is given of the control framework of Van de Weg et al. (2016b) used in Section 4-6. Note that the text in this appendix is equivalent to the text of Van de Weg et al. (2016b).

### B-1 Control framework

The hierarchical control framework can be seen in Figure B-1 and consists out of two layers:

1. The first layer is the network coordination layer. This layer uses a prediction model to optimize the network performance every  $T^{\text{ref}}$  seconds. The produced control signal only consists out of splits. Therefore, the control signal is not directly applicable to traffic signal controllers. The network coordination layer derives a reference trajectory (the prediction of  $N_{\text{out}} \forall$  links) from the optimized control signal.  $T^{\text{ref}}$  is in the range of one or several minutes and where it holds that
2. The second layer is the local intersection layer. This layer consists out of a controller per intersection. The aim of the local controller is to track the reference signal. Every  $T^{\text{local}}$  the possible stages are evaluated. The stage with the smallest error to the reference trajectory in the next  $T^{\text{local}}$  seconds is actuated.

According to Van de Weg et al. (2016b) the advantage of using this framework is that there is no need for a computationally demanding optimization. However, the local intersection controllers are still capable of realizing improvement of the networks' performance, due to the tracking of the optimized reference. Section B-2 shows the various assumptions that are made. Section B-3 elaborates the network coordination strategy and its features, and Section B-4 shows the theory behind the local intersection layer.



- **Measurements:** it is assumed that perfect measurements are available so that there is no need for the design of an observer.

Discrete timing is considered in this paper. The time step  $k$  (-) and sampling time  $T$  ( refer to the period  $t \in [Tk, T(k+1))$  (h). It is assumed that the sampling time of the measurements is equal to  $T$ . The prediction model has a sampling time step  $k^c$  (-) and sampling time  $T^c$  (h). It holds that  $T^c = \epsilon^c T$  with the factor  $\epsilon^c \in \mathcal{I}^+$ . The control signal is updated every controller sampling time step  $k^{\text{local}}$  (-) with controller sampling time step  $T^{\text{local}}$  for which it holds that  $T^{\text{local}} = \epsilon^{\text{local}} T$  with the factor  $\epsilon^{\text{local}} \in \mathcal{I}^+$ .

The main task of the traffic control strategy is to select, based on the measurements from time step  $k-1$ , at every controller sampling time step  $k^{\text{local}}$  (-) and every intersection  $i^{\text{inter}}$  the stage  $p_{i^{\text{inter}}}^*(k^{\text{local}}|k-1)$  with index  $i^s$  (-) that will be actuated for the coming period  $t^{\text{local}} = [k^{\text{local}}T^{\text{local}}, (k^{\text{local}}+1)T^{\text{local}})$  that minimizes the TTS of all the vehicles in the network over a time horizon  $N^{\text{P}}$ :

$$p_{i^{\text{inter}}}^*(k^{\text{local}}|k-1) = \arg \min_{i^s \in \mathcal{P}(p_{i^{\text{inter}}}^*(k^{\text{local}}-1))} J^{\text{TTS}}(x_0(k-1), i^s, u, d), \quad (\text{B-1})$$

where the set  $\mathcal{P}(p_{i^{\text{inter}}}^*(k^{\text{local}}-1))$  is the set of stages that can be reached from the currently active stage  $i^s$  at intersection  $i^{\text{inter}}$ .

## B-3 Network control

### The reference trajectory

The outcome of the optimization problem (3-20) is the vector  $\bar{u}^*(k^c)$  (-):

$$\bar{u}^*(k^{\text{ref}}) = \arg \min_{\bar{u}(k^{\text{ref}})} Z \tilde{A} \bar{u}(k^{\text{ref}}). \quad (\text{B-2})$$

As noted before, this signal cannot be directly applied to the local intersection controllers due to the aggregated nature of the traffic flow model that is used to formulate the linear optimization problem. Instead, a reference trajectory is derived from the optimized signal  $\bar{u}^*(k^{\text{ref}})$ .

To realize this, note that a prediction of the traffic states  $\bar{x}(k^{\text{ref}})$  can be obtained by multiplying  $\bar{u}(k^{\text{ref}})$  with the matrix  $\tilde{A}$ :

$$\bar{x}(k^{\text{ref}}) = \tilde{A} \bar{u}(k^{\text{ref}}). \quad (\text{B-3})$$

The prediction of the state  $\bar{x}(k^{\text{ref}})$  consists of the traffic states  $x(k^c)$  at time steps  $k^c = k^{\text{ref}} + 1 : \dots : k^{\text{ref}} + N^{\text{P}} + 1$ :

$$\bar{x} = [x(k^{\text{ref}} + 1) \quad \dots \quad x(k^{\text{ref}} + N^{\text{P}} + 1)]^{\top}. \quad (\text{B-4})$$

In its turn, the state  $x(k^c)$  consists of the states of the links  $x_{iL}^L(k^c)$  and origins  $x_{iO}^L(k^c)$  at time step  $k^c$ :

$$x(k^c) = [x_1^L(k^c) \quad \dots \quad x_{nL}^L(k^c) \quad x_1^O(k^c) \quad \dots \quad x_{nO}^O(k^c)]^{\top}. \quad (\text{B-5})$$

Finally, the state of link  $x_{iL}^L(k^c)$  and origin  $x_{IO}^O(k^c)$  are defined as:

$$x_{iL}^L(k^c) = \left[ N_{iL}^{\text{out}}(k^c) \quad \dots \quad N_{iL}^{\text{out}}(k^c - k_{iL}^{\text{c,shock}}) \quad N_{iL}^{\text{in}}(k^c) \quad \dots \quad N_{iL}^{\text{in}}(k^c - k_{iL}^{\text{c,free}}) \right]^\top, \quad (\text{B-6})$$

$$x_{IO}^O(k^c) = \left[ N_{IO}^{\text{O,out}}(k^c) \quad N_{IO}^{\text{O,in}}(k^c) \right]^\top. \quad (\text{B-7})$$

$$(\text{B-8})$$

Now, from  $\bar{x}(k^{\text{ref}})$  a reference cumulative outflow trajectory  $N_{iL}^{\text{out,ref}}(\hat{k}^{\text{ref}})$  is derived for every controlled link  $i^L \in \mathcal{I}^{\text{controlled}}$ :

$$N_{iL}^{\text{out,ref}}(k^{\text{ref}}) = \left[ N_{iL}^{\text{out}}(k^{\text{ref}}) \quad N_{iL}^{\text{out}}(k^{\text{ref}} + 1) \quad \dots \quad N_{iL}^{\text{out}}(k^{\text{ref}} + N^{\text{p}} + 1) \right]^\top. \quad (\text{B-9})$$

$$(\text{B-10})$$

where  $\hat{k}^{\text{ref}} = k^{\text{ref}} : \dots : k^{\text{ref}} + N^{\text{p}} + 1$ .

Since,  $T^c = \epsilon^c T$ , the signal  $N_{iL}^{\text{out,ref}}(\hat{k}^{\text{ref}})$  has to be resampled. This is done via the following procedure:

$$\hat{N}_{iL}^{\text{out,ref}}(\hat{k}) = (1 - \gamma^{\text{ref}}(\hat{k})) N_{iL}^{\text{out,ref}}(\hat{k}^{\text{ref,p}}(\hat{k})) + \gamma^{\text{ref}}(\hat{k}) N_{iL}^{\text{out,ref}}(\hat{k}^{\text{ref,p}}(\hat{k}) + 1), \quad (\text{B-11})$$

$$\hat{k}^{\text{ref,p}}(\hat{k}) = \lfloor \hat{k} / T^c \rfloor, \quad (\text{B-12})$$

$$\gamma^{\text{ref}}(\hat{k}) = \frac{\hat{k} - \hat{k}^{\text{ref,p}}(\hat{k})}{T^c}, \quad (\text{B-13})$$

$$\forall \hat{k} \in k^{\text{ref}} \epsilon^{\text{ref}} : \dots : (k^{\text{ref}} + N^{\text{p}} + 1) \epsilon^{\text{ref}}. \quad (\text{B-14})$$

## B-4 Local control

In this paper a greedy reference tracking policy is chosen. This is realized by selecting at every time step  $k^{\text{local}}$  the stage that is expected to minimize the reference tracking error during the next  $T^{\text{local}}$  seconds. The reason that a greedy policy is chosen is that it requires limited computation time. Additionally, including longer horizon predictions is not trivial and requires further theoretical extensions. For instance, when the prediction horizon exceeds the free flow link travel time, it may become necessary to include intersection interaction effects.

The greedy policy is computed for every intersection separately. So, for every intersection the following steps are computed:

1. For every stage that may be actuated:
  - (a) predict the potential cumulative outflow of every link in the intersection when actuating the stage (see Section B-4);
  - (b) compute the resulting reference tracking error (see Section B-4);
2. Actuate the stage that is expected to realize the smallest reference tracking error (see Section B-4).

### Potential cumulative outflow prediction

The first step is to predict, for every intersection and possible stage, the potential cumulative outflows

$N_{iL}^{\text{out,P}}(\hat{k}|k, p_{i^s, i^{\text{inter}}}(k^{\text{local}}))$  (veh) (inflows  $N_{iL}^{\text{in,P}}(\hat{k}|k, p_{i^s, i^{\text{inter}}}(k^{\text{local}}))$  (veh)) of the links  $i_{i^{\text{inter}}}^{\text{us}}$  ( $i_{i^{\text{inter}}}^{\text{ds}}$ ) directly upstream (downstream) of the intersection when actuating the stage  $i^s$  for the time steps  $\hat{k} = k + 1 : \dots : k + \epsilon^{\text{local}} + 1$ . Note that not every stage can be actuated at every time step due to conflicts between stages. This depends on the currently active stage  $p_{i^s, i^{\text{inter}}}(k^{\text{local}} - 1)$ . Hence, denote with  $\mathcal{P}^{\text{reach}}(p_{i^s, i^{\text{inter}}}(k^{\text{local}} - 1))$  the set of stages at intersection  $i^{\text{inter}}$  that can be reached from stage  $p_{i^s, i^{\text{inter}}}(k^{\text{local}} - 1)$ .

When it holds that:

$$T^{\text{local}} < t_{iL}^{\text{free}} \forall i^L \in i_{i^{\text{inter}}}^{\text{us}}, \quad (\text{B-15})$$

$$T^{\text{local}} < t_{iL}^{\text{shock}} \forall i^L \in i_{i^{\text{inter}}}^{\text{ds}}, \quad (\text{B-16})$$

the potential cumulative outflows and inflows at a next time step can be computed as:

$$N_{iL}^{\text{out,P}}(\hat{k} + 1|k, p_{i^s, i^{\text{inter}}}(k^{\text{local}})) = \min \left\{ N_{iL}^{\text{out,P}}(\hat{k}|k, p_{i^s, i^{\text{inter}}}(k^{\text{local}})) + q_{iL}^{\text{sat}} T b_{iL}(\hat{k}, N_{iL}^{\text{out,free}}(\hat{k} + 1), N_{iL}^{\text{out,sb}}(\hat{k} + 1)) \right\} \forall i^L \in i_{i^{\text{inter}}}^{\text{us}}, \quad (\text{B-17})$$

$$N_{iL}^{\text{in,P}}(\hat{k} + 1|k, p_{i^s, i^{\text{inter}}}(k^{\text{local}})) = N_{iL}^{\text{in,P}}(\hat{k}|k, p_{i^s, i^{\text{inter}}}(k^{\text{local}})) + \dots \sum_{j^s \in i_{i^{\text{inter}}}^{\text{us}}} \eta_{j^s, i^L}(\hat{k}) \left( N_{iL}^{\text{out,P}}(\hat{k} + 1|k, p_{i^s, i^{\text{inter}}}(k^{\text{local}})) - N_{iL}^{\text{out,P}}(\hat{k}|k, p_{i^s, i^{\text{inter}}}(k^{\text{local}})) \right) \forall i^L \in i_{i^{\text{inter}}}^{\text{ds}}. \quad (\text{B-18})$$

In this equation, the number of vehicles  $N_i^{\text{out,free}}(k + 1)$  (veh) is given as:

$$N_{iL}^{\text{out,free}}(k + 1) = \gamma_{iL}^{\text{fr}} N_{iL}^{\text{in}}(k - k_{iL}^{\text{free}} + 2) + (1 - \gamma_{iL}^{\text{fr}}) N_{iL}^{\text{in}}(k - k_{iL}^{\text{free}} + 1). \quad (\text{B-19})$$

The maximum possible cumulative outflow caused by spillback from a downstream link  $j^s \in i_{iL}^{\text{ds}}$  is given as:

$$N_{iL}^{\text{out,sb}}(k + 1) = N_{iL}^{\text{out,P}}(k) + \gamma_{j^s}^{\text{sh}} N_{j^s}^{\text{out}}(k - k_{j^s}^{\text{shock}} + 2) + (1 - \gamma_{j^s}^{\text{sh}}) N_{j^s}^{\text{out}}(k - k_{j^s}^{\text{shock}} + 1) + N_{j^s}^{\text{max}} - N_{j^s}^{\text{in,P}}(k), \quad (\text{B-20})$$

where it is assumed that at an intersection one link leads to just one downstream link and it is never the case that two links have an outflow to the same link at the same time step. This assumption is mainly included for simplicity.

### Reference tracking error

Now that the predictions of the link outflows are available when actuating the different stages, the expected reference tracking error  $\bar{e}_{i^s, i^{\text{inter}}}(k^{\text{local}})$  can be computed. This reference is computed as the square of the area between the reference outflow  $\hat{e}_{i^s, i^{\text{inter}}}^{\text{a}}(k^{\text{local}})$  and the predicted

outflow combined with the error between the total intersection reference outflow and total predicted intersection outflow  $\hat{e}_{i^s, i^{\text{inter}}}^b(k^{\text{local}})$ .

The first error is computed as follows:

$$\hat{e}_{i^s, i^{\text{inter}}}^a(k^{\text{local}}) = \sum_{\hat{k}=k+2}^{k+\epsilon^{\text{local}}+1} \sum_{i^L \in i_{i^{\text{inter}}}^{\text{us}}} \left( \hat{N}_{i^L}^{\text{out,ref}}(\hat{k}) - N_{i^L}^{\text{out,p}}(\hat{k}) \right)^2. \quad (\text{B-21})$$

The second error is computed as follows:

$$\hat{e}_{i^s, i^{\text{inter}}}^b(k^{\text{local}}) = \sum_{\hat{k}=k+2}^{k+\epsilon^{\text{local}}+1} \left| \left( \sum_{i^L \in i_{i^{\text{inter}}}^{\text{us}}} \hat{N}_{i^L}^{\text{out,ref}}(\hat{k}) - \sum_{i^L \in i_{i^{\text{inter}}}^{\text{us}}} N_{i^L}^{\text{out,p}}(\hat{k}) \right) \right|. \quad (\text{B-22})$$

Now, the total reference tracking error is computed by adding the two errors multiplied with the tuning parameter  $\gamma^e$  (-):

$$\bar{e}_{i^s, i^{\text{inter}}}(k^{\text{local}}) = \gamma^e \hat{e}_{i^s, i^{\text{inter}}}^a(k^{\text{local}}) + (1 - \gamma^e) \hat{e}_{i^s, i^{\text{inter}}}^b(k^{\text{local}}). \quad (\text{B-23})$$

The parameter  $\gamma^e$  is introduced to trade off the current reference tracking cost and the final reference tracking costs.

### Stage actuation

The final step is the actuation of the stage  $p_{i^s, i^{\text{inter}}}^*(k^{\text{local}})$  that leads to the smallest expected reference tracking error:

$$p_{i^s, i^{\text{inter}}}^*(k^{\text{local}}) = \arg \min_{p_{i^s, i^{\text{inter}}} \in \mathcal{P}^{\text{reach}}(p_{i^s, i^{\text{inter}}}(k^{\text{local}}-1))} \bar{e}_{i^s, i^{\text{inter}}}(k^{\text{local}}). \quad (\text{B-24})$$

---

## Bibliography

- K. Aboudolas, M. Papageorgiou, A. Kouvelas, and E. Kosmatopoulos. A rolling-horizon quadratic programming approach to the signal control problem in large-scale congested urban road networks. *Transportation Research Part C: Emerging Technologies*, 18:680–694, 2010.
- B.D.O. Anderson and J.B. Moore. *Optimal control: linear quadratic methods*. Prentice-Hall, Englewood Cliffs, New Jersey, 1990.
- A. Bemporad and M. Morari. *Robust model predictive control: A survey*. Springer, London, 1999.
- C.F. Daganzo. The cell transmission model, part II: network traffic. *Transportation Research Part B: Methodological*, 29(2):79–93, 1995.
- C. Diakaki, M. Papageorgiou, and K. Aboudolas. A multivariable regulator approach to traffic-responsive networkwide signal control. *Control Engineering Practice*, 10:183–195, 2002.
- C. Diakaki, V. Dinopoulou, K. Aboudolas, M. Papageorgiou, E. Ben-Shabat, E. Seider, and A. Leibov. Extensions and new applications of the traffic-responsive urban control strategy. *Transportation Research Record: Journal of the TRB*, 1856:202–211, 2003.
- F. Dion and S. Yagar. Real-time control of signalised networks, different approaches for different needs. In *Proceedings of the eighth IEE international conference on road traffic monitoring and control*, pages 56–60, 1996.
- L. El Ghaoui, F. Oustry, and H. Lebret. Robust solutions to uncertain semidefinite programs. *SIAM J. Optim.*, 9:33–52, 1998.
- N.H. Gartner, S.F. Assmann, F. Lasaga, and D.L. Hou. A multi-band approach to arterial traffic signal optimization. *Transportation Research Part B: Methodological*, 25(1):55–74, 1991.

- V.V. Gayah and C.F. Daganzo. Clockwise hysteresis loops in the macroscopic fundamental diagram: An effect of network instability. *Transportation Research Part B: Methodological*, 45:643–655, 2011.
- J. Gregoire, X. Qian, E. Frazzoli, A. De La Fortelle, and T. Wongpiromsarn. Capacity-aware back-pressure traffic signal control. *IEEE Transactions on Control of Network Systems*, 2(2):164–173, 2015.
- B. Heydecker. Uncertainty and variability in traffic signal calculations. *Transportation Research Part B: Methodological*, 21(1):79–85, 1987.
- T. Le, H.L. Vu, Y. Nazarathy, and S. Hoogendoorn. Linear-quadratic model predictive control for urban traffic networks. *Procedia - Social and Behavioral Sciences*, 80:512–530, 2013.
- T. Le, P. Kovács, N. Walton, H.L. Vu, L.L.H. Andrew, and S.P. Hoogendoorn. Decentralized signal control for urban road networks. *Transportation Research Part C: Emerging Technologies*, 58:431–450, 2015.
- S. Lin, B.D. Schutter, Y. Xi, and H. Hellendoorn. Fast model predictive control for urban road networks via milp. *IEEE Transactions on Intelligent Transportation Systems (ITSC)*, 12(3):846–856, 2011.
- S. Lin, B. De Schutter, Y. Xi, and H. Hellendoorn. Efficient network-wide model-based predictive control for urban traffic networks. *Transportation Research Part C: Emerging Technologies*, 24:122–140, 2012.
- J.D.C. Little, M.D. Kelson, and N.H. Gartner. Maxband: a versatile program for setting signal on arteries and triangular networks. *Transportation Research Record: Journal of the TRB*, 795:40–46, 1981.
- H.K. Lo. A novel traffic signal control formulation. *Transportation Research Part A*, 33:433–448, 1999.
- J. Löfberg. *Minimax approaches to robust model predictive control*, volume 812. Linköping University Electronic Press, 2003.
- P.R. Lowrie. The sydney coordinated adaptive traffic system; principles, methodology, algorithms. In *Proceedings of Institute of Electrical Engineers International Conference on Road Traffic Signalling*, pages 67–70, 1982.
- C. Osorio and M. Bierlaire. A multiple model approach for traffic signal optimization in the city of lausanne. *Swiss Transport Research Conference*, 2008.
- M. Papageorgiou, C. Diakaki, V. Dinopoulou, A. Kotsialos, and Y. Wang. Review of road traffic control strategies. *Proceedings of IEEE*, 91(12):2043–2067, 2003.
- B.Y. Quan, J.C. Greenough, and Kelman W.L. The metropolitan scoot demonstration project, 1993.
- D.I. Robertson. Transyt method for area traffic control. *Traffic engineering and control*, 10:276–281, 1969.

- D.I. Robertson and R.D. Bretherton. Optimizing networks of traffic signals in real time - the SCOOT method. *IEEE Transactions on Vehicular Technology*, 40(1):11–15, 1991.
- S. Skogestad and I. Postlethwaite. *Multivariable Feedback Control: Analysis and Design*. John Wiley and Sons Ltd., Chichester, West Sussex, UK, second edition edition, 2005.
- A.A. Stoorvogel. The  $h_\infty$  control problem: a state space approach, 2000.
- T. Tettamanti, T. Luspay, B. Kulcsár, T. Péni, and Varga. Robust control for urban road traffic networks. *IEEE Transactions on Intelligent Transportation Systems*, 15(1):385–398, 2014.
- S.V. Ukkusuri, G. Ramadurai, and G. Patil. A robust transportation signal control problem accounting for traffic dynamics. *Computers and Operations Research*, 37:869–879, 2010.
- G.S. Van de Weg, M. Keyvan-Ekbatani, A. Hegyi, and S.P. Hoogendoorn. Urban network throughput optimization via model predictive control using the link transmission model, 2016a.
- G.S. Van de Weg, H. Le Vu, A. Hegyi, and S.P. Hoogendoorn. Coordinated control of intersection stage switching via a two layer control framework for throughput improvement in all traffic regimes. -, 2016b.
- M. Van den Berg, A. Hegy, B. De Schutter, and H. Hellendoorn. Integrated traffic control for mixed urban and freeway networks: A model predictive control approach. *European Journal of Transport and Infrastructure Research*, 7(3):233–250, 2007.
- L. Xie and G. Li, P.and Wozny. *Chance Constrained Nonlinear Model Predictive Control*. Springer Berlin Heidelberg, 2007.
- Y. Yin. Robust optimal traffic signal timing. *Transportation Research Part B: Methodological*, 42(10):911–924, 2008.
- I. Yperman. The link transmission model for dynamic network loading. *PhD thesis, KU Leuven*, 2007.



---

# Glossary

## List of Acronyms

<b>MPC</b>	Model Predictive Control
<b>LQG</b>	Linear Quadratic Gaussian
<b>LTM</b>	Link Transmission Model
<b>CTM</b>	Cell Transmission Model
<b>TTS</b>	Total Time Spent
<b>QP</b>	Quadratic Programming
<b>LP</b>	Linear Programming
<b>SQP</b>	Sequential Quadratic Programming
<b>MILP</b>	Mixed-Integer Linear Programming
<b>SISO</b>	Single Input Single Output
<b>MIMO</b>	Multiple Input Multiple Output
<b>LTI</b>	Linear Time Invariant
<b>CFL</b>	Courant-Friedrichs-Lewy

## List of Symbols

### Variables

$\alpha$	[-] control variable - threshold for the penalty
$b^{L,eff}$	[-] effective fraction of green time

$b^{O,eff}$	[-] effective fraction of green time of an origin
$\beta$	[-] control variable - maximum value of the penalty
$\Delta$	[-] random variable between -1 and 1 with uniform distribution
$\eta_{j,i}$	[-] turn fraction from link $j$ to link $i$
$\eta^{act}$	[-] nominal turn fraction
$\eta^{nom}$	[-] actual turn fraction
$\gamma$	[-] uncertainty weight
$k^{c,free}$	[-] discrete free-flow travel time sampled with $k^c$
$k^{c,shock}$	[-] discrete shock wave travel time sampled with $k^c$
$N^{in}$	[veh] cumulative inflow
$N^{O,in}$	[veh] cumulative inflow of an origin
$N_i^{max}$	[veh] maximum number of vehicles in link $i$
$N^{out}$	[veh] cumulative outflow
$N^{O,out}$	[veh] cumulative outflow of an origin
$q^{bn,act}$	[veh/h] actual bottleneck link outflow
$q^{bn,nom}$	[veh/h] nominal bottleneck link outflow
$q_j^{in}$	[veh/h] inflow of origin $j$
$q^{in,act}$	[veh/h] actual inflow
$q^{in,nom}$	[veh/h] nominal inflow
$q^{out,max}$	[veh/h] maximum link outflow
$q^{realized}$	[veh/h] realized link outflow
$q^{sat}$	[veh/h] saturation outflow
$\gamma^{c,fr}$	[-] residual of a sampling time step that the free-flow travel time is exceeded by $k^{c,free}$
$\gamma^{c,sh}$	[-] residual of a sampling time step that the shock wave travel time is exceeded by $k^{c,shock}$
$t^{free}$	[s] free-flow travel time
$t^{shock}$	[s] shock wave travel time
$v^{free}$	[km/h] free-flow speed
$v^{shock}$	[km/h] shock wave speed
$N$	[veh] number of vehicles

### Timing

$k^c$	[-] control time step
$T^c$	[s] control sampling time
$k$	[-] simulation time step
$T$	[s] model sampling time

### Indices and sets

$I_y^{conflict}$	[-] set of conflicts for intersection $y$
------------------	---

---

$I^{\text{Exit}}$	[-] set of exit links
$I_i^{\text{in}}$	[-] set of all directly upstream links of link $i$
$J_i^{\text{in}}$	[-] set of all origins directly upstream of link $i$
$I$	[-] set of links
$i$	[-] link index
$J$	[-] set of origins
$j$	[-] origin index

